Cdc48-dependent Chromatin Ubiquitylation Hotspots in *Saccharomyces Cerevisiae*

DISSERTATION DER FAKULTÄT FÜR BIOLOGIE
DER LUDWIG-MAXIMILIANS-UNIVERSITÄT MÜNCHEN

vorgelegt von
Maximilian Josef Kern, M.Sc. Biochemie

Oktober 2013

EIDESSTATTLICHE ERKLÄRUNG

Hiermit erkläre ich an Eides statt, dass ich die vorliegende Dissertation selbstständig und ohne unerlaubte Hilfe angefertigt habe. Ich habe weder anderweitig versucht, eine Dissertation einzureichen oder eine Doktorprüfung durchzuführen, noch habe ich diese Dissertation oder Teile derselben einer anderen Prüfungskommission vorgelegt.

München, den……. ……..……..

(Unterschrift)

Promotionsgesuch eingereicht am: 29.10.2013
Datum der mündlichen Prüfung: 25.02.2014
Erster Gutachter: Prof. Dr. Stefan Jentsch
Zweiter Gutachter: Prof. Dr. Barbara Conradt

Die vorliegende Arbeit wurde zwischen Januar 2009 und Oktober 2013 unter der Anleitung von Prof. Dr. Stefan Jentsch am Max-Planck-Institut für Biochemie in Martinsried durchgeführt.

TABLE OF CONTENTS

SUMMARY **1**

1 INTRODUCTION **2**

1.1 The Ubiquitin System 2
1.1.1 Ubiquitin Conjugation and Deconjugation 2
1.1.2 Recognition of Ubiquitin Conjugates 4
1.1.3 Protein Degradation - 26S Proteasome 5
1.1.4 Non-proteolytic Functions of Ubiquitin 6
1.2 The SUMO System 7
1.2.1 SUMO Conjugation and Deconjugation 7
1.2.2 Molecular and Cellular Functions of SUMOylation 9
1.2.3 SUMO-targeted Ubiquitin E3 Ligases (STUbLs) 10
1.3 The AAA ATPase Cdc48/p97 12
1.3.1 Molecular Function of Cdc48/p97 12
1.3.2 Cdc48/p97 Structure 12
1.3.3 Cdc48/p97 Co-factors 14
1.3.4 Cellular Functions of Cdc48/p97 17
1.3.5 Chromatin-related Functions of Cdc48/p97 20

2 AIMS OF THIS STUDY **23**

3 RESULTS **24**

3.1 Genome-wide Monitoring of Chromatin-associated Ubiquitin Conjugates by Chromatin Immunoprecipitation 24
3.2 Identification of Cdc48-dependent Ub-hotspots 26
3.3 K48-linked Ubiquitin Chains Accumulate at Cdc48-dependent Ub-hotspots 29
3.4 Cdc48 Function at Cdc48-dependent Ub-hotspots Requires the Cdc48 Co-factors Ufd1-Npl4, Ubx4 and Ubx5 31
3.5 A Short DNA Sequence Motif Is Sufficient for Ectopic Cdc48-dependent Ub-hotspot Formation 34
3.6 Identification of Proteins That Bind the Conserved DNA Sequence Motif of Ub-hotspots 38
3.7 Ymr111c Is Required for the Formation of 7 Cdc48-dependent Ub-hotspots 40
3.8 Ymr111c Is SUMOylated on Lysine-231 43
3.9 SUMOylation of Ymr111c Is Required for Formation of Ymr111c-dependent Ub-hotspots 46
3.10 Slx5-Slx8 Mediates Ubiquitylation at Ymr111c-dependent Ub-hotspots in a Ymr111c SUMOylation-dependent Manner 47
3.11 Cdc48 Is Recruited to Ymr111c-dependent Ub-hotspots by Ubiquitylation but Does not Seem to Extract Ymr111c 51

3.12 Gene Expression Profiling Suggests That Ymr111c Does not Regulate Gene Transcription 53

4 DISCUSSION 56

4.1 Identification of 9 Cdc48-dependent Ub-hotspots 56
4.2 Cdc48-dependent Chromatin Extraction of Ubiquitylated Proteins Involves a Distinct Cdc48 Co-factor Subset 58
4.3 Ubiquitylation Mechanism and Substrate(s) at Ymr111c-dependent Ub-hotspots 60
4.4 Speculative Models for the Physiological Role of Cdc48-dependent Chromatin Extraction at Ymr111c-dependent Ub-hotspots 63

5 MATERIALS AND METHODS 67

5.1 Microbiological Techniques 67
5.1.1 *Escherichia Coli (E. Coli)* Techniques 67
5.1.2 *Saccharomyces Cerevisiae (S. Cerevisiae)* Techniques 68
5.2 Molecular Biological Techniques 78
5.2.1 DNA Purification and Analysis 78
5.2.2 Polymerase Chain Reaction (PCR) 79
5.2.3 Molecular Cloning 81
5.3 Biochemical and Cell Biological Techniques 83
5.3.1 Protein Methods 83
5.3.2 Chromatin Immunoprecipitation (ChIP) 87
5.3.3 Gene Expression Profiling 91
5.4 Bioinformatic Analysis, Online Resources, and Computer Programs 92

6 REFERENCES 94

7 ABBREVIATIONS 103

DANKSAGUNG 105

Summary

The conserved ATPase Cdc48 (referred to as p97 in humans) is a critical component of the ubiquitin system. Empowered by its ATPase activity, Cdc48/p97 typically segregates ubiquitylated proteins from their environments such as membranes or protein-protein complexes. Recent studies have expanded the spectra of Cdc48/p97 substrates to ubiquitylated chromatin proteins, which are dislodged from DNA by the Cdc48/p97 segregase activity. However, despite the identification of first substrates, it has still remained unclear whether Cdc48/p97-dependent chromatin extraction globally regulates chromatin association of ubiquitylated proteins.

To globally study Cdc48-dependent chromatin extraction in *Saccharomyces cerevisiae*, I established ubiquitin-directed chromatin immunoprecipitation (ChIP) in combination with genome-wide tiling microarrays (Ub-ChIP-chip). Using this method, this study revealed that the genome-wide distribution pattern of ubiquitylated proteins in wild-type *(WT)* yeast cells is vastly dominated by monoubiquitylation of the core histone H2B (H2B-Ub). In line with a global importance of Cdc48-dependent chromatin extraction, steady-state chromatin ubiquitylation appears to increase in Cdc48-deficient cells, resulting in a flattening of the ubiquitin enrichment at H2B-Ub sites compared to *WT* cells. Intriguingly, Cdc48 dysfunction also gives rise to a strong accumulation of predominantly K48-linked polyubiquitin conjugates at 9 genomic positions (Cdc48-dependent Ub-hotspots) that seem to particularly depend on Cdc48-dependent chromatin extraction. Notably, chromatin extraction at all 9 Cdc48-dependent Ub-hotspots not only involves Cdc48 but also its co-factors Ufd1-Npl4, Ubx4, and Ubx5. *In silico* and experimental analysis revealed that 7 out of 9 Cdc48-dependent Ub-hotspots contain a short DNA motif, which is sufficient to trigger ubiquitin conjugate accumulation. This DNA motif is associated with a previously uncharacterised yeast protein, Ymr111c, that is strictly required for ubiquitylation at all 7 DNA motif-containing (Ymr111c-dependent Ub-hotspots) but not at the remaining Cdc48-dependent Ub-hotspots. Ubiquitylation at Ymr111c-dependent Ub-hotspots is mediated in a two-step mechanism, involving SUMOylation of Ymr111c, followed by the recruitment of the SUMO-targeted E3 ubiquitin ligase (STUbL) Slx5-Slx8. First evidence suggests that the ubiquitylation occurs at the nuclear pore and might not target Ymr111c, but rather a currently unknown binding partner. Taken together, this study provides first evidence for a global role of Cdc48-dependent chromatin extraction in yeast and gives detailed insights into its mechanism by identifying and characterising discrete genomic loci at which this pathway is particularly active.

1 Introduction

1.1 The Ubiquitin System

1.1.1 Ubiquitin Conjugation and Deconjugation

Covalent attachment of the 8.5 kDa protein ubiquitin to a substrate protein (referred to as ubiquitylation) is a prominent posttranslational protein modification conserved among all eukaryotes. Ubiquitylation is typically achieved by the formation of an isopeptide bond between the carboxy-terminus of ubiquitin and the ε-amino group of a substrate lysine residue[1]. In very rare cases, ubiquitin is also attached to the amino-terminus, or to none-lysine residues (cysteine, serine, and threonine) of substrate proteins[2,3].

Ubiquitin conjugation is catalysed by a three-enzyme cascade reaction (see Figure 1). First, the ubiquitin-activating enzyme (E1) forms a high-energy thioester with the carboxy-terminus of ubiquitin in an ATP-dependent manner. Second, ubiquitin is transferred to a cysteine residue of a ubiquitin-conjugating enzyme (E2) by transesterification, and finally, a ubiquitin ligase (E3) catalyses ubiquitin attachment to a substrate protein[4].

Substrate proteins are often not only modified by a single ubiquitin moiety (monoubiquitylation), but rather by a polyubiquitin chain that is formed by successive rounds of ubiquitin conjugation to a previously substrate-attached ubiquitin moiety. All seven lysine residues (resulting in K6-, K11-, K27-, K29-, K33-, K48-, and K63-linked ubiquitin chains) as well as the amino-terminus of ubiquitin (resulting in a linear ubiquitin chain) can serve as isopeptide bond acceptor sites. Accordingly, polyubiquitin chains with distinct linkage type and chain topologies can be synthesised[5]. Formation of polyubiquitin chains does sometimes not only involve E1, E2, and E3 enzymes but also so-called E4 ubiquitin ligases. E4 enzymes (like Ufd2 in *S. cerevisiae*) are specialised ubiquitin ligases, which catalyse polyubiquitylation of previously monoubiquitylated proteins[6]. In addition to mono- and polyubiquitylation, substrate proteins can also be multiubiquitylated by the attachment of single ubiquitin moieties to different lysine residues[1].

The ubiquitin conjugation machinery is organised in a hierarchical manner, consisting of one E1 (in *S. cerevisiae,* in *Homo sapiens* two E1s), several E2 (11 in *S. cerevisiae*), and a large family of E3 enzymes (60-100 in *S. cerevisiae*)[1]. Substrate selectivity is mainly conferred by the large family of E3 enzymes[1], which can be subdivided in two major classes, HECT domain and RING domain E3 ligases. HECT domain E3 ligases contain an active site cysteine residue that forms a thioester bond with

ubiquitin prior to its transfer to a target protein[7]. In contrast, RING domain E3 ligases do not form thioester intermediates, but rather facilitate ubiquitylation by promoting E2-substrate interaction[8].

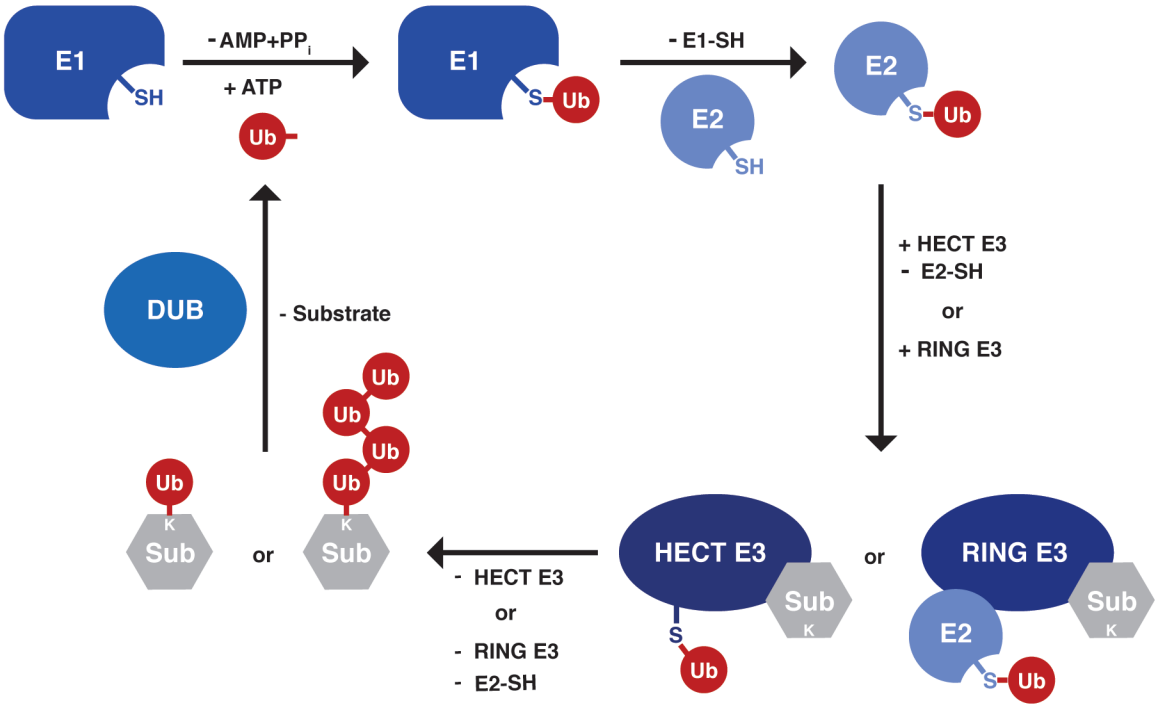

Figure 1: The Ubiquitin Conjugation and Deconjugation System.
Ubiquitin (Ub) conjugation to its substrate proteins requires three enzymatic steps. Initially the ubiquitin-activating enzyme (E1) forms a high-energy thioester bond with the carboxy-terminus of ubiquitin. Next, ubiquitin is transferred to a cysteine residue of a ubiquitin-conjugating enzyme, and finally, a ubiquitin ligase (E3) catalyses ubiquitin conjugation to a lysine residue (K) of its substrate protein (Sub). Ubiquitin ligases of the RING (RING E3) or HECT (HECT E3) family trigger ubiquitin conjugation by different mechanisms. Whereas HECT domain E3 ligases form a thioester bond with ubiquitin prior to ubiquitin conjugation, RING domain E3 ligases facilitate ubiquitylation by promoting E2-substrate interaction. A ubiquitylation substrate is modified either with a single ubiquitin moiety or rather with a polyubiquitin chain. The assembly of polyubiquitin chains requires several rounds of ubiquitin conjugation. Protein ubiquitylation can be reversed by deubiquitylating enzymes (DUBs), which hydrolyse the isopeptide bond between ubiquitin and its substrate proteins.

Like other posttranslational protein modifications, ubiquitylation is a highly regulated and reversible reaction. A family of so-called deubiquitylating enzymes (DUBs) catalyses the hydrolysis of isopeptide bonds that link ubiquitin to its target proteins (see Figure 1). The substrate spectra of some DUBs is limited to polyubiquitin chains of distinct linkage types[9]. Notably, DUB activity is not only required for disassembly of protein-ubiquitin conjugates and efficient ubiquitin recycling, but also for release of free ubiquitin from its precursors. Ubiquitin is exclusively translated in precursors, which are head-to-tail fusion proteins of ubiquitin with itself (*UBI4* gene product) or ribosomal proteins (*UBI1-UBI3* gene

products)[1]. In *S. cerevisiae* twenty DUBs have been identified, which are categorised in four families (Ubp, Otu, JAMM, and Uch) according to their catalytic domain structures[1].

1.1.2 Recognition of Ubiquitin Conjugates

Ubiquitin attachment to substrates usually affects protein stability or function (see 1.1.3 and 1.1.4). To transmit protein ubiquitylation to cellular functions, substrate-attached ubiquitin is typically recognised by ubiquitin-binding proteins. These proteins contain one or several structural features, so-called ubiquitin-binding domains (UBDs), which interact with ubiquitin in a non-covalent manner. Structurally, UBDs (to date more than 20 identified) can be classified in α-helical (e.g. UBA, UIM and Cue domains), zinc finger (e.g. UBZ and NZF domains), pleckstrin homology (e.g. Pru and Glue domains), and ubiquitin-conjugating-like (e.g. UEV and UBC domains) domain containing proteins. Despite their structural diversity UBDs typically interact with similar surfaces of ubiquitin, sharing isoleucine-44 of ubiquitin as a key interaction residue[10].

As discussed above, proteins can be decorated either with single ubiquitin moieties (mono- and multiubiquitylation) or differentially linked polyubiquitin chains. The recent finding that polyubiquitin chains of the same linkage type can adopt several conformations adds even more complexity to the so-called “ubiquitin code”[11]. One mechanism to decode diverse ubiquitin assemblies to different cellular functions is the variable affinity of UBDs towards ubiquitin conjugates of particular length, linkage, and conformation[10]. For instance, the carboxy-terminal UBA domain of Rad23, a ubiquitin receptor that targets proteins for degradation, shows higher affinity for K48-linked than for K63-linked ubiquitin chains[12]. Moreover, as observed for many other UBDs, the Rad23 UBA domain binds monoubiquitin much less strongly than K48-linked ubiquitin chains[12]. Intriguingly, despite their high structural similarity, even members of the same UBD family often differ in their ubiquitin conjugate binding preference.

In many cases binding specificity to distinct ubiquitin assemblies is not only achieved by a single UBD, but rather by a combination of multiple UBDs[10]. Arrays of multiple UBDs provide several surfaces with a defined distance that can interact with ubiquitin conjugates of particular linkage, length and conformation. To get further insight in ubiquitin signalling, it will be of particular importance to increase the knowledge about chain selectivity of single UBDs and UBD arrays in future.

1.1.3 Protein Degradation - 26S Proteasome

Depending on the nature of the attached ubiquitin assembly, ubiquitylation of substrate proteins promotes different functional consequences. The first identified and most intensively studied function of ubiquitylation is its ability to target proteins for degradation by the 26S proteasome, a 2.5 Mega Dalton multi subunit protease[13]. Protein degradation by the 26S proteasome plays a key role in a multitude of cellular pathways such as protein quality control, cell cycle regulation, recycling of amino acids, and production of peptides for antigen presentation[14].

K48-linked polyubiquitin chains, ideally in a length of four ubiquitin moieties, are the most frequent and best characterised signals for proteasomal degradation[15]. However, other ubiquitin chains (in particular K11- and K29-linked ubiquitin chains) can also trigger proteasomal degradation efficiently[16,17]. Depending on the substrate even K63-linked chains can be sufficient for proteasomal targeting[18], although this chain type is generally considered to exclusively promote non-proteolytic functions (see 1.1.4).

Degradation of ubiquitylated proteins is mediated by the 26S proteasome, which consists of the 20S core particle and the 19S regulatory particle[19]. The 20S core particle adopts a barrel-shaped structure that is formed by four stacked rings of seven subunits and harbours proteolytic activity in its cavity. A narrow translocation channel closes the cavity of the 20S core particle and its opening is controlled by the 19S regulatory particle in an ATP-dependent manner. Additionally, the 19S regulatory particle mediates unfolding of substrate proteins, an ATP-dependent reaction that is required for substrate feeding into the proteolytic cavity of the 20S particle[19].

The 26S proteasome recognises its substrates by two different means. On the one hand Rpn10 and Rpn13, two subunits of the 19S regulatory particle, bind polyubiquitylated proteins via ubiquitin-binding domains (UBDs). On the other hand the 19S regulatory particle associates with so-called shuttling ubiquitin receptors, which are non-stoichiometric binding partners of the 26S proteasome[20-24]. Shuttling ubiquitin receptors, such as Rad23, Dsk2, and Ddi1 in *S. cerevisiae*, contain a ubiquitin-like domain (UBL), which serves as a docking site to the 26S proteasome. UBL domains are recognised by Rpn1, Rpn10, or Rpn13, three subunits of the 19S regulatory particle[20,23].

Notably, the proteasome is also linked to deubiquitylation. The deubiquitylating enzymes (DUBs) Rpn11 and Ubp6 (Usp14 in mammalians) ensure efficient deubiquitylation prior to substrate degradation in order to recycle conjugated ubiquitin and to regulate proteasomal substrate selection[25,26]. Whereas Rpn11 is a subunit of the 19S

regulatory particle[25], Ubp6 is a non-stoichiometric binding partner of the 26S proteasome[26].

1.1.4 Non-proteolytic Functions of Ubiquitin

Despite its key role in targeting proteins for proteasomal degradation, ubiquitylation also triggers a multitude of non-proteolytic functions. On the molecular level ubiquitin modulates protein-protein interactions or enzymatic activities of modified proteins. Prominent proteasome-independent functions have been mainly described for mono-, K63-linked, and linear (linked via amino-terminus) ubiquitylation[27-29].

Monoubiquitylation has been implicated in the regulation of numerous cellular processes such as endocytosis, transcription, and DNA repair[30-32]. A very prominent example is its function in postreplicative DNA repair, in which monoubiquitylation of the sliding clamp PCNA (proliferating cell nuclear antigen) stimulates DNA damage tolerance by the recruitment of error-prone translesion DNA-polymerases[33]. Another example, monoubiquitylation of the core histone H2B (H2B-Ub) is one of the most abundant ubiquitylation reactions in eukaryotic cells[34]. Monoubiquitylation of H2B regulates transcription and DNA repair by modulating chromatin structure[35,36].

K63-linked ubiquitylation is a key regulator in a variety of cellular pathways. One of the most prominent functions of K63-linked ubiquitin chains is their role in activation of the pro-inflammatory transcription factor NFκB (nuclear factor kappa-light-chain-enhancer of activated B cells). In this pathway K63-linked ubiquitylation of several proteins, including TRAF6 and NEMO, stimulates a signalling cascade that results in subsequent NFκB activation[28]. In addition to its function in NFκB signalling, K63-linked ubiquitylation triggers several DNA repair processes like DNA double-strand break (DSB) repair and the error-free branch of postreplicative DNA repair[27,32,37].

Linear ubiquitin chains represent a third class of non-proteolytic ubiquitin marks, which has only been identified very recently[38]. Similar to K63-linked ubiquitin chains, linear ubiquitylation promotes NFκB activation[29]. To which extent linear ubiquitin chains also regulate other cellular pathways remains to be determined.

1.2 The SUMO System

1.2.1 SUMO Conjugation and Deconjugation

Apart from ubiquitin, also other structurally related proteins (referred to as ubiquitin-like proteins) are covalently attached to substrate proteins[39]. The most intensively studied member of the ubiquitin-like protein family is the small ubiquitin-like modifier (SUMO), a highly conserved protein, which shares less than 20% sequence similarity with ubiquitin[40]. Despite the low degree of sequence conservation, the three-dimensional structure of SUMO and ubiquitin are highly similar except for a short (10-25 amino acids) amino-terminal extension of SUMO[40].

In some organisms like *S. cerevisiae* or *Caenorhabditis elegans* SUMO is expressed from a single gene copy (e.g. *SMT3* in *S. cerevisiae*), whereas other organisms like plants or vertebrates express several SUMO variants (e.g. in *Homo sapiens* SUMO1-4). All SUMO proteins are expressed as immature precursors with a carboxy-terminal extension of variable length (2-11 amino acids). Proteolytic cleavage by SUMO isopeptidases activates SUMO, resulting in a mature protein with a carboxy-terminally exposed double glycine motif required for conjugation[41].

Similar to ubiquitin, SUMO is attached to target proteins by formation of an isopeptide bond with a substrate lysine residue (see Figure 2). However, SUMO conjugation (SUMOylation) involves specialised E1, E2, and usually E3 enzymes[42]. Notably, E3 enzymes are sometimes dispensable, but usually strongly facilitate SUMOylation[43]. Substrate proteins are modified either by a single SUMO moiety or by polySUMO chains. SUMOylation can be reversed by SUMO isopeptidases, the same class of enzyme that is required for initial SUMO maturation[44].

SUMO attachment sites are frequently surrounded by a conserved sequence motif, the consensus SUMOylation site (ΨKxE, in which Ψ is an aliphatic branched-chain amino acid and x is any amino acid). Although not all consensus sites are SUMOylated and SUMOylation can also occur on other lysine residues, this observation allows *in silico* prediction of some SUMOylation sites[45].

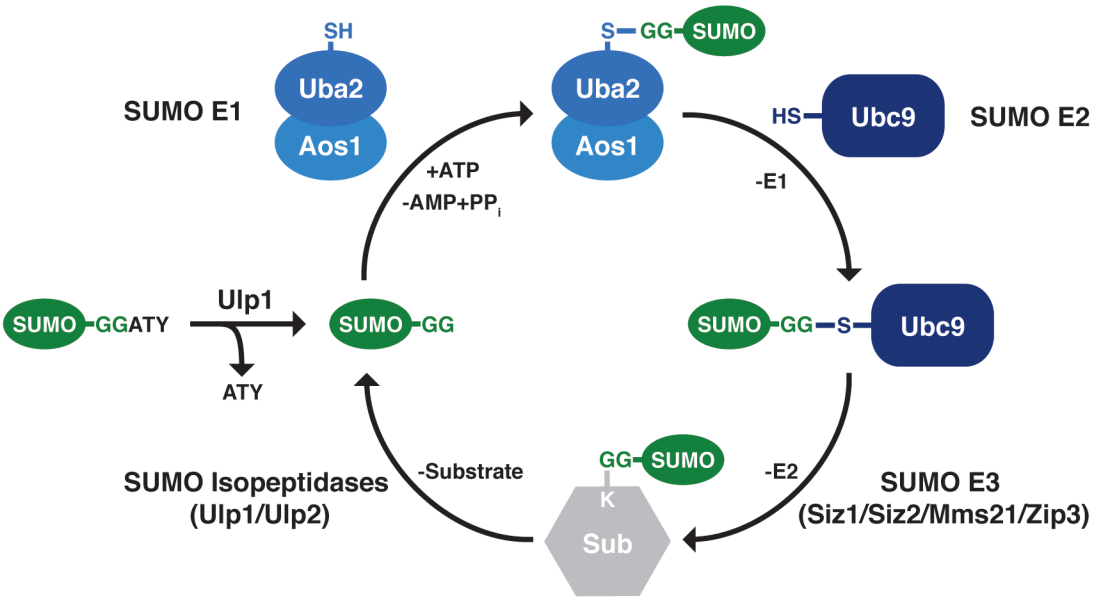

Figure 2: The SUMO Conjugation and Deconjugation System (in *S. Cerevisiae*).
The ubiquitin-like modifier SUMO (Smt3 in *S. cerevisiae*) is synthesised as an inactive precursor protein with a carboxy-terminal extension (in *S. cerevisiae* the peptide ATY). SUMO is activated by proteolytic cleavage (by the SUMO isopeptidase Ulp1), which results in the exposure of the carboxy-terminal double glycine motif (GG) of SUMO. Similar to ubiquitin (see Figure 1), SUMO conjugation to its substrate protein (Sub) typically involves three enzymes. First, the heterodimeric SUMO-activating enzyme (SUMO E1) forms a high-energy thioester with the carboxy-terminus of SUMO. Second, activated SUMO is transferred to a cysteine of the SUMO-conjugating enzyme Ubc9 (SUMO E2), and finally SUMO attachment to a lysine residue of the substrate protein is facilitated by SUMO ligases (SUMO E3). SUMOylation of substrate proteins can be reversed by SUMO isopeptidases, which hydrolyse the isopeptide bond between SUMO and its substrate protein.

The most striking difference between the SUMO and the ubiquitin conjugation system is the simplicity of the SUMO conjugation and deconjugation apparatus. The enzymatic machinery is limited to one E1 (Aos1-Uba2 dimer), one E2 (Ubc9), several E3s, and few SUMO isopeptidases. *S. cerevisiae* expresses four SUMO E3 ligases, Siz1, Siz2, Mms21, and the meiosis-specific Zip3 compared to 60-100 ubiquitin E3 ligases. Likewise in *S. cerevisiae* only two SUMO isopeptidases, Ulp1 and Ulp2, but 20 deubiquitylating enzymes have been identified[1,46].

Curiously, despite the simplicity of the conjugation pathway, SUMOylation targets numerous substrates[47], thereby raising the question how substrate specificity in the SUMOylation pathway is achieved. To this end it has been suggested recently that distinct localisation and targeting of SUMO E3 ligases to cellular compartments is a key mechanism to achieve substrate specificity[48,49].

1.2.2 Molecular and Cellular Functions of SUMOylation

Functional consequences of SUMOylation can be changes in localisation, activity, folding, or even stability of target proteins. On a molecular level these consequences of SUMO attachment can be triggered by different mechanisms. First, SUMO can compete with other lysine-directed posttranslational modifications like acetylation or ubiquitylation. Second, SUMOylation can modulate protein-protein interactions by inducing conformational changes, occupying binding sites or providing an additional interaction surface[45]. To foster protein-protein interactions, substrate-attached SUMO moieties are usually recognised with a moderate affinity by short linear motifs of partner proteins, so-called SUMO-interaction motifs (SIMs). SIMs typically share a hydrophobic core sequence ([V/I]-x-[V/I]-[V/I] or [V/I]-[V/I]-x-[V/I]), which is flanked by acidic and serine residues in a subset of proteins[50,51]. SUMO-SIM interactions can be modulated by posttranslational modifications like phosphorylation of SIMs, or acetylation of SUMO itself[52,53].

Protein SUMOylation affects cellular pathways like transcription, stress response, DNA repair, and many others[40]. Although most SUMO substrates are localised in the nucleus, SUMOylation also targets a number of cytosolic proteins. For several proteins a functional consequence of SUMOylation has been demonstrated by mutation of the corresponding SUMO acceptor sites. One of the most prominent functions of SUMO is its ability to modulate gene expression by modifying a large subset of transcription regulators[54]. For a long time SUMOylation had been primarily linked to inhibition of gene expression, but a growing list of transcription activating functions of SUMO highlighted that it can affect gene expression both negatively and positively[55,56]. A second prominent SUMO modification is the SUMOylation of the replicative sliding clamp PCNA. SUMOylation of PCNA facilitates the recruitment of the helicase Srs2 by SUMO-SIM interactions, thus preventing homologous recombination by disruption of Rad51 recombinase filaments[57].

A key feature of the SUMO pathway is that frequently multiple proteins of complexes or cellular pathways (“protein groups”) are simultaneously modified by SUMO. Moreover, SUMOylation is often triggered by external stimuli such as heat stress or DNA damage[48,58,59]. For instance DNA double-strand breaks (DSBs) induce SUMOylation of many proteins involved in homologous recombination[48,59]. Whereas individual mutations of SUMO acceptor sites in these proteins have only very mild or no phenotypes, the simultaneous mutation of several SUMOylated lysine residues causes a kinetic delay of homologous recombination[48]. Based on this example and the observation that several

proteins of other cellular pathways are also simultaneously SUMOylated, it has been postulated that protein group SUMOylation might be a general mechanism[48,49]. Protein group SUMOylation might foster or “glue” protein-protein interactions in larger protein assemblies by SUMO-SIM interactions and could thereby explain why many individual SUMO substrate acceptor site mutants in previous studies did not show severe phenotypes[49].

1.2.3 SUMO-targeted Ubiquitin E3 Ligases (STUbLs)

Although the SUMO and the ubiquitin system act independently of each other in many cases, an enzyme class of so-called SUMO-targeted ubiquitin ligases (STUbLs) interconnects both pathways. STUbLs are specialised E3 ubiquitin ligases that contain SUMO-interaction motifs (SIMs), which target them to SUMOylated proteins (see Figure 3). They attach polyubiquitin chains to substrate proteins, thereby typically subjecting them to proteasomal degradation[60].

In *S. cerevisiae* three ubiquitin E3 ligases, Ris1 (also called Uls1), the Slx5-Slx8 heterodimer, and Rad18 have been implicated as STUbLs[49]. The RING domain E3 ligase Ris1 has been functionally linked to mating type silencing, replication stress response, and inhibition of telomeric non-homologous end joining[61-63]. Interestingly, Ris1 contains not only a RING but also a DNA-dependent ATPase domain of the Swi/Snf family that is crucial for most of its cellular functions[61,62].

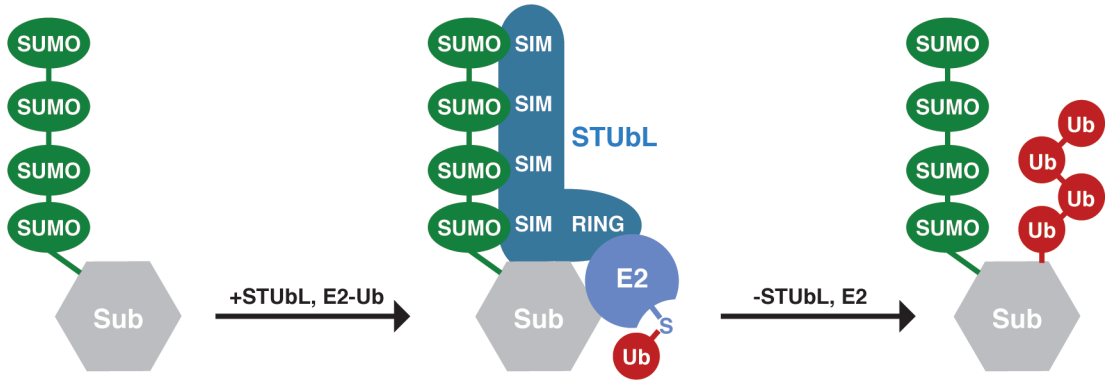

Figure 3: Molecular Mechanism of SUMO-targeted Ubiquitin E3 Ligases (STUbLs).
SUMO-targeted ubiquitin ligases (STUbLs) typically contain several SUMO-interaction motifs (SIMs) by which they are targeted to SUMOylated (typically polySUMOylated) substrate proteins (Sub). Subsequently to recruitment, STUbLs trigger attachment of several ubiquitin (Ub) moieties to their substrate proteins, which are in most cases targeted for proteasomal degradation afterwards. The STUbL depicted in this scheme is a RING domain containing ubiquitin ligase (like Slx5-Slx8 and RNF4), which promotes ubiquitylation by facilitating the interaction between a ubiquitin-conjugating enzyme (E2) and the substrate protein.

The second known STUbL in *S. cerevisiae* consists of a heterodimer of the two RING domain proteins Slx5 (also called Hex3) and Slx8. Slx5 harbours multiple SIMs[64], which target Slx5-Slx8 typically to polySUMO conjugates[65]. Whereas Slx5 mediates substrate binding, ubiquitylation of substrate proteins is exclusively mediated by the Slx8 RING domain[64,65]. Genetic experiments indicate an important function of Slx5-Slx8 in genome maintenance in the presence of DNA double-strand breaks (DSBs) or stalled replication forks[66]. It has been suggested that Slx5-Slx8 is required for a repair pathway that involves relocation of persistent DSBs and collapsed replication forks to the nuclear periphery, although the underlying substrates of this process remain unknown[67]. In line with this function, a large fraction of the Slx5-Slx8 protein pool co-localises with the nuclear pore complex and interacts with the nuclear pore component Nup84[67]. In addition to its prominent role in genome maintenance, Slx5-Slx8 also targets the yeast transcription repressor Matα2 for proteasomal degradation[64]. Notably, Matα2 is recognised in a SUMO-independent manner by Slx5-Slx8, thus suggesting that Slx5-Slx8, and maybe STUbLs in general, might not exclusively act on SUMOylated proteins[64].

Very recently, the E3 ubiquitin ligase Rad18 has been implicated as the third member of the STUbL family in *S. cerevisiae*[68]. It has been demonstrated that a SIM in Rad18 strongly facilitates the recruitment of Rad18 to the sliding clamp PCNA[68]. As already previously identified, Rad18 promotes non-proteolytic mono-ubiquitylation of PCNA[37], indicating that STUbLs are not always directly coupled to proteasomal degradation. Instead, monoubiquitylation of PCNA stimulates DNA damage tolerance by recruiting error-prone translesion DNA-polymerases[33]. If Rad18 might also act as a STUbL in a different cellular context has not been investigated so far.

STUbLs have not only been identified in *S. cerevisiae* but also higher eukaryotes. The vertebrate homologue of Slx5-Slx8, RNF4, is probably the most intensively studied STUbL to date. RNF4 forms a homodimer that localises to promyelocytic leukaemia (PML) bodies and specifically ubiquitylates polySUMOylated PML proteins[69,70]. Ubiquitylation targets PML proteins for proteasomal degradation, which in turn destabilises PML bodies. Notably, PML protein ubiquitylation and degradation is strongly stimulated by arsenic[69,70].

In addition to its crucial role in degradation of PML proteins, RNF4 has also been implicated in other cellular processes such as DSB repair[71,72]. Intriguingly, RNF4 appears to have a non-proteolytic role in DSB repair, since it promotes the formation of K63-linked ubiquitin chains in this pathway[71]. To which extent also other STUbLs possess both proteolytic and non-proteolytical functions remains to be analysed.

1.3 The AAA ATPase Cdc48/p97

1.3.1 Molecular Function of Cdc48/p97

The AAA (ATPases associated with various cellular activities) ATPase Cdc48 (p97 or VCP in humans) is a highly conserved protein among all eukaryotes that has been tightly linked to the ubiquitin system. Together with a subset of other proteins, referred to as substrate-recruiting co-factors, Cdc48/p97 specifically targets ubiquitylated proteins[73]. By converting chemical energy from ATP hydrolysis to mechanical force, Cdc48/p97 segregates its ubiquitylated substrates from protein assemblies or cellular compartments[74]. Subsequent to segregation, Cdc48/p97 either targets its substrates for proteasomal degradation or releases them as stable proteins[75]. The fate of Cdc48/p97 substrates is usually determined by a second class of Cdc48/p97 binding partners, the so-called substrate-processing co-factors. Substrate-processing co-factors tightly regulate the ubiquitylation status of Cdc48/p97 substrates. Due to its function in ubiquitin chain editing, Cdc48/p97 has also been termed a “molecular gearbox”[73].

Cdc48/p97 has been considered for a long time as a ubiquitin-selective segregase. However, very recently, it has been reported that Cdc48/p97 curbs the interaction between the homologous recombination proteins Rad52 and Rad51 in a SUMO-dependent manner[76]. Moreover, Cdc48/p97 was also linked to Atg8, another ubiquitin-like modifier that triggers autophagy by its conjugation to the lipid phosphatidylethanolamine[77]. Both findings expand the spectra of Cdc48 substrate recognition signals to other ubiquitin-like modifiers, but whether both substrates resemble exceptions or rather examples for general principles remains to be investigated.

1.3.2 Cdc48/p97 Structure

Cdc48/p97 is a homohexameric complex with a ring-like structure around a central pore (see Figure 4A and Figure 4B)[78]. Each Cdc48/p97 protomer contains a flexible amino-terminal domain (referred to as N-domain), two AAA domains (referred to as D1 and D2 domains), and a presumably disordered carboxy-terminal tail (see Figure 4C). The D1 and D2 domains of the six protomers are assembled in two stacked rings, which form the ring-shaped core of the Cdc48/p97 hexamer. The hexameric structure of Cdc48/p97 is mainly sustained by the D1 domain and does not require nucleotide binding[74].

The D1 and D2 domain contain a nucleotide binding (Walker A), a nucleotide hydrolysis (Walker B), and a second region of homology (SRH) motif[79]. In line with a

binding preference for ADP[80], the D1 domains have only very moderate ATPase activity under physiological conditions[81]. However, at elevated temperatures D1 ATPase activity is markedly increased[81]. The D2 domains of Cdc48/p97 mediate the bulk of ATP hydrolysis, which induces cooperative conformational changes in all six protomers[82,83]. Cooperativity between the protomers is facilitated either by arginine residues in the D2 domain (referred to as arginine collar) or by the linker between the D1 and D2 domains[74,80,83].

Different structural approaches demonstrated that ATP hydrolysis induces global conformational changes in the Cdc48/p97 hexamer, although their precise localisation and extent is still controversially discussed[84]. Despite all discrepancies it is generally accepted that nucleotide hydrolysis converts chemical energy into mechanical force, which is the molecular basis for Cdc48/p97 segregase activity[74].

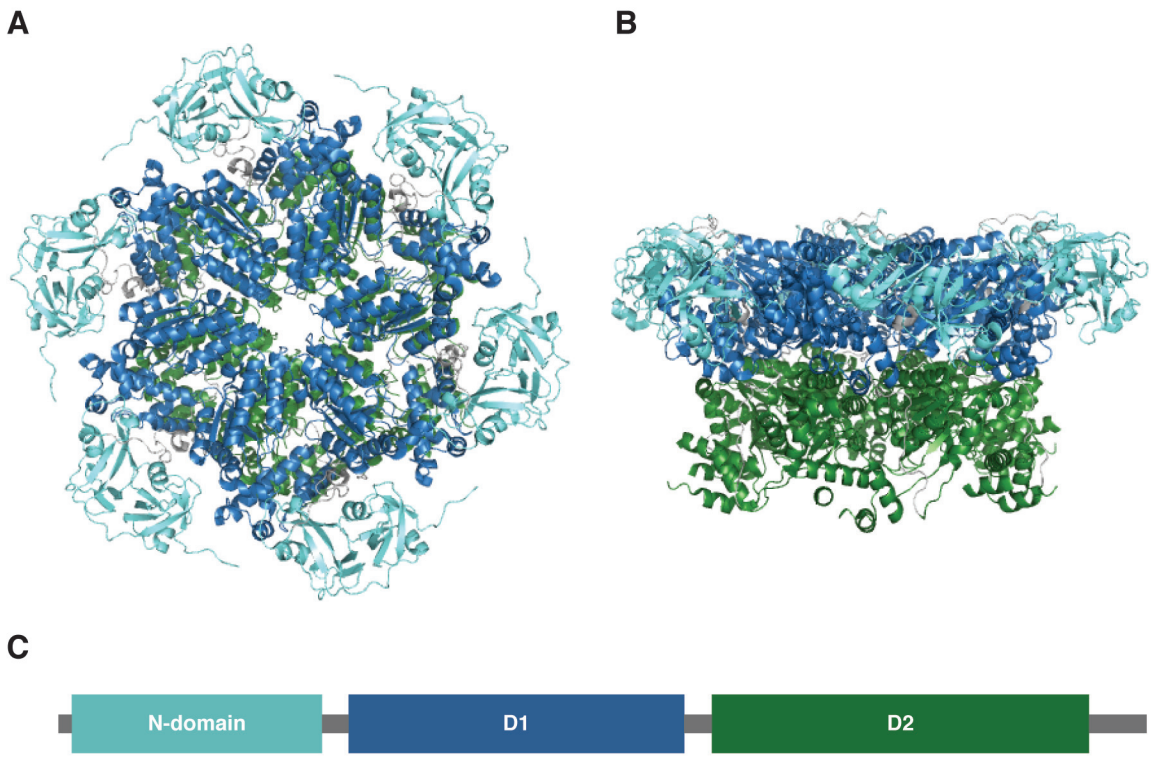

Figure 4: Three-dimensional and Domain Structure of Cdc48/p97.
(A) Top view of the three-dimensional structure of murine p97 (PDB ID: 1r7r) in cartoon presentation (only amino acid residues 17-735 are resolved in the crystal structure)[78]. The N- (cyan), D1 (blue) and D2 (green) domains are presented in the same colours as in C. **(B)** Side-view of the three-dimensional structure of murine p97 presented in A. **(C)** Schematic view of Cdc48/p97 domain structure (the domains are presented in the same colours as in A and B).

1.3.3 Cdc48/p97 Co-factors

1.3.3.1 Cdc48/p97 Binding Modules

To act as a segregase in different cellular contexts, Cdc48/p97 requires a large number of co-factors. Cdc48/p97 co-factors contain at least one Cdc48/p97 binding module, which interacts either with the N-domain or the carboxy-terminal tail of Cdc48/p97[85]. Whereas the UBX domain (a ubiquitin-like domain), the UBX-like domain, the SHP box (also called Binding Site 1), the VBM, and the VIM motif bind to the N-domain[75], other binding modules such as the PUB (only found in higher eukaryotes) and the PUL domain interact with the carboxy-terminus of Cdc48/p97[86-88].

Although many binding modules compete for the same interaction surfaces of Cdc48/p97, competing co-factors can still bind to different protomers of the same Cdc48/p97 hexamer[89]. Functionally distinct Cdc48/p97 complexes differ in co-factor composition, but how the recruitment of distinct co-factor combinations is regulated in time and space is still poorly understood. On the one hand hierarchical binding of co-factors might facilitate stepwise assembly of distinct Cdc48/p97 complexes[90,91]. On the other hand posttranslational modifications might regulate interaction between Cdc48/p97 and its co-factors. Indeed, phosphorylation of a conserved tyrosine residue in the very carboxy-terminus of Cdc48/p97 interferes with binding of PUB or PUL domain containing co-factors[88,92,93].

1.3.3.2 Functional Classification of Cdc48/p97 Co-factors

Although a diverse variety of Cdc48/p97 co-factors has been identified, most of them can be functionally grouped[73]. The first class of Cdc48/p97 co-factors (substrate-recruiting co-factors) mediates substrate binding and pathway choice. The second class of co-factors (substrate-processing co-factors) alters substrate fate (see Figure 5)[73].

Binding of Cdc48/p97 substrates is mainly achieved by Shp1 (also called Ubx1; p47 in mammalian cells) or the Ufd1-Npl4 heterodimer, two substrate-recruiting co-factors that interact with the N-domain of Cdc48/p97 in a mutually exclusive manner[94]. Ufd1-Npl4 and Shp1 form distinct Cdc48/p97 complexes (referred to as Cdc48/p97$^{Ufd1\text{-}Npl4}$ and Cdc48/p97$^{Shp1/p47}$) that promote different cellular functions[89,95]. Both Ufd1-Npl4 and Shp1/p47 contain ubiquitin-binding domains by which they specifically target Cdc48/p97 to ubiquitylated substrates[94]. In addition, Ufd1-Npl4 harbours a SUMO-interaction motif (SIM) that recruits SUMOylated proteins to Cdc48/p97[76,96]. Likewise, yeast Shp1 does not only

bind ubiquitin but also Atg8, a different ubiquitin-like modifier that is required for autophagy induction[77].

Besides Shp1/p47 (the founding member of the UBX protein family) also most other members of the UBX protein family have been implicated in substrate recruitment. Like the major substrate-recruiting co-factors Ufd1-Npl4 and Shp1/p47, most UBX proteins contain ubiquitin-binding domains (UBDs) and interact with the N-domain of Cdc48/p97[89,97]. Despite these similarities the precise role of most UBX proteins in substrate recruitment is still poorly understood. The best-studied member of the UBX family is the membrane protein Ubx2, which targets Cdc48/p97 to the endoplasmic reticulum (ER) and assists Ufd1-Npl4 in substrate recruitment[91,98]. Like Ubx2, other UBX proteins may also bind to the $Cdc48/p97^{Ufd1\text{-}Npl4}$ and $Cdc48/p97^{Shp1}$ core complexes in order to promote substrate recognition.

For years, Cdc48/p97 functions have been exclusively linked to either Ufd1-Npl4 or Shp1/p47, suggesting two major substrate-recruiting co-factors that are assisted by other co-factors like the UBX protein family. However, it has recently been reported that the mammalian co-factor Ubxd1 targets p97 to endosomes independently of Ufd1-Npl4 and p47[99-101]. Therefore it has been proposed that Ubxd1 acts as a independent substrate-recruiting co-factor that forms a third functionally distinct complex with p97[101].

Substrate-processing co-factors are the second functional class of Cdc48/p97 co-factors. They typically regulate the ubiquitylation status of Cdc48 substrates and either target them for proteasomal degradation or trigger their release as stable proteins[73].

The first identified substrate-processing Cdc48/p97 co-factor is the E4 ubiquitin ligase Ufd2, which triggers polyubiquitylation and proteasomal degradation of previously monoubiquitylated Cdc48/p97 substrates[6,102,103]. In addition to Ufd2, a number of other Cdc48/p97-associated ubiquitin ligases (probably most of them also act as an E4 in this context) promote substrate ubiquitylation[104]. However, except for Ufd2, most of them do not bind Cdc48 directly, but are rather recruited to Cdc48/97 by co-factors like UBX family proteins[104].

To counteract proteasomal degradation if desired, Cdc48/p97 binds to co-factors, which interfere with substrate ubiquitylation. On the one hand, Cdc48/p97 interacts with deubiquitylating enzymes such as Otu1 or Ubp3[103,105]. On the other hand, the Cdc48/p97 co-factor Ufd3 abolishes polyubiquitylation of Ufd2 substrates by competing with Ufd2 for Cdc48/p97 binding[103].

Although most substrate-processing co-factors affect protein ubiquitylation, some modify their substrates by different means. The best characterised member of this

subgroup is the mammalian peptide:N-glycanase (PNGase), which removes sugar moieties from glycosylated ER-associated degradation (ERAD) substrates prior to their degradation[106].

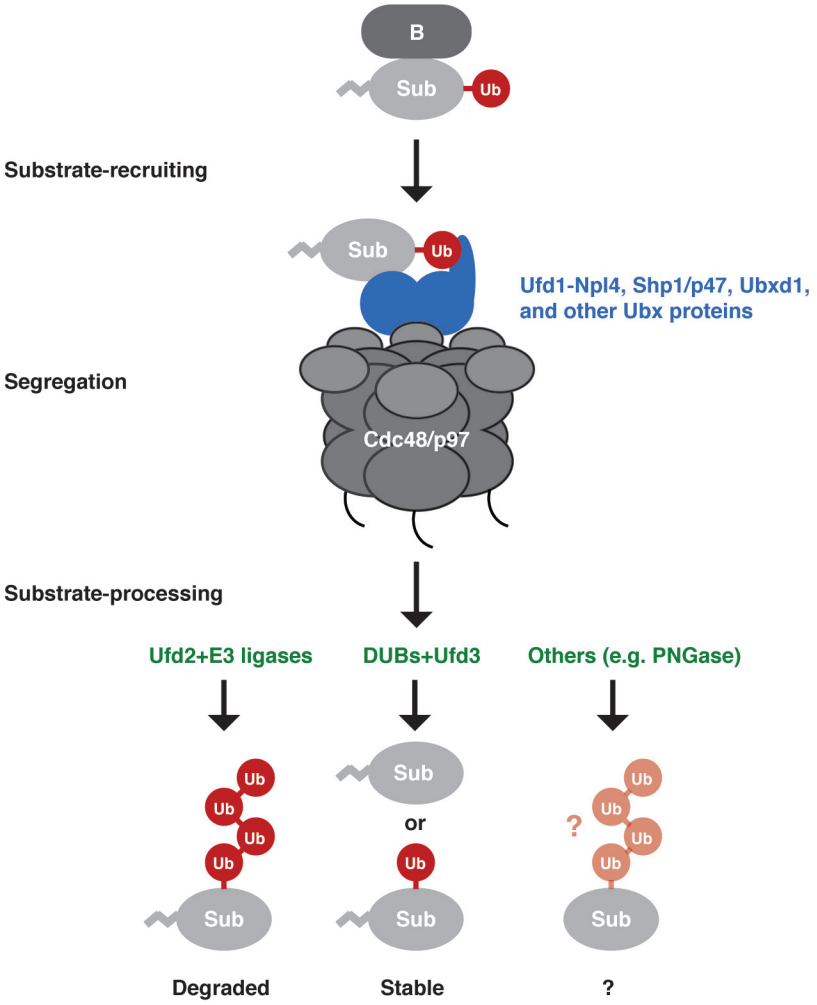

Figure 5: Functional Classification of Cdc48/97 Co-factors.
Cdc48/p97 co-factors can be functionally grouped in substrate-recruiting (blue) and substrate-processing co-factors (green). Substrate-recruiting co-factors target Cdc48/p97 to substrate proteins (Sub), which are typically modified with ubiquitin (Ub) and are engaged in environments (B) such as protein-protein complexes or membranes. The major substrate-recruiting co-factors are Ufd1-Npl4 and Shp1/p47, which bind Cdc48 in a mutually exclusive manner. In mammalian cells the co-factor Ubxd1 has been described as a third substrate-recruiting co-factor. Moreover, other members of the UBX protein family have been linked to substrate recruitment. Notably, some UBX proteins are not sufficient for substrate recruitment, but rather facilitate substrate binding by major substrate-recruiting co-factors.
Substrate-processing co-factors of Cdc48/p97 usually determine the fate of substrates by modulating their ubiquitylation status. Substrates are released as poly- (left), mono- (middle, bottom), or deubiquitylated (middle, top) proteins from Cdc48/p97. Whereas polyubiquitylated proteins are typically subjected to proteasomal degradation, mono- or deubiquitylated proteins remain stable. Some substrate-processing co-factors (referred to as others) do probably not influence the ubiquitylation status of Cdc48/p97 substrates but rather process substrate proteins by different means (right). One example for this class of substrate-processing co-factor is the mammalian PNGase.

1.3.4 Cellular Functions of Cdc48/p97

Cdc48/p97 has been implicated in numerous cellular functions (see Figure 6). In this section the most important functions and substrates of Cdc48/p97 will be discussed (chromatin-related functions will be discussed separately in 1.3.5).

The most intensively studied function of Cdc48/p97 is its role in endoplasmic reticulum-associated degradation (ERAD). By proteasomal clearance of misfolded or damaged proteins from the endoplasmic reticulum (ER), ERAD ensures ER integrity[75,107]. Notably, degradation of ERAD substrates does not take place in the ER lumen, but at the cytosolic face of the ER membrane. By its ATP-dependent segregase activity, Cdc48/p97 drives the dislocation of ERAD substrates from the ER lumen to the cytosolic face of the ER membrane[108-110]. Targeting of Cdc48/p97 to the ER and its ERAD substrates is mediated by Ufd1-Npl4 together with the ER membrane located co-factor Ubx2 (Ubxd8 in humans)[91,98]. In addition to its role in substrate recruitment, Ubx2 also couples Cdc48/p97 to the ERAD ubiquitin ligases Hrd1 and Doa10, as well as to the putative retrotranslocation pore component Der1[91]. Thereby, Ubx2/Ubxd8 spaciously links ubiquitylation of ERAD substrates to their recognition by Cdc48/p97. Cdc48/p97 not only dislocates proteins to the cytosolic face of the ER membrane, but also promotes their subsequent proteasomal degradation. The E4 ubiquitin ligase Ufd2 triggers polyubiquitylation of ERAD substrates, which are subsequently escorted to the proteasome by the Ufd2-associated ubiquitin receptors Rad23 and Dsk2[102].

Cdc48/p97 also plays a critical role in protein quality control in the cytosol and mitochondria, although it has been much less intensively studied than ERAD[101]. In the cytosol Cdc48/p97 has been linked to the ribosome-associated quality control pathway and the disassembly of protein aggregates[101,111,112]. The ribosomal quality control pathway triggers ubiquitylation and subsequent proteasomal degradation of aberrant nascent chains[111,112]. Recent evidence suggests that Cdc48/p97$^{Ufd1\text{-}Npl4}$ extracts defective nascent chains from ribosomes in a ubiquitin-dependent manner[111,112]. Moreover, Cdc48/p97 has been implicated in disassembly and degradation of cytosolic protein aggregates[113-115]. First, Cdc48/p97 physically interacts and co-localises with different types of protein aggregates[114,115]. Second, Cdc48/p97 appears to be genetically important to deal with toxic protein aggregates[113-115].

In contrast to the ER, mitochondria have internal proteolytic machineries to eliminate aberrant proteins[116]. Nevertheless, some proteins of the outer mitochondrial membrane are subjected to proteasomal degradation in a pathway that has been termed

mitochondria-associated protein degradation[116,117]. Recent evidence points to a critical role of Cdc48/p97 in extracting proteins from the outer mitochondrial membrane[118,119]. A controversially discussed study proposed that the conserved Cdc48/p97 co-factor Vms1 forms a heterodimer with Npl4 (excluding Ufd1) that acts as a mitochondria-specific substrate-recruiting co-factor[118].

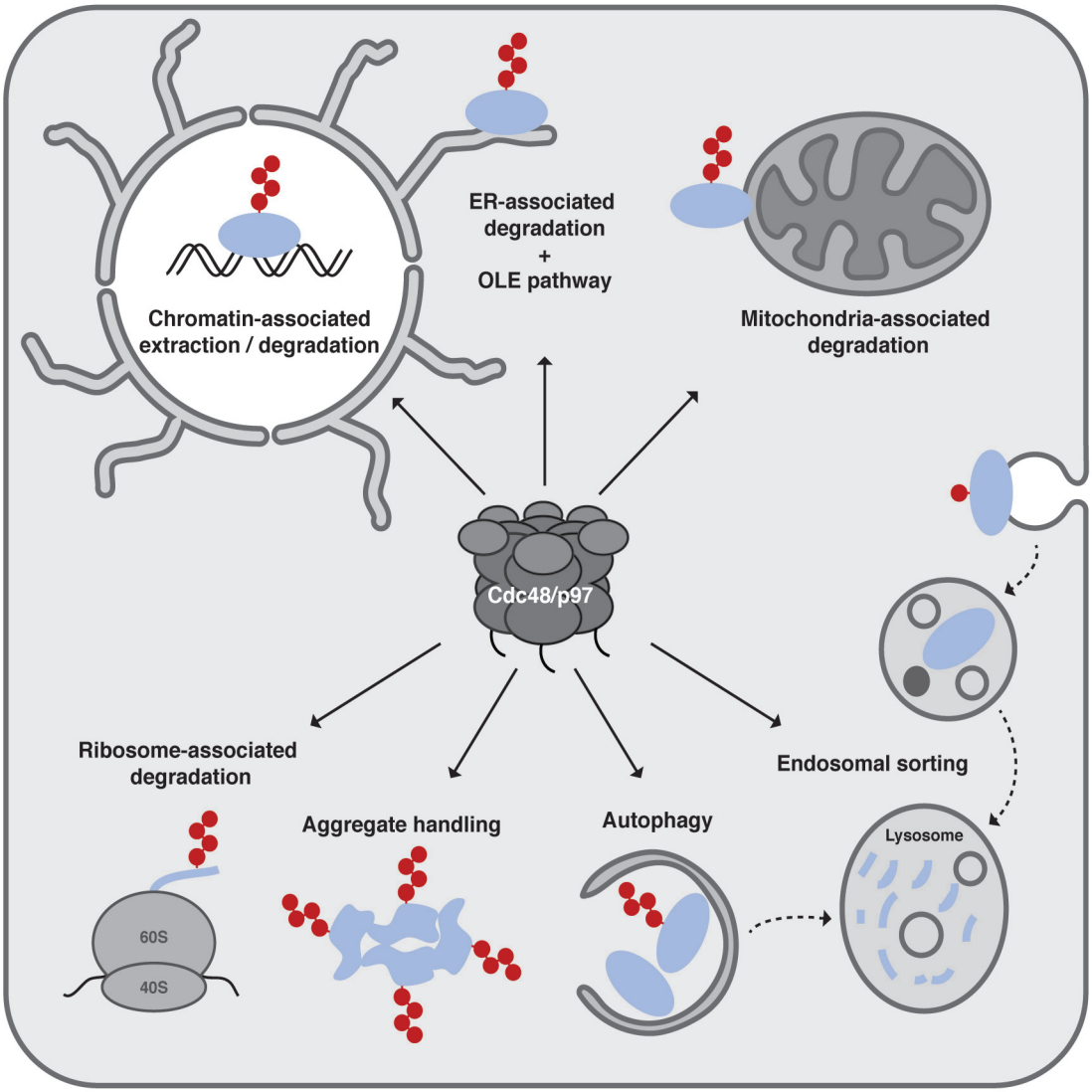

Figure 6: Schematic View of Cellular Cdc48/p97 Functions.
Cdc48/p97 is an essential protein that has been implicated in various cellular functions such as chromatin-associated extraction/degradation, ER-associated degradation, the OLE pathway, mitochondria-associated degradation, endosomal sorting, autophagy, the ribosome-associated degradation and the handling of protein aggregates. Cdc48/p97 substrates that are typically modified by ubiquitin (red) are depicted in blue.

In addition to its importance in protein quality control, Cdc48/p97 regulates the abundance of the ER-associated fatty acid desaturase Ole1 (OLE pathway)[109,120,121]. Ole1 is an essential component in synthesis of unsaturated fatty acids in yeast. The expression level

of Ole1 is tightly controlled by ERAD[109] and transcriptional regulation[120,122]. The transcription of *OLE1* is regulated by the transcription factor Spt23 (and its homologue Mga2), which is anchored to the ER membrane in its inactive precursor state (called p120). A shortage of unsaturated fatty acids triggers Spt23 dimerisation at the ER membrane that promotes monoubiquitylation of one p120 subunit per dimer (probably by a stochastic mechanism)[120]. Monoubiquitylated p120 is subsequently processed by the 26S proteasome in order to remove the Spt23 ER membrane anchor[122]. The amino-terminal fragment of Spt23 (called p90) is spared from degradation, but remains tethered to the ER membrane due to its tight interaction with a p120 partner molecule[120]. To liberate p90 from this complex, the ATP-dependent segregase activity of Cdc48 is required[120]. Cdc48 is targeted to monoubiquitylated p90 by its substrate-recruiting co-factor Ufd1-Npl4[120]. After mobilization from the ER membrane, p90 enters the nucleus and activates *OLE1* transcription[120]. Intriguingly, Cdc48 is not only involved in initiation but also termination of *OLE1* transcription. Nuclear p90 is degraded in an at least partially Cdc48-dependent manner[102]. Similar to ERAD substrates, p90 is polyubiquitylated by Ufd2 and escorted to the proteasome by the ubiquitin receptors Rad23 and Dsk2[102].

In ERAD and the OLE pathway Cdc48/p97 is tightly linked to proteasomal degradation and processing, respectively. However, Cdc48/p97 also facilitates lysosomal protein degradation (in yeast vacuolar protein degradation) by the autophagy pathway[100]. In *S. cerevisiae* it has been demonstrated that several autophagy pathways depend on Cdc48 function[77,100,105]. These studies suggested that Shp1 (binds Cdc48 mutually exclusive with Ufd1-Npl4) is the substrate-recruiting co-factor in Cdc48/p97-dependent autophagy pathways[77,100]. Notably, Shp1 targets Cdc48 to the ubiquitin-like modifier Atg8, which is conjugated to the lipid phosphatidylethanolamine (PE) in order to trigger autophagy induction[77]. Based on this finding it has been speculated that Atg8-PE is the respective Cdc48 substrate in the autophagy pathway[75,77]. In addition to Shp1, the Cdc48 co-factors Ubp3 and Ufd3 are involved in at least some autophagy pathways in yeast[105].

In mammalian cells Cdc48/p97 has recently been implicated in endocytosis (in particular in endosomal sorting), another pathway that often results in lysosomal protein degradation[99-101]. Several lines of evidence support that p97 targets the ubiquitylated plasma membrane protein Caveolin-1, a component of a specialised endocytosis pathway[99]. Intriguingly, this pathway appears to be independent of the two major substrate-recruiting co-factors Ufd1-Npl4 and p47, but involves the mammalian-specific co-factor Ubxd1[99]. Thus, this study suggests that p97 and Ubxd1 form a third functionally distinct p97 core complex that regulates endosomal trafficking[101,123].

1.3.5 Chromatin-related Functions of Cdc48/p97

As described above Cdc48/p97 has important functions at different cellular compartments. In the last years Cdc48/p97 has particularly been implicated in chromatin-related processes such as mitosis, DNA replication, transcriptional regulation, and the DNA damage response[124]. These findings highlight a crucial role of Cdc48/p97 in modulating chromatin-association and activity of typically ubiquitylated chromatin proteins.

The first identified chromatin substrate of Cdc48/p97 is the Aurora B kinase (Ipl1 in *S. cerevisiae*), which triggers nuclear envelope formation and chromatin decondensation in late mitosis[125]. A series of experiments using *Xenopus laevis* egg extracts showed that $p97^{Ufd1\text{-}Npl4}$ removes ubiquitylated Aurora B kinase from chromatin at the exit of mitosis. Notably, Aurora B kinase remains stable upon chromatin extraction, thus suggesting that it is not targeted for proteasomal degradation by p97. However, protein degradation might not be required for Aurora B kinase inactivation, because its kinase activity is strongly stimulated by chromatin binding[125].

Cdc48/p97 function has also been tightly linked to DNA replication, a second cell cycle progression-related pathway[126]. Two recent studies demonstrated that Cdc48/p97 (together with Ufd1-Npl4) segregates the replication licensing factor Cdt1 from chromatin[127,128]. As a component of the pre-replication complex, Cdt1 licenses replication origins in the G1 phase[129]. To ensure that DNA is only replicated once per cell cycle, Cdt1 protein levels are tightly regulated by proteasomal degradation in almost all eukaryotes (but not in *S. cerevisiae*)[130]. Efficient degradation requires chromatin extraction of ubiquitylated Cdt1 by Cdc48/p97. Notably, Cdt1 is not only degraded during cell cycle progression but also after DNA damage[127,131]. DNA damage-induced Cdt1 degradation avoids replication of damaged DNA and also depends on $Cdc48/p97^{Ufd1\text{-}Npl4}$ function[127].

Notably, Cdc48/p97 has a much broader role in the DNA damage response than only mobilising Cdt1 for proteasomal degradation[123,124]. This broad role is particularly stressed by the DNA damaging agent sensitivity of organisms and cells impaired in Cdc48/p97 function[76,132,133].

A series of studies highlighted an important function of Cdc48/p97 in DNA double-strand break (DSB) repair[76,132,133]. In mammalian cells the ubiquitin ligases RNF8 and RNF168 (in an RNF8-dependent manner) are recruited to DSBs, where they assemble transient K48-linked and persistent K63-linked ubiquitin chains[132,134]. These ubiquitin chains facilitate protein degradation and the recruitment of repair factors, respectively[132,134]. RNF8-dependent ubiquitylation recruits p97 in complex with its

ubiquitin-binding co-factor Ufd1-Npl4 to DSBs[132]. Inhibition of $p97^{Ufd1\text{-}Npl4}$ function results in prolonged accumulation of K48-linked ubiquitin chains, but does not affect the level of K63-linked ubiquitin conjugates[132]. This finding suggests that $p97^{Ufd1\text{-}Npl4}$ extracts K48-ubiquitylated proteins from chromatin and subsequently targets them for proteasomal degradation. One of the proteins that are subjected to proteasomal degradation upon DNA damage in a $p97^{Ufd1\text{-}Npl4}$-dependent manner is the tumour suppressor L3MBTL1[133]. Notably, L3MBTL1 binds the histone H4 lysine-20 dimethylation mark ($H4K20me_2$) that is also recognised by the DSB repair factor 53BP1[135,136]. In line with a model that L3MBTL1 and 53BP1 compete for $H4K20me_2$ marks, L3MBTL1 gets extracted and targeted for proteasomal degradation after DSB induction, whereas 53BP1 simultaneously accumulates at DSB sites[124]. A competition between 53BP1 and L3MBTL1 could explain why $p97^{Ufd1\text{-}Npl4}$ function is crucial for efficient DSB recruitment of 53BP1 and other DNA repair factors like BRCA1 and Rad51, although it does not affect DSB-induced K63-linked ubiquitin chains[124,132,133].

Very recently an additional function of Cdc48/p97 in DSB repair (by homologous recombination) has been described[76]. Using its segregase activity Cdc48/p97 curbs the physical interaction between the homologous recombination factors Rad52 and Rad51[76]. Intriguingly, Cdc48/p97 is targeted to the Rad52-Rad51 complex not by ubiquitylation but SUMOylation of Rad52. In *S. cerevisiae* SUMOylated Rad52 is recognised by a carboxy-terminal SUMO-interacting motif (SIM) of Ufd1[76,96]. Interfering with Ufd1-SUMO interaction or Cdc48/p97 function results in abnormal Rad51 foci and an increased spontaneous recombination rate[76]. Despite the fact that in mammalian cells Rad51 loading depends more on BRCA2 than Rad52, p97 depletion in human cell lines also induces abnormal Rad51 assemblies that depend on Rad52 function[76]. Accordingly, the function of Cdc48/p97 in counterbalancing Rad52 activity is conserved from yeast to humans[76]. Although it is not yet clear if Cdc48/p97 acts on the chromatin-associated or free Rad52-Rad51 complex, its segregase activity is crucial to avoid abnormal Rad51 filaments.

Cdc48/p97 functions in DNA repair have been recently expanded to stalled replication forks[137-139]. Several studies suggest that the p97 co-factor Dvc1 (also referred to as Spartan or C1orf124) targets p97 to laser induced DNA damage tracks[137-139]. Dvc1 (predicted to be a protease) appears to be recruited by monoubiquitylated PCNA that triggers translesion synthesis (TLS). Therefore it has been speculated that p97 together with Dvc1 extracts translesion DNA-polymerases in a ubiquitin-dependent manner[123].

In addition to DNA repair, transcription is another pathway in which Cdc48/p97 regulates DNA-protein interactions[124]. A study in *S. cerevisiae* revealed a function of

$Cdc48^{Ufd1\text{-}Npl4}$ in chromatin extraction of the transcriptional inhibitor Matα2 that represses mating type a (*MATa*) specific genes[140]. To facilitate α-to-a mating type switch, Matα2 is rapidly inactivated by Cdc48-dependent chromatin extraction and proteasomal degradation[140,141]. To date, Matα2 is the only described example for a transcriptional regulator that is extracted from chromatin in a Cdc48/p97-dependent manner. However, many other transcription regulators are also ubiquitylated and targeted for proteasomal degradation. Therefore it is attractive to assume that Cdc48/p97 also extracts other transcription regulators from chromatin[140].

Intriguingly, Cdc48/p97 does not only modulate expression of single genes by extraction of transcriptional regulators, but also affects transcription by targeting irreversibly stalled RNA-polymerase II (RNA Pol II) for proteasomal degradation[142]. Bulky DNA lesions (e.g. induced by UV-light) and other transcriptional obstacles cause RNA Pol II stalling, which is typically repaired by transcription-coupled DNA repair (TCR) or polymerase backtracking[143]. If these repair pathways fail, RNA Pol II is cleared from chromatin by the proteasomal degradation of its largest subunit Rpb1[144,145]. Efficient degradation of Rpb1 requires its previous segregation from chromatin by Cdc48/p97. In addition to Cdc48, its co-factors Ufd1-Npl4, Ubx4, and Ubx5 are involved in Rpb1 degradation[142].

Collectively, Cdc48/p97 has been implicated in a large variety of chromatin-associated pathways. In all these pathways the extraction of its ubiquitylated or SUMOylated substrates from chromatin and chromatin-associated protein assemblies is the crucial Cdc48/p97 function[76,124]. Interestingly, the segregation of all currently reported chromatin substrates involves the substrate-recruiting co-factor Ufd1-Npl4, which might represent a general component of the Cdc48/p97 chromatin extraction pathway[101,123,124]. In line with other cellular functions of Cdc48/p97, chromatin extraction by Cdc48/p97 is not always coupled to proteasomal degradation. Therefore Cdc48/p97 chromatin functions can be discriminated in chromatin-associated protein extraction and degradation[101,124].

2 Aims of this Study

Cdc48/p97 is a critical component of the ubiquitin system and typically segregates ubiquitylated proteins from their partner environments such as membranes or protein-protein complexes[73,101]. Recent studies have expanded the substrate spectra of Cdc48/p97 to ubiquitylated chromatin proteins, such as the aurora B kinase[125], the mammalian replication regulator Cdt1[127,128], the largest subunit of RNA polymerase II Rpb1[142], or the transcriptional repressor Matα2[140] (see 1.3.5.). However, despite the identification of individual Cdc48/p97 substrates on chromatin, it sill remains unclear whether Cdc48-dependent chromatin extraction affects also other proteins and might be of global importance to regulate chromatin-association of ubiquitylated proteins. In addition, it has not been investigated systematically if Cdc48/p97-dependent chromatin extraction usually involves a specific set of Cdc48/p97 co-factors.

To address these questions, the first aim of this study was to establish a method that enables monitoring of the relative abundance of ubiquitylated proteins on chromatin in a genome-wide manner using *S. cerevisiae* cells. The method of choice was ubiquitin-directed chromatin immunoprecipitation in combination with genome-wide tiling microarrays (Ub-ChIP-chip). Using this method I not only expected to monitor the relative genome-wide distribution of ubiquitin conjugates in wild-type *(WT)* cells for the first time, but also hoped to answer the question if Cdc48-dependent chromatin extraction is globally important to regulate chromatin distribution of ubiquitylated proteins. In particular, a major aim was to identify genomic positions at which ubiquitylated proteins accumulate in Cdc48-deficient cells compared to *WT* cells. On the one hand, such genomic positions would provide a powerful tool to investigate which Cdc48 co-factors are mechanistically important for the process of chromatin extraction. On the other hand, detailed analysis of these genomic regions could lead to the identification of novel Cdc48 substrates and might reveal novel functions of Cdc48-dependent chromatin extraction.

3 Results

3.1 Genome-wide Monitoring of Chromatin-associated Ubiquitin Conjugates by Chromatin Immunoprecipitation

Many chromatin-bound proteins are modified by ubiquitin, but the distribution of ubiquitin conjugates on chromatin, as well as the impact of ubiquitin-dependent chromatin extraction by Cdc48/p97 on this distribution, has not been studied. To monitor the genome-wide distribution of ubiquitylated proteins on DNA, I established chromatin immunoprecipitation (ChIP) of ubiquitin for the first time. Feasibility of ubiquitin-directed ChIP required an antibody that efficiently immunoprecipitates formaldehyde-fixed ubiquitin conjugates under partially denaturing conditions. Among all commercially available anti-ubiquitin antibodies, the FK2 antibody (Millipore) appeared best suited to specifically monitor ubiquitylated chromatin proteins, because it recognises mono- and polyubiquitylated (different linkage types) proteins but not free ubiquitin[146]. To test the feasibility of ChIP using the FK2 anti-ubiquitin antibody (FK2-Ub-ChIP), FK2-Ub-ChIP material from *S. cerevisiae* was analysed for ubiquitin content by western blotting (ChIP-Western). The ChIP-Western experiment demonstrated that the FK2 anti-ubiquitin antibody but not an unspecific IgG efficiently pulls down ubiquitylated proteins in ChIP assays (see Figure 7A).

To identify genomic positions that are enriched in ubiquitylated proteins in a genome-wide manner, FK2-Ub-ChIP was combined with DNA hybridisation to genome-wide tiling microarrays (referred to as FK2-Ub-ChIP-chip). Notably, FK2-Ub-ChIP-chip experiments using wild-type *(WT) S. cerevisiae* cells demonstrated that ubiquitin conjugates are not equally distributed on chromatin, but are enriched at many genomic positions (see Figure 7B). Strikingly, almost all of these genomic positions overlap with a subset of open reading frames (ORFs) that has been previously linked to monoubiquitylation of the histone H2B on lysine-123 (H2B-Ub)[147]. To test whether H2B-Ub indeed causes the observed enrichment of ubiquitin conjugates at these genomic loci, FK2-Ub-ChIP-chip was performed with yeast cells that were either deleted for the E2 enzyme responsible for H2B-Ub (*rad6Δ*) or mutated in the ubiquitin attachment site of H2B *(h2B-K123R)*. Importantly, interference with H2B ubiquitylation abolished enrichment of ubiquitin conjugates at almost all genomic positions (see a representative region on chromosome III in Figure 7B), indicating that H2B-Ub is indeed the cause of the observed ubiquitin enrichment. Given that H2B is very abundant and that up to 10% of the steady-

state H2B levels are ubiquitylated in yeast[148], this finding suggests that H2B monoubiquitylation is by far the most prominent ubiquitylation event on chromatin in yeast.

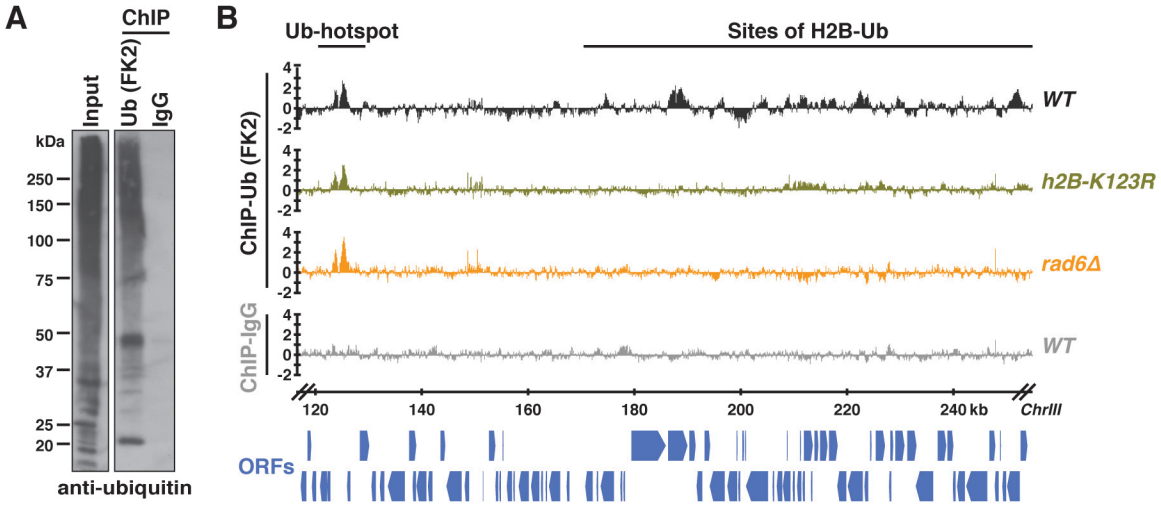

Figure 7: Genome-wide Monitoring of Chromatin-associated Ubiquitin Conjugates.
(A) The anti-ubiquitin antibody FK2 efficiently pulls down ubiquitylated proteins in chromatin immunoprecipitation (ChIP) experiments. ChIPs from *WT* yeast cells using FK2 anti-ubiquitin antibody (Millipore) or unspecific murine IgG1 (Bethyl Laboratories Inc.) were analysed by western blotting (ChIP-Western) with anti-ubiquitin antibody (P4D1, Santa Cruz). The left panel shows ubiquitin levels in the input material.
(B) ChIP-chip experiments using the anti-ubiquitin FK2 antibody indicate that monoubiquitylation of histone H2B (H2B-Ub) is the most abundant ubiquitin conjugate on chromatin. In addition, ubiquitylation hotspots (Ub-hotpots) that are also present in H2B-Ub-deficient cells (*h2B-K123R* and *rad6Δ*) were identified. Shown are FK2-ChIP-chip profiles of a representative region of chromosome III *(ChrIII)* that contains several H2B-Ub-dependent (right) and one H2B-Ub-independent (left) Ub-hotspots. A ChIP-chip experiment (from *WT* cells) using an unspecific rabbit IgG antibody is depicted as control. ChIP signals are plotted as $\log_2$ values of the IP/Input ratios. All experiments except the FK2-Ub-ChIP from *rad6Δ* cells and the IgG control (only performed once) represent the mean of two independent experiments, which include a hybridisation dye swap (for details see 5.3.2). Blue arrows (bottom) indicate the genomic positions of open reading frames (ORFs) in the presented region of ChrIII. Genes are grouped in two rows depending on the respective coding strands.

Intriguingly, ubiquitin conjugate accumulation at a small number of genomic loci (subsequently referred to as ubiquitylation hotspots) was unaffected by genetic interference with H2B ubiquitylation (see an example on chromosome III in Figure 7B), suggesting a high density of other ubiquitylated proteins at these positions. In *h2b-K123R* cells, 4 high-enrichment† and 14 low-enrichment‡ ubiquitylation hotspots (Ub-hotspots), which were absent in the IgG control experiment, could be identified. All 4 high-enrichment as well as 4 of the low-enrichment Ub-hotpots were also detected in *rad6Δ* cells.

† ChIP-chip signal of several neighbouring oligonucleotides above 1
‡ ChIP-chip signal of several neighbouring oligonucleotides above 0.8

3.2 Identification of Cdc48-dependent Ub-hotspots

Detection of Ub-hotspots and H2B-Ub sites by FK2-Ub-ChIP-chip demonstrated that this method effectively monitors chromatin distribution of ubiquitylated proteins. Given the exemplary evidence that Cdc48 acts on ubiquitylated proteins on chromatin[124], we next addressed if Cdc48 plays a general role in regulating the abundance and distribution of ubiquitylated proteins on chromatin. To this end, FK2-Ub-ChIP-chip in a temperature-sensitive *CDC48* mutant *(cdc48-6)* that is impaired in Cdc48 function was performed. Intriguingly, this experiment revealed that the chromatin distribution of ubiquitin conjugates is dramatically altered in *cdc48-6* cells (see Figure 8A and Figure 9A).

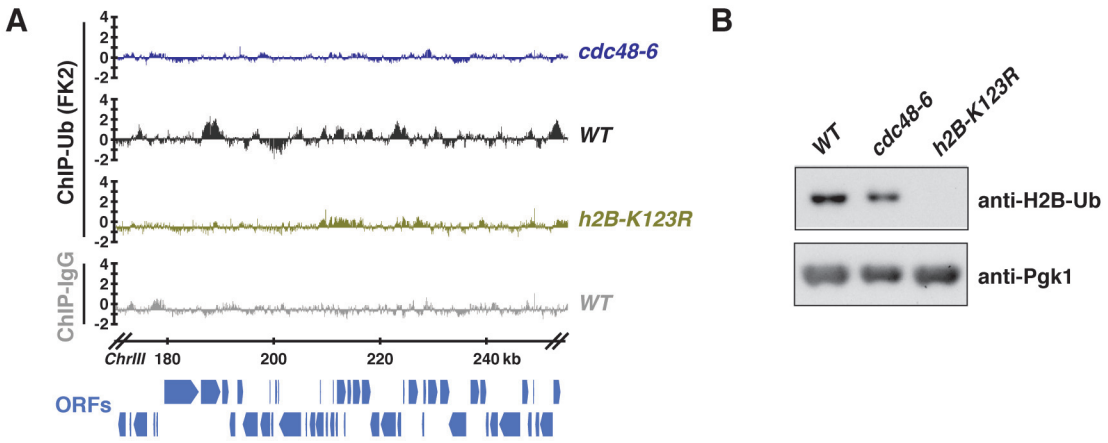

Figure 8: Ubiquitin Enrichment Pattern Is Flattened at Sites of H2B Monoubiquitylation in *cdc48-6* Cells.
(A) Relative enrichment pattern of ubiquitin conjugates is flattened at sites of H2B monoubiquitylation (H2B-Ub) in cells that are impaired in Cdc48 function *(cdc48-6)*. Shown are FK2-ChIP-chip profiles of a representative region on chromosome III *(ChrIII)* that contains several areas with increased abundance of monoubiquitylated H2B in *WT* cells. A ChIP-chip experiment (from *WT* cells) using an unspecific rabbit IgG antibody is presented as control. ChIP-chip signals are depicted as normalised $\log_2$ values of the IP/Input ratios. Notably, all profiles except for the FK2-Ub-ChIP-chip profile from *cdc48-6* cells (which represents the mean of two independent experiments, including a dye swap) are identical with the profiles presented in Figure 7B. Blue arrows (bottom) indicate the genomic positions of open reading frames (ORFs) in the presented region of *ChrIII*. Genes are grouped in two rows depending on the respective coding strands.
(B) Steady-state levels of monoubiquitylated H2B (H2B-Ub) are only mildly reduced in *cdc48-6* cells. Western blot analysis was performed with whole cell extracts (WCEs) from *WT* and *cdc48-6* cells using an H2B-Ub-directed antibody. The specificity of the H2B-Ub-specific antibody was verified by simultaneous western blotting of a WCE isolated from a mutant yeast strain, which is impaired in H2B-Ub *(h2B-K123R)*. Equal loading of samples was verified by Pgk1-directed western blotting.

First, in *cdc48-6* cells the relative enrichment pattern of ubiquitylated proteins is flattened at sites of H2B-Ub (see Figure 8A). Given that ChIP-chip signals are depicted as relative fold change to the genome-wide average (ChIP-chip signal of 0), the relative loss of ubiquitin enrichment at H2B-Ub sites in *cdc48-6* cells could result either from defects in

H2B-Ub, or from a global increase in steady-state ubiquitylation levels at chromatin. As verified by western blotting with an H2B-Ub-specific antibody, cellular levels of H2B-Ub are only mildly reduced in *cdc48-6* cells (see Figure 8B). Therefore it appears more likely that the changes in the FK2-Ub-ChIP-chip pattern of *cdc48-6* cells mainly result from a global increase in steady-state chromatin ubiquitylation levels due to impaired chromatin extraction by Cdc48.

Second, and even more strikingly, in *cdc48-6* cells ubiquitylation levels dramatically increase at a very limited number of 9 genomic positions that are distributed to only 5 chromosomes (see Figure 9A). Intriguingly, 8 of these 9 positions overlap with the Ub-hotspots (including all 4 high-enrichment Ub-hotspots and all 4 low-enrichment Ub-hotspots that were identified in *h2B-K123R* as well as *rad6Δ* cells) that appear to be the major sites of H2B-Ub-independent chromatin ubiquitylation in *WT*, *h2B-K123R*, and *rad6Δ* cells (see 3.1). The increase in FK2-Ub-ChIP-chip signal indicates that ubiquitylated proteins accumulate at these loci (referred to as Cdc48-dependent Ub-hotspots in the following) in Cdc48-deficient cells, most likely because they are not efficiently extracted from chromatin. Ubiquitin conjugates do not accumulate to the same extent at all Cdc48-dependent Ub-hotspots, which is, however, also reflected by differences in the ubiquitylation levels in *WT* cells (see Figure 9A). The observed enrichment of ubiquitin conjugates at most of the Cdc48-dependent Ub-hotspots in *WT* cells indicates that ubiquitylation and subsequent extraction are processes that constantly take place under the analysed growth conditions.

The FK2-Ub-ChIP-chip signal of all Cdc48-dependent Ub-hotspots peaks in intergenic regions, but the distance to neighbouring open reading frames varies significantly from only 100 to more than 1000 base pairs (see Figure 9A). Despite the intergenic localisation, the genomic position of the Cdc48-dependent Ub-hotspots does not hint to a particular cellular function, because they do not systematically overlap with other genomic features such as centromeres, replication start sites, or known recombination hotspots.

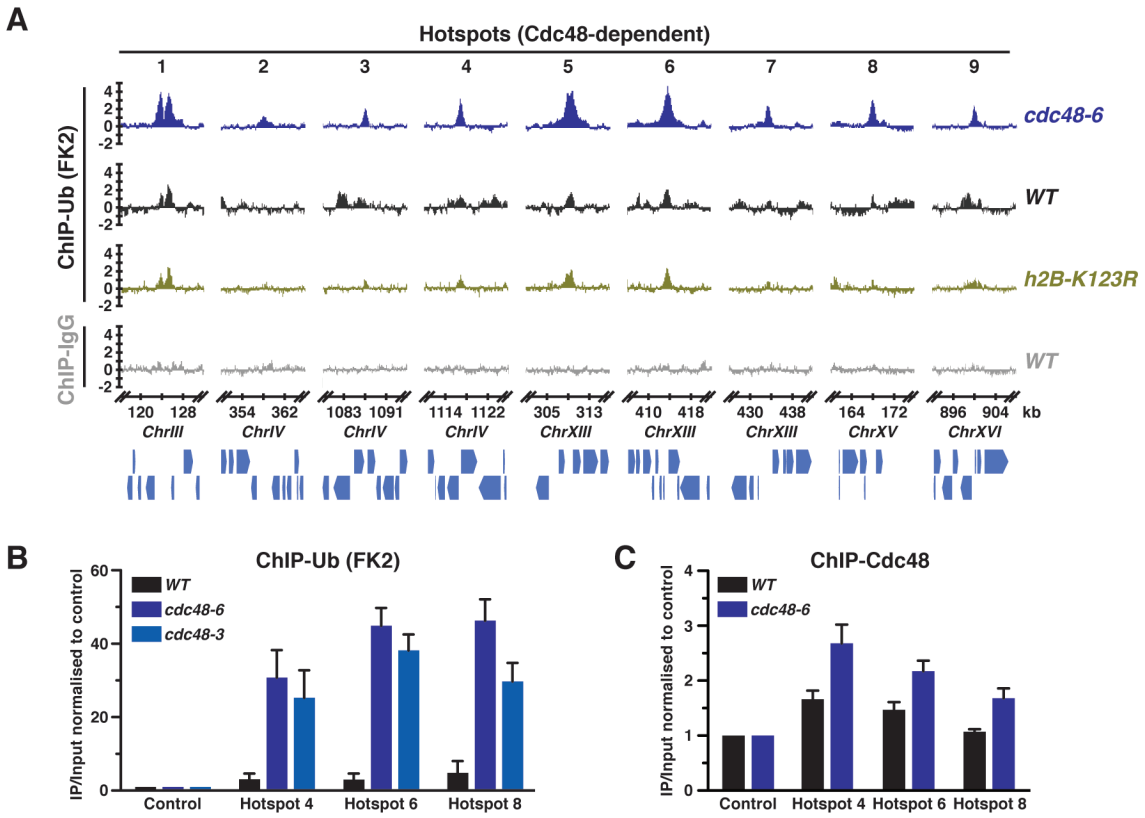

Figure 9: Identification of 9 Cdc48-dependent Ub-hotspots.

(A) Cells with impaired Cdc48 function *(cdc48-6)* accumulate ubiquitin conjugates at 9 genomic loci (Cdc48-dependent Ub-hotspots). Strikingly, 8 of these 9 genomic positions overlap with the previously identified H2B monoubiquitylation-independent Ub-hotspots (see *WT* and *h2B-K123R*). Shown are sections of FK2-ChIP-chip profiles and a control experiment (from *WT* cells) using an unspecific rabbit IgG antibody. ChIP-chip signals are presented as normalised $\log_2$ values of the IP/Input ratios. All profiles except for the IgG control experiment (only performed once) represent the mean of two independent experiments, including a hybridisation dye swap. All profile sections result from the same experiments that are presented in Figure 7 and Figure 8. Blue arrows (bottom) indicate the genomic positions of open reading frames (ORFs) in the presented regions. Genes are grouped in two rows depending on the respective coding strands.

(B) Quantitative Real-Time-PCR (RT-PCR) analysis of FK2-Ub-ChIP experiments (FK2-Ub-ChIP-RT-PCR) confirms the strong accumulation of ubiquitin conjugates at Cdc48-dependent Ub-hotspots in cells that are impaired in Cdc48 function *(cdc48-6 and cdc48-3)*. Ubiquitin enrichments at the indicated Ub-hotspots and a control region on chromosome II are shown. Depicted are the IP/Input ratios that were normalised to the control region (IP/Input at control regions is set to 1). Data represents the mean (and the standard deviation) of three independent experiments.

(C) Cdc48 is enriched at Cdc48-dependent Ub-hotspots. Cdc48-directed ChIP analysed by RT-PCR demonstrates that Cdc48 mildly accumulates at the indicated Cdc48-dependent Ub-hotspots compared to a control region on chromosome II. Cdc48 enrichment at Ub-hotspots is much more pronounced in cells expressing the mutant variant cdc48-6, which interacts with Cdc48 substrates more robustly (substrate-trap)[76,91]. Depicted are the IP/Input ratios that were normalised to the control region (IP/Input at control regions is set to 1). Data represents the mean (and the standard deviation) of three independent experiments.

ChIP-chip is a semi-quantitative method, because it involves whole-genome DNA amplification and microarray hybridisation. To measure the accumulation of ubiquitin conjugates at Cdc48-dependent Ub-hotspots more quantitatively, FK2-Ub-ChIPs were analysed by quantitative Real-Time PCR (RT-PCR), using primer pairs that enabled

detection of selected Ub-hotspots (Hotspots 4, 6, and 8) and an unaffected control region on chromosome II (control). In line with the FK2-Ub-ChIP-chip results, the RT-PCR analysis of FK2-Ub-ChIP experiments (FK2-Ub-ChIP-RT-PCR) confirmed that ubiquitin conjugates are significantly enriched (up to 4.8-fold relative to control) at Cdc48-dependent Ub-hotspots in *WT* cells (see Figure 9B). In *cdc48-6* cells even up to 14.6-fold (compared to *WT*) higher ubiquitin enrichments at Cdc48-dependent Ub-hotpots were detected (see Figure 9B). Importantly, a similar increase in ubiquitin conjugate enrichment compared to *WT* cells was also observed in a second temperature-sensitive *CDC48* mutant (*cdc48-3*; see Figure 9B). Moreover, FK2-Ub-ChIP-RT-PCR analysis confirmed that the extent of ubiquitin enrichment significantly differs between the tested hotspots (see Figure 9B).

A direct function of Cdc48 in segregating ubiquitylated proteins from Cdc48-dependent Ub-hotspots requires Cdc48 interaction with these genomic loci. To test if Cdc48 interacts with Cdc48-dependent Ub-hotspots, ChIP experiments using a Cdc48-specific antibody were performed (see Figure 9C). Indeed, Cdc48 mildly accumulates at the analysed Cdc48-dependent Ub-hotspots (Hotspots 4,6, and 8) compared to a control region (see *WT* in Figure 9C). The mild enrichment was substantially increased in cells that express the mutated cdc48-6 protein (see *cdc48-6* in Figure 9C). Notably, the cdc48-6 protein acts as a “substrate trap”, which is known to bind substrates more robustly[76,91]. The rather mild Cdc48 enrichment at Ub-hotspots, which is predominantly detected in *cdc48-6* cells, indicates a very transient interaction between Cdc48 and the Cdc48-dependent Ub-hotspots. Moreover, cross-linking between DNA and Cdc48 might be particularly difficult, because the DNA interaction is not direct but bridged by the ubiquitylated substrate protein(s). Alternatively, the rather mild Cdc48 enrichment could be explained by a generally high chromatin abundance of Cdc48.

3.3 K48-linked Ubiquitin Chains Accumulate at Cdc48-dependent Ub-hotspots

The dramatic accumulation of ubiquitin conjugates at Cdc48-dependent Ub-hotspots in *CDC48* mutants, and the rather small number of 9 hotspots, suggest an important cellular function of Cdc48 at these genomic positions. As discussed in the introduction, ubiquitylation (in particular K48-linked ubiquitin chains) as well as Cdc48 function are often coupled to proteasomal degradation. To address if ubiquitin conjugates might trigger proteasomal degradation at Cdc48-dependent Ub-hotspots, I next tested if K48-linked

ubiquitin chains accumulate at these genomic positions. To this end ChIP with a monoclonal antibody that is specifically directed against K48-linked ubiquitin chains (Millipore) was established (Figure 10A and data not shown). Indeed, K48-linked ubiquitin chain-directed ChIP experiments demonstrated that K48-linked ubiquitin conjugates strongly accumulate at all tested Cdc48-dependent Ub-hotspots (Hotspots 4,6, and 8) in Cdc48-deficient cells (*cdc48-6* and *cdc48-3*; see Figure 10A). The detected enrichments of K48-linked ubiquitin chains and total ubiquitylated proteins (detected by FK2-Ub-ChIP) are similar (see Figure 9B and Figure 10A). Notably, compared to a control region, K48-linked ubiquitin chains are already mildly enriched in *WT* cells at all analysed Cdc48-dependent Ub-hotspots (see Figure 10A).

ChIP-chip experiments using the K48-linked ubiquitin chain-specific antibody (K48-Ub-ChIP-chip) demonstrated that K48-linked ubiquitin conjugates accumulate at all 9 Cdc48-dependent Ub-hotspots in *cdc48-6* cells (see Figure 10B). Similar to the FK2-Ub-ChIP-chip experiments, the levels of K48-linked ubiquitin chain enrichments differ between the Ub-hotspots, but typically correlate with the intensity of the K48 ubiquitin accumulation in *WT* cells. K48-Ub-ChIP-chip experiments in *WT* cells confirmed that most of the Cdc48-dependent Ub-hotspots are among the genomic loci with the highest K48-linked ubiquitin chain abundance on a genome-wide level. However, in contrast to ubiquitin conjugates that were detected by FK2-Ub-ChIP, K48-linked ubiquitin chains accumulated at numerous additional genomic positions to a similar extent in a Cdc48-independent manner (data not shown).

The high abundance of K48-linked ubiquitin chains at Cdc48-dependent Ub-hotspots suggests that ubiquitylated proteins are extracted by Cdc48 and subsequently subjected to proteasomal degradation. A previous study on proteasome delivery by Cdc48 has proposed that Cdc48 substrates are escorted to the proteasome by a sequential pathway involving the shuttling ubiquitin receptors Rad23 and Dsk2[102]. In line with a sequential pathway, in which Cdc48 acts upstream of the 26S proteasome, K48-linked ubiquitin conjugates at Cdc48-dependent Ub-hotpots accumulated neither in cells that lack Rad23 and Dsk2 (*rad23Δ dsk2Δ*), nor in cells that are impaired in proteasome activity by the deletion of the proteasome assembly chaperone *UMP1* (*ump1Δ*; see Figure 10C). Although this result could also indicate that K48-linked ubiquitin chains do not trigger proteasomal degradation in this particular case, it appears more likely that one or several K48-ubiquitylated proteins are targeted for proteasomal degradation in a Cdc48-dependent manner. Since Cdc48 function is not impaired in *rad23Δ dsk2Δ* and *ump1Δ*

cells, these proteins are probably still effectively extracted from chromatin despite of defects in proteasome delivery and protein degradation.

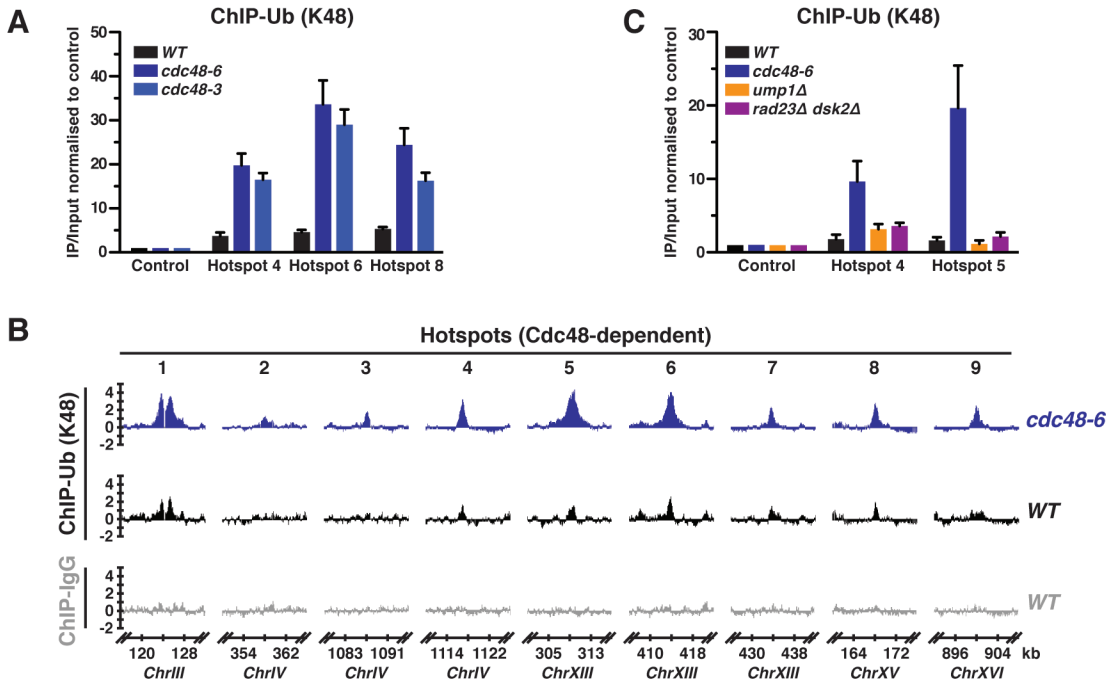

Figure 10: K48-linked Ubiquitin Chains Accumulate at Cdc48-dependent Ub-hotspots.
(A) K48-linked ubiquitin chains accumulate at Cdc48-dependent Ub-hotspots. ChIP-RT-PCR experiments were performed with *WT* and two Cdc48-deficient yeast strains *(cdc48-6 and cdc48-3)* using an antibody that is specifically directed against K48-linked ubiquitin chains. Depicted are IP/Input ratios that were normalised to the control region (IP/Input at control regions is set to 1). Data represents the mean (and the standard deviation) of four independent experiments.
(B) K48-linked ubiquitin chains accumulate at all 9 Cdc48-dependent Ub-hotspots in *cdc48-6* cells. ChIP-chip experiments using a K48-linked ubiquitin chain-specific antibody were performed with *WT* and *cdc48-6* cells. A ChIP-chip experiment (from *WT* cells) using an unspecific rabbit IgG antibody is depicted as control (same control experiment as presented in Figure 9). Shown are sections of ChIP-chip profiles that cover all 9 Cdc48-dependent Ub-hotspots. ChIP-chip signals are presented as normalised $\log_2$ values of the IP/Input ratios. All profiles except for the IgG control experiment (only performed once) represent the mean of two independent experiments, including a hybridisation dye swap.
(C) K48-linked ubiquitin chains accumulate at Cdc48-dependent Ub-hotspots in *cdc48-6* cells but not in cells that are impaired in proteasome delivery (*rad23Δ dsk2Δ*) or activity (*ump1Δ*). Shown are IP/Input ratios normalised to the control region (IP/Input at control regions is set to 1) from K48-Ub-ChIP-RT-PCR experiments using *WT*, *cdc48-6*, *rad23Δ dsk2Δ*, and *ump1Δ* cells. Data represents the mean (and the standard deviation) of three independent experiments. Notably, enrichment of K48-linked ubiquitin chains in both *WT* and *cdc48-6* cells is lower than in Figure 10A, because a different sonication protocol was used (see 5.3.2).

3.4 Cdc48 Function at Cdc48-dependent Ub-hotspots Requires the Cdc48 Co-factors Ufd1-Npl4, Ubx4 and Ubx5

Cdc48 typically interacts with a subset of co-factors that facilitate substrate recruitment and processing. To identify co-factors that are crucial for Cdc48 function on Cdc48-

dependent Ub-hotspots, I addressed how ubiquitylation at Ub-hotpots is affected in cells that are functionally impaired in known Cdc48 co-factors. First, cells expressing mutant variants of the two major substrate-recruiting Cdc48 co-factors Ufd1-Npl4 (*ufd1-2* and *npl4-1*) and Shp1 *(shp1-7)* were analysed by K48-ChIP-RT-PCR (see Figure 11A). At both tested Cdc48-dependent Ub-hotspots, K48-linked ubiquitin conjugates accumulate dramatically in *ufd1-2* and *npl4-1*, but only mildly in *shp1-7* cells (see Figure 11A). In line with previous studies on chromatin substrates of Cdc48 or its mammalian homologue p97[125,127,128,133], this finding suggests that Ufd1-Npl4 is the major substrate-recruiting co-factor that targets Cdc48 to chromatin Ub-hotspots.

In other cellular pathways, such as endoplasmic reticulum-associated protein degradation (ERAD), Ufd1-Npl4 is usually assisted in Cdc48 substrate recruitment by additional co-factors. In particular, some members of the rather poorly characterised UBX protein family have been previously implicated in substrate recruitment[89,91,98]. Interestingly, K48-Ub-ChIP-RT-PCR experiments with yeast cells carrying deletions of individual Ubx protein-encoding genes (*ubx2Δ*, *ubx3Δ*, *ubx4Δ*, *ubx5Δ*, *ubx6Δ*, and *ubx7Δ*) revealed that *ubx4Δ* and *ubx5Δ* mutants accumulate K48-linked ubiquitin chains at two tested Ub-hotspots (Hotspots 4 and 5) to a comparable degree as in *cdc48-6* cells (see Figure 11B). Given that K48-Ub-ChIP measures chromatin abundance of K48-linked ubiquitin conjugates, Ubx4 and Ubx5 appear to be crucial for efficient chromatin extraction by Cdc48 at Ub-hotspots. In contrast to Ubx4 and Ubx5, all other Ubx proteins, as well as the Cdc48 co-factor Vms1 that has been linked to Cdc48 function at mitochondria, do not affect Cdc48-dependent Ub-hotspots (see Figure 11B). Likewise, deletions of genes encoding for the substrate-processing co-factors Ufd2, Ufd3, and Otu1 (*ufd2Δ*, *ufd3Δ*, and *otu1Δ*) do not affect K48-Ub-ChIP-RT-PCR signals compared to *WT* cells (see Figure 11B). However, based on this experiment it cannot be excluded that some of these co-factors are involved in the pathway downstream of chromatin extraction.

To test if all 9 Cdc48-dependent Ub-hotspots depend on the same Cdc48 co-factors, K48-Ub-ChIP-chip experiments in *ufd1-2, ubx4Δ,* and *ubx5Δ* cells were performed (see Figure 11C). Despite small differences in signal intensities, the K48-Ub-ChIP-chip profiles of all three mutant yeast strains strongly resemble the profile in *cdc48-6* cells (see Figure 11C and data not shown). Compared to *WT* cells, K48-linked ubiquitin chains accumulated at all 9 Cdc48-dependent Ub-hotspots in *ufd1-2, ubx4Δ,* and *ubx5Δ* cells (see Figure 11C). This finding strongly suggests that Cdc48 and its co-factors Ufd1-Npl4, Ubx4 and Ubx5 form a complex that specifically targets K48-ubiquitylated chromatin proteins at Cdc48-dependent Ub-hotspots.

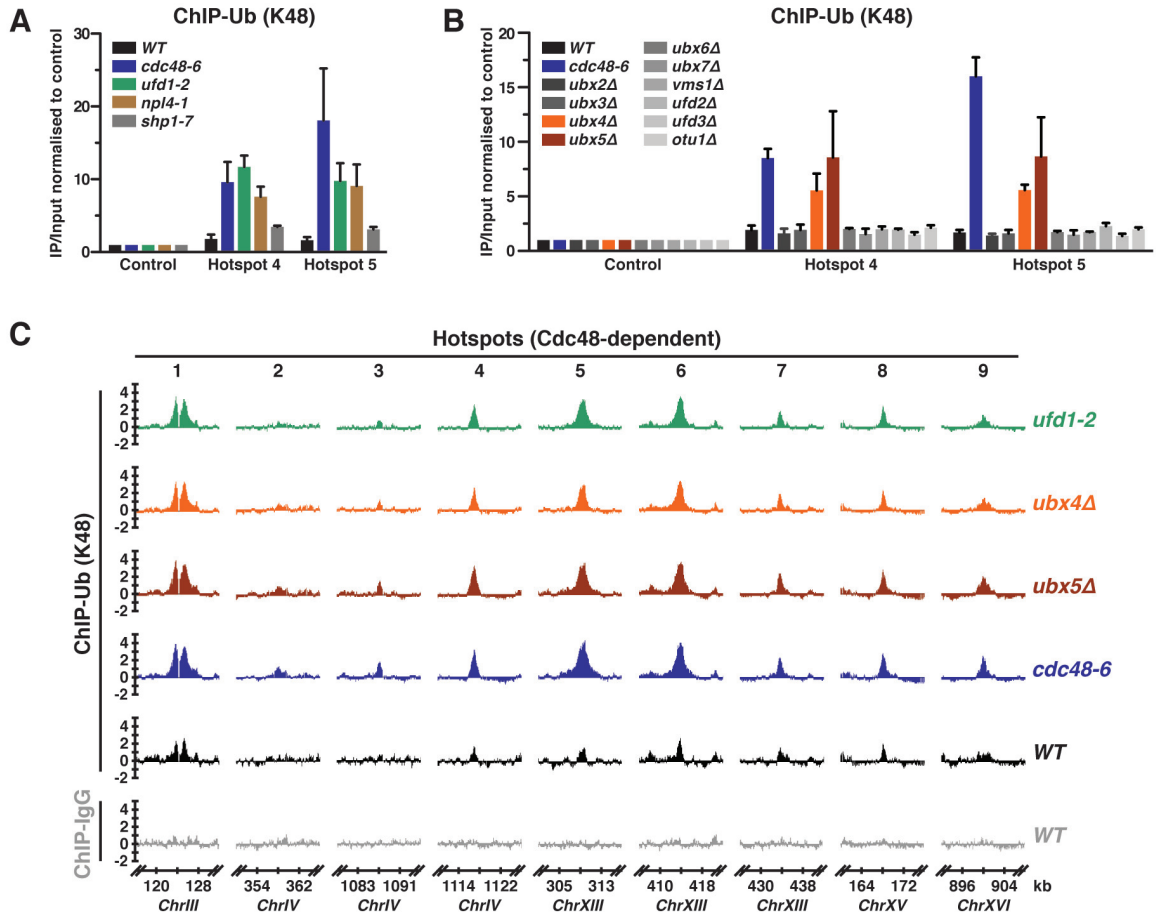

Figure 11: Cdc48-dependent Ub-hotspots Depend on the Cdc48 Co-factors Ufd1-Npl4, Ubx4 and Ubx5.
(A) K48-linked ubiquitin chains accumulate at Cdc48-dependent Ub-hotspots in cells that are impaired in the function of the heterodimeric substrate-recruiting co-factor Ufd1-Npl4 (*ufd1-2* and *npl4-1*). K48-Ub-ChIP-RT-PCR experiments using *WT*, *ufd1-2*, *npl4-1,* and *shp1-7* (cells do not express Shp1 due to the deletion of the translation start site) cells were performed. Shown are IP/Input ratios that were normalised to the control region (IP/Input at control regions is set to 1). Data represents the mean (and the standard deviation) of three independent experiments.
(B) K48-linked ubiquitin chains accumulate at Cdc48-dependent Ub-hotspots in cells lacking the Cdc48 co-factors Ubx4 and Ubx5 (*ubx4Δ* and *ubx5Δ*). In contrast, deletion of other Cdc48 co-factors (*ubx2Δ*, *ubx3Δ*, *ubx6Δ*, *ubx7Δ*, *vms1Δ*, *ufd2Δ*, *ufd3Δ*, and *otu1Δ*) does not affect the enrichment of K48-linked ubiquitin chains at Cdc48-dependent Ub-hotspots. Depicted are IP/Input ratios of K48-Ub-ChIP-RT-PCR experiments that were normalised to the control region (IP/Input at control regions is set to 1). Data represents the mean (and the standard deviation) of three independent experiments.
(C) K48-linked ubiquitin chains accumulate at all 9 Cdc48-dependent Ub-hotspots in cells that are deficient in Cdc48 *(cdc48-6)* and its co-factors Ufd1-Npl4 *(ufd1-2)*, Ubx4 (*ubx4Δ*), and Ubx5 (*ubx5Δ*) compared to *WT* cells. K48-Ub-ChIP-chip experiments were performed with the indicated yeast strains. A ChIP-chip experiment (from *WT* cells) using an unspecific rabbit IgG antibody is depicted as control (same control experiment as presented in Figure 9). Shown are sections of ChIP-chip profiles that cover all 9 Cdc48-dependent Ub-hotspots. ChIP-chip signals are presented as normalised $\log_2$ values of the IP/Input ratios. All profiles except for the IgG control experiment (only performed once) represent the mean of two independent experiments, including a hybridisation dye swap.

3.5 A Short DNA Sequence Motif Is Sufficient for Ectopic Cdc48-dependent Ub-hotspot Formation

The rather limited number of 9 Cdc48-dependent Ub-hotspots and their dependence on the same set of Cdc48 co-factors raised the question if these genomic loci are functionally linked. An attractive idea is that the Cdc48-dependent Ub-hotspots harbour DNA-sequence properties that trigger the accumulation of ubiquitin conjugates at these genomic loci.

To address if the DNA sequence is sufficient to generate a Cdc48-dependent Ub-hotspot, a yeast strain containing an ectopic copy of a DNA sequence segment of Hotspot 5 was generated (see Figure 12A). To this end an integrative plasmid that contained the central DNA sequence segment of Hotspot 5 (*YI128-Hotspot 5*) was targeted to the *leu2-3* loci on chromosome III of *cdc48-6* cells (see Figure 12A). K48-Ub-ChIP-RT-PCR experiments using this strain revealed that the DNA sequence is indeed sufficient to create an ectopic Ub-hotspot (see Figure 12B). In contrast, integration of an empty plasmid (*YI128-empty*) did not increase ubiquitin conjugate abundance (see Figure 12B). Notably, ubiquitin enrichment at the endogenous Hotspot 6 was not affected by integration of the ectopic Ub-hotspot (see Figure 12B). To allow direct comparison between all strains, the accumulation of ubiquitin conjugates at the ectopic positions was measured with the same primer pair (YI128/ectopic Hotspot 5) that amplifies a DNA sequence directly next to the multiple cloning site of the integrative plasmid (see Figure 12A). Due to the shearing of DNA to 250-500 base pairs fragments, this primer pair can be used to indirectly measure the abundance of the Ub-hotspot sequence in the multiple cloning site of the integrative plasmid.

To identify the crucial components of the DNA sequence of Hotspot 5, the DNA sequence was systematically truncated (see Figure 12B and Figure 12C). First, plasmids containing 4 partially overlapping DNA fragments of Hotspot 5 (*YI128* with *F1-F4*; see Figure 12B) were generated and integrated in the *leu2-3* locus of *cdc48-6* cells. Surprisingly, K48-Ub-ChIP-RT-PCR experiments using these yeast strains revealed that three of the truncated DNA fragments were sufficient to trigger Ub-hotspot formation (see Figure 12B). Given that the DNA fragments *F3* and *F4* share a large overlap of 189 base pairs, this finding strongly suggests that the DNA sequence of Hotspot 5 contains at least two independent motifs (in *F1* and the overlap of *F3* and *F4)* that are sufficient to trigger ectopic Ub-hotspot formation.

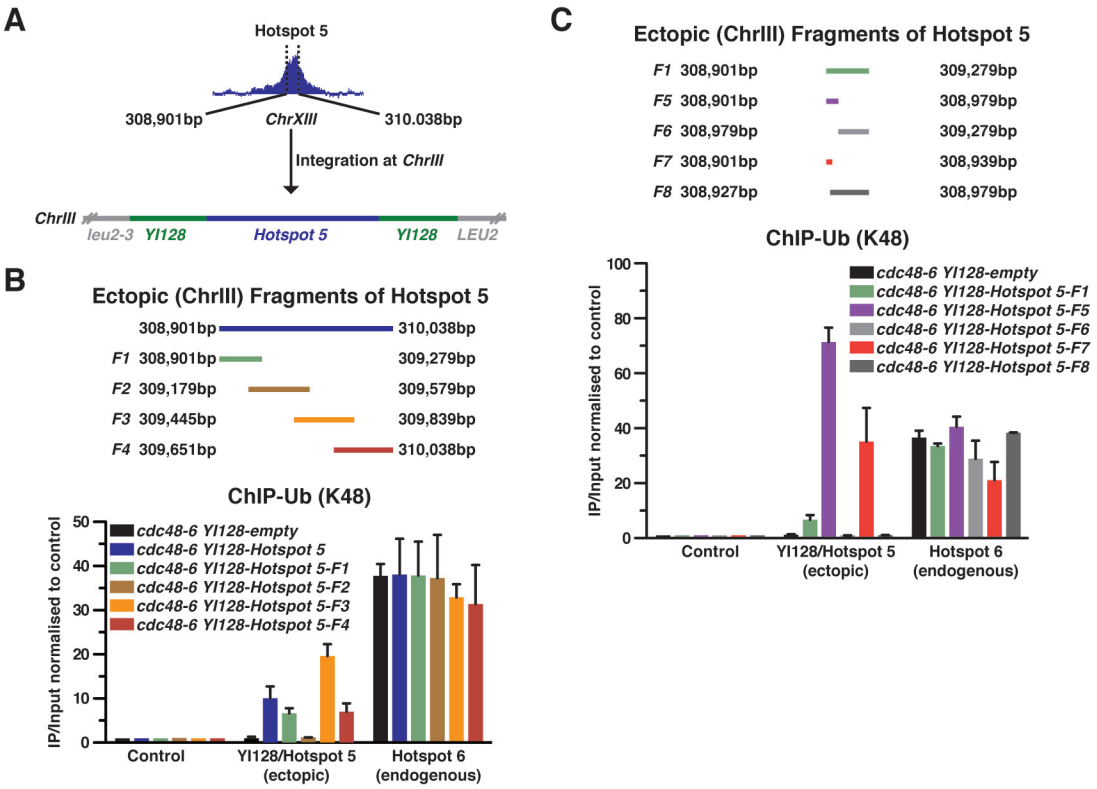

Figure 12: A Short DNA Sequence Motif Is Sufficient for Formation of an Ectopic Cdc48-dependent Ub-hotspot.

(A) Schematic view illustrating the construction of yeast strains (shown is the construction of *cdc48-6 YI128-Hotspot 5* cells) that contain an ectopic Ub-hotspot DNA sequence on chromosome III *(ChrIII)*. A DNA fragment from Hotspot 5 (dashed lines indicate the borders) on chromosome XIII *(ChrXIII)* was cloned in an integrative plasmid (*YI128*) and integrated at the *leu2-3* locus (on *ChrIII)* of *cdc48-6* cells.

(B) DNA sequence fragments of Hotspot 5 are sufficient to trigger ectopic Ub-hotspot formation on chromosome III *(ChrIII)*. Upper panel: Schematic view of the constructed DNA fragments of Hotspot 5 (borders of DNA fragments are indicated by the original genomic positions on chromosome XIII in bp). Lower panel: K48-Ub-ChIP-RT-PCR analysis of yeast strains containing the indicated Hotspot 5 fragments. Relative ubiquitin enrichments at a control region on chromosome II (control), the ectopic Hotspot 5 (YI128/Hotspot 5), and the endogenous Hotspot 6 (Hotspot 6) are depicted. Shown are IP/Input ratios that were normalised to the control region (IP/Input at control regions is set to 1). Data represents the mean (and the standard deviation) of three independent experiments.

(C) Specific DNA fragments of 79 bp *(F5)* and 39 bp *(F7)* are sufficient to trigger ectopic Ub-hotspot formation on chromosome III *(ChrIII)*. Upper panel: Schematic view of the constructed DNA fragments of Hotspot 5 (borders of DNA fragments are indicated by the original genomic position on chromosome XIII in bp) in the same scale as in B. Lower panel: K48-Ub-ChIP-RT-PCR analysis of yeast strains containing the indicated Hotspot 5 fragments. Relative ubiquitin abundance at a control region on chromosome II (control), the ectopic Hotspot 5 (YI128/Hotspot 5), and the endogenous Hotspot 6 (Hotspot 6) are depicted. Shown are IP/Input ratios that were normalised to the control region (IP/Input at control regions is set to 1). Data represents the mean (and the standard deviation) of two independent experiments.

To map one of these motifs precisely, additional fragments of *F1* (*F5-F8*; see Figure 12C) were constructed and integrated in *cdc48-6* cells. K48-Ub-ChIP-RT-PCR experiments using these strains limited the minimal DNA sequence to 79 *(F5)* and even 39 base pairs *(F7)*, respectively (see Figure 12C). Further truncation of the 39 base pairs motif (by 10

base pairs from both ends) resulted in loss of the ectopic Ub-hotspot (data not shown), suggesting that the 39 base pairs motif *(F7)* is indeed the minimal DNA sequence that triggers Ub-hotspot formation. Notably, the accumulation of ubiquitin conjugates was slightly higher for the longer 80 base pairs motif *(F5)*, indicating that DNA sequences neighbouring the minimal 39 base pairs motif *(F7)* might further enhance Ub-hotspot formation (see Figure 12C). However, neither the 80 base pairs motif nor the initial DNA sequence segment *(F1)* consist additional DNA fragments that are sufficient to trigger ectopic Ub-hotpot formation (see *YI128-F6* and *YI128-F8* in Figure 12C). Importantly, the big differences in the levels of K48-linked ubiquitin chain accumulation between the Hotspot 5 fragments of different length (see *F1*, *F5*, and *F7* in Figure 12C) do not indicate that the shorter DNA motifs (*F5* and *F7*) trigger Ub-hotspot formation more efficiently. Instead the strong differences in the K48-Ub-ChIP-RT-PCR signals are rather caused by a dramatic decrease in the distance between the site of DNA detection (the binding site of the YI128/ectopic Hotspot 5 RT-PCR primers) and the DNA binding site of ubiquitin conjugates. Since DNA is sheared to 250-500 base pairs fragments for ChIP experiments, a smaller distance between the actual DNA binding sites of ubiquitin conjugates and the detection primers (binding to the *YI128* vector backbone) increases the ChIP-RT-PCR signal.

The observation that the DNA sequence at Hotspot 5 contains a very short sequence motif of 39 base pairs, which is sufficient to trigger ubiquitin accumulation at an ectopic genomic locus, raised the question whether the 8 additional Ub-hotspots contain a similar sequence motif. Indeed, *in silico* prediction of DNA sequence motifs, using the MEME software[149], identified a conserved 36 base pairs sequence motif in 7 of the 9 Ub-hotspot sequences with a strikingly low expectation value (see Figure 13A). Intriguingly, the predicted sequence motif is nearly identical with the experimentally mapped DNA motif (see Figure 13B), although the experimentally gained information had not been used for bioinformatic prediction. In line with the experimental data that Hotspot 5 contains at least a second DNA motif that can trigger Ub-hotspot formation (see Figure 12B), the MEME software predicted a second Ub-hotspot motif in the overlap between the DNA fragments *F3* and *F4* (see Figure 13A). K48-Ub-ChIP-RT-PCR experiments indeed verified that this sequence, which is very similar to the experimentally identified 39 base pairs motif *(F7)*, is sufficient to trigger ectopic Ub-hotspot formation (data not shown). In addition to Hotspot 5, also the Hotspots 1 and 8 appear to contain more than one copy of the conserved DNA motif (see Figure 13A).

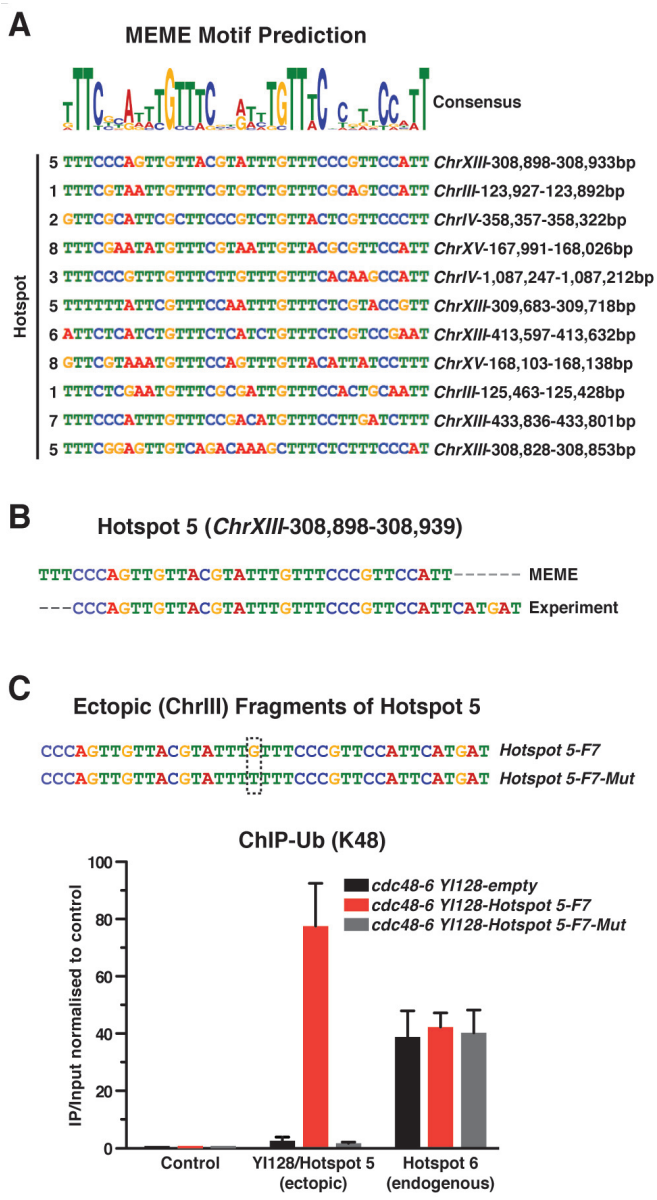

Figure 13: 7 out of 9 Cdc48-dependent Ub-hotspots Share a Conserved DNA Sequence Motif.

(A) The DNA sequence motif prediction software MEME predicts that 7 out of 9 Cdc48-dependent Ub-hotspots contain a conserved DNA sequence motif (for further details see 5.4). All predicted motifs and their genomic positions are listed (highest to lowest prediction e-value). The resulting consensus motif is depicted above (letter size is proportional to the degree of conservation).

(B) The predicted (top) and experimentally mapped (bottom) DNA sequence motifs for Hotspot 5 are nearly identical. Shown are the minimal DNA sequence motifs that were predicted *in silico* or experimentally.

(C) A single base pair exchange in the DNA motif of Hotspot 5 abolishes ectopic Cdc48-dependent Ub-hotspot formation. The upper panel shows the DNA sequence of the minimal Hotspot 5 DNA sequence motif *(Hotspot 5-F7)* and its mutant variant *(Hotspot 5-F7-Mut)*. The position of the mutation is highlighted (dashed black box). The lower panel shows the K48-Ub-ChIP-RT-PCR analysis of yeast strains containing the indicated Hotspot 5 fragments. Relative ubiquitin enrichments at a control region on chromosome II (control), the ectopic Hotspot 5 (YI128/Hotspot 5), and the endogenous Hotspot 6 (Hotspot 6) are depicted. Shown are IP/Input ratios that were normalised to the control region (IP/Input at control regions is set to 1). Data represents the mean (and the standard deviation) of five independent experiments.

The alignment of all predicted Ub-hotspot sequences and the resulting consensus motif suggest that the identified DNA motif contains a central and highly conserved tandem repeat of a TGTTTC motif (see Figure 13A). To verify the critical importance of these residues within the DNA motif, a mutant variant of the experimentally mapped 39 base pairs sequence (*Hotspot 5-F7-Mut*; see Figure 13C) was generated and integrated in *cdc48-6* cells. In line with the predicted importance of these residues, the mutation of a single residue was sufficient to result in a complete loss of the ability to generate an ectopic Ub-hotspot (see Figure 13C).

MEME prediction suggests that the experimentally mapped DNA sequence is at least responsible for Ub-hotspot formation at 7 out of 9 identified Ub-hotspots. Together with the observation that all 9 Cdc48-dependent Ub-hotspots peak in intergenic regions,

the presence of such a DNA sequence implicates that at least most Ub-hotspots are functionally identical.

3.6 Identification of Proteins That Bind the Conserved DNA Sequence Motif of Ub-hotspots

The presence of a conserved DNA sequence motif at 7 of the 9 Cdc48-dependent Ub-hotspots strongly suggests that the same protein or set of proteins binds to these loci. Given that the DNA motif is sufficient to trigger *de novo* formation of a Cdc48-dependent Ub-hotspot, the DNA motif recruits either the ubiquitylation substrate or machinery. To identify proteins that bind the DNA motif at Ub-hotspots, a yeast-one-hybrid screen was performed. To this end, a bait yeast strain containing a reporter gene *(HIS3)* under the control of a minimal promoter and three repeats of the experimentally mapped DNA sequence motif of Hotspot 5 (*Hotspot5-F7*; see Figure 13C) was generated (see Figure 14A). This bait strain was transformed with a prey cDNA library (Dualsystems) that encodes for approximately 10^7 different *S. cerevisiae* protein fragments, which are carboxy-terminally fused to a Gal4 transcription-activation domain (AD). Only AD-fusion proteins that interact with the bait DNA sequence motifs lead to transcriptional activation of the *HIS3* reporter gene, resulting in cell growth on media lacking histidine (see Figure 14A). Notably, the bait strain was additionally deleted for *UBX5* in order to interfere with proper chromatin extraction by Cdc48. Interference with chromatin extraction by Cdc48 might facilitate reporter gene activation by increased chromatin abundance of the AD-fusion protein.

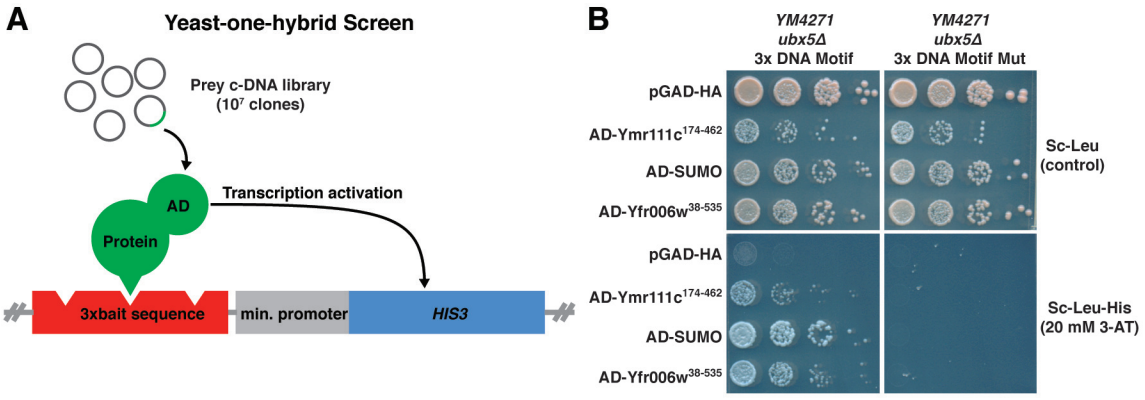

C Hits Y1H Screen (in *ubx5Δ* cells)

Gene name	Clones	Protein start site(s) (aa)	Frame	Stop codon
SUMO (SMT3)	18	several 5'UTR positions	IF (18x)	no
YFR006W	4	38 (4x)	IF (4x)	no
YMR111C	1	174	IF	no

D Hits Y1H Screen (Hybrigenics) (in *WT* cells)

Gene name	Clones	Protein start site(s) (aa)	Frame	Stop codon
SLX5/HEX3	16	nd (4x), 152 (1x), 153 (9x), 197 (1x), 218 (1x)	IF (11x)	no (11x)
YMR111C	3	38	IF	yes

Figure 14: Yeast-one-hybrid Screen Identified Proteins That Bind the Conserved DNA Sequence Motif of Ub-hotspots.

(A) Schematic cartoon explaining the basic principle of a yeast-one-hybrid screen. As depicted in the lower panel, the bait yeast strain contains a *HIS3* reporter gene (blue) under control of a minimal promoter (grey; contains a TATA box and a transcription start site) and three repeats of the bait sequence (red). The *HIS3* reporter gene is only efficiently activated in cells that were transformed with a plasmid of the prey c-DNA library that expresses an AD-fusion protein (AD: Gal4 transcription-activation domain), which interacts with the bait sequence.

(B) AD-Ymr111c, AD-SUMO, and AD-Yfr006w are verified hits of the yeast-one-hybrid screen. Yeast-one-hybrid bait strains lacking *UBX5* that expressed either the *HIS3* reporter gene under control of three repeats of the 39 bp DNA sequence motif of Hotspot 5 (*YM4271 ubx5Δ* 3x DNA motif) or its mutant variant (*YM4271 ubx5Δ* 3x DNA motif Mut) were transformed with plasmids expressing AD-Ymr111c$^{174-462}$, AD-SUMO, or AD-Yfr006w$^{38-535}$ (these plasmids were isolated in the yeast-one-hybrid screen). An empty vector (pGAD-HA) was transformed as control. Shown are spottings of serial dilutions (1:8) of the transformed bait strains on a control plate (Sc-Leu, only selecting for plasmid presence) and plates that additionally lack histidine (Sc-Leu-His, containing 20 mM 3-aminotriazol to supress *HIS3* background activity). Cell growth on plates lacking histidine indicates interaction between the AD-protein and the bait DNA motifs upstream of the *HIS3* reporter. Plates were incubated at 30°C for 3 (control) or 4 days (Sc-Leu-His 20 mM 3-AT), respectively.

(C) Summary of yeast-one-hybrid (Y1H) screen hits. Listed are the gene names, the number of independent clones that were identified in the screen, the respective protein start site (amino acid (aa) position) of the expressed protein fragments, the frame (IF: in frame), and the presence of a premature stop codon (e.g. due to 5'UTR which is present in the c-DNA construct).

(D) Summary of yeast-one-hybrid (Y1H) screen hits resulting from a second screen that was performed by the company *Hybrigenics*. Listed are the gene names, the number of independent clones that were identified in the screen, the respective protein start site of the expressed protein fragments (nd: not determined), the frame (IF: in frame), and the presence of a premature stop codon (e.g. due to 5'UTR which is present in the c-DNA construct). Notably, *S. cerevisiae* translation can in some cases read through premature stop codons, resulting in expression of the expected fusion protein. Plates were incubated at 30°C for 3 (control) or 4 days (Sc-Leu-His 20 mM 3-AT), respectively.

Isolation and sequencing of c-DNA constructs expressing AD-fusion proteins conferring cell growth on media lacking histidine revealed in total 7 candidate proteins. To exclude non-specific activators from this candidate list, two control bait strains expressing either the *HIS3* reporter gene exclusively under the control of a minimal promoter, or in

combination with three mutated copies of the experimentally mapped DNA sequence motif (*Hotspot5-F7-Mut*; see Figure 13C) were generated. Given that Cdc48-dependent Ub-hotpots critically depend on the presence and the integrity of the conserved DNA sequence motif, AD-fusion proteins that activated *HIS3* in one or both control strains were considered as non-specific (data not shown). Spotting assays revealed that only 3 of the 7 initial candidate proteins, including Ymr111c, Yfr006w, and SUMO (Smt3) exclusively activate *HIS3* transcription in the screen bait strain, but not in the two control strains (see Figure 14B and 14C). Whereas Ymr111c and Yfr006w are annotated but previously uncharacterised *S. cerevisiae* proteins, SUMO (Smt3) is a very well studied member of the ubiquitin-like protein family that is conjugated to many substrate proteins. It appears very likely that reporter gene activation by AD-SUMO results from SUMO modification of another protein that interacts with the DNA sequence motif.

To potentially extend the results of the first yeast-one-hybrid screen (summarised in Figure 14C), in parallel a second yeast-one-hybrid screen with a slightly different setup was performed in collaboration with the company *Hybrigenics*. Using a mating-based yeast-one-hybrid system, *Hybrigenics* screened a different c-DNA prey library in a *WT* bait strain (expressing *UBX5*) using a similar *HIS3* reporter system (see Figure 14A). Strikingly, in accordance with the first screen, the uncharacterised protein Ymr111c was again identified as potential binding partner of the conserved DNA sequence motif at Cdc48-dependent Ub-hotspots (see Figure 14D). In addition, the screen also revealed Slx5, a subunit of the heterodimeric SUMO-targeted E3 ubiquitin ligase Slx5-Slx8, as a second candidate (see Figure 14D). This finding implicates that the Slx5-Slx8 E3 ligase might catalyse ubiquitylation at Cdc48-dependent Ub-hotspots. Similar to SUMO, a direct DNA binding by Slx5 appears rather unlikely.

All together, the two yeast-one-hybrid screens suggest that the yeast proteins Ymr111c and Yfr006w, as well as SUMO and Slx5-Slx8 might be important components in the formation of Cdc48-dependent Ub-hotspots. Whereas Ymr111c and Yfr006w are very promising candidates for direct binding of the conserved DNA sequence motif, Slx5 and SUMO might rather be important for the ubiquitylation reaction.

3.7 Ymr111c Is Required for the Formation of 7 Cdc48-dependent Ub-hotspots

The results obtained from two yeast-one-hybrid screens suggest that the previously uncharacterised proteins Ymr111c and Yfr006w are potential interaction partners of the

conserved DNA sequence motif at Cdc48-dependent Ub-hotspots. To test the impact of these proteins on formation of Cdc48-dependent Ub-hotspots, *ubx5Δ* cells lacking either Ymr111c (*ubx5Δ ymr111cΔ*) or Yfr006w (*ubx5Δ yfr006wΔ*) were subjected to K48-Ub-ChIP-RT-PCR experiments (see Figure 15A). Intriguingly, the deletion of *YMR111C* but not *YFR006W* completely blocked the accumulation of K48-linked ubiquitin chains at 2 of 3 tested Cdc48-dependent Ub-hotspots (Hotspots 5 and 6; see Figure 15A). In contrast, ubiquitylation at another Ub-hotspot (Hotspot 4) was unaffected in both mutant strains (see Figure 15A), strongly suggesting that ubiquitylation at this genomic locus depends neither on Ymr111c nor on Yfr006w. Interestingly, at both Ub-hotspots (Hotspot 5 and 6) that were affected by *YMR111C* deletion but not at the unaffected Hotspot 4, the MEME software predicted the conserved 36 base pairs DNA sequence (see Figure 13A). Additional K48-Ub-ChIP-RT-PCR experiments confirmed that *YMR111C* deletion indeed only affects the 7 Cdc48-dependent Ub-hotspots that were predicted to contain the conserved DNA motif (data not shown, summarised in Figure 15C). Based on this result the Cdc48-dependent Ub-hotspots were subsequently subdivided in Ymr111c-dependent and -independent Ub-hotspots. The intriguing loss of ubiquitin accumulation in cells lacking Ymr111c strongly suggests that Ymr111c is either ubiquitylated or is involved in the recruitment of the ubiquitylation machinery to Ymr111c-dependent Ub-hotspots.

To verify that Ymr111c is directly involved in the formation of 7 Cdc48-dependent Ub-hotspots, the interaction between of Ymr111c and these genomic loci was analysed by Ymr111c-directed ChIP (see Figure 15B). Since epitope tagging of Ymr111c (with TAP, 6HA, and GFP tags) strongly interfered with the ubiquitin accumulation at all Ymr111c-dependent Ub-hotspots (data not shown), a polyclonal antibody directed against Ymr111c was generated. ChIP using this Ymr111c antibody revealed that Ymr111c indeed specifically binds to Ymr111c-dependent but not -independent Ub-hotspots (see Figure 15B). In line with a specific recognition of Ymr111c by the newly generated antibody, Ymr111c-ChIP from cells deleted for *YMR111C* did not result in enrichment at Ub-hotspots (see Figure 15B). Additional Ymr111c-ChIP-RT-PCR experiments revealed that indeed all Ymr111c-dependent Ub-hotspots are enriched in Ymr111c binding (data not shown, summarised in Figure 15C). Notably, the levels of Ymr111c enrichment differ significantly between the Ymr111c-dependent Ub-hotspots (see Figure 15B and data not shown). Interestingly, the differences in Ymr111c enrichments do not correlate with the extent of ubiquitin accumulation at these genomic loci (compare Figure 10B and Figure 15A with Figure 15B), suggesting that Ymr111c may not be the direct ubiquitylation target.

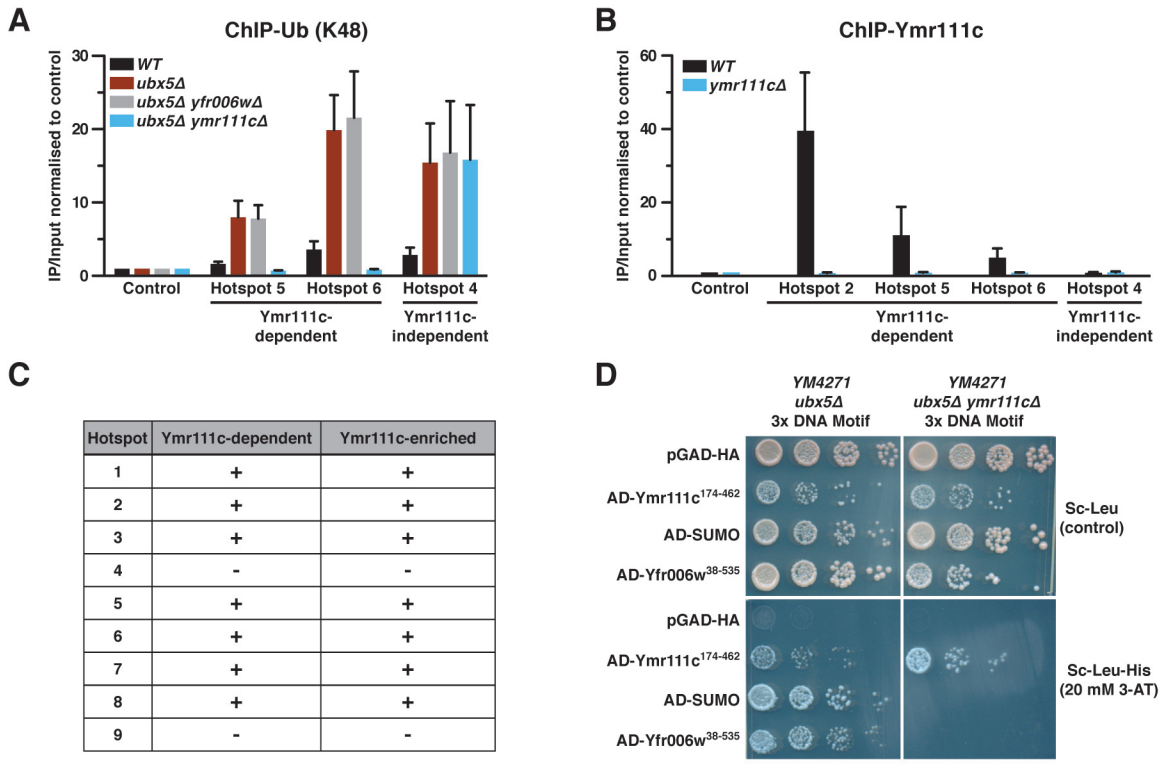

Hotspot	Ymr111c-dependent	Ymr111c-enriched
1	+	+
2	+	+
3	+	+
4	-	-
5	+	+
6	+	+
7	+	+
8	+	+
9	-	-

Figure 15: Ubiquitin Accumulation at 7 out of 9 Cdc48-dependent Ub-hotspots Depends on Ymr111c.
(A) Deletion of *YMR111C* but not *YFR006W* abolishes accumulation of K48-linked ubiquitin conjugates at 2 of 3 tested Cdc48-dependent Ub-hotspots. K48-Ub-ChIP-RT-PCR analysis was performed with *WT*, *ubx5Δ*, *ubx5Δ yfr006wΔ,* and *ubx5Δ ymr111cΔ* yeast cells. Ubiquitin abundance was analysed at a control region on chromosome II (control) and three Cdc48-dependent Ub-hotspots (Hotspot 4,5, and 6). Shown are IP/Input ratios that were normalised to the control region (IP/Input at control regions is set to 1). Data represents the mean (and the standard deviation) of four independent experiments.
(B) Ymr111c physically interacts with Ymr111c-dependent Ub-hotspots. Ymr111c-directed ChIP (Ymr111c-ChIP) was performed with *WT* and *ymr111cΔ* (to control for antibody specificity) cells. Ymr111c abundance was analysed at a control region on chromosome II (control), three Ymr111c-dependent Ub-hotspots (Hotspots 2, 5, and 6), and the Ymr111c-independent Ub-hotspot 4. Shown are IP/Input ratios that were normalised to the control region (IP/Input at control regions is set to 1). Data represents the mean (and the standard deviation) of three independent experiments.
(C) Summary of the Ymr111c-dependence of ubiquitin accumulation (detected by K48-Ub-ChIP-RT-PCR) and the enrichment of Ymr111c (detected by Ymr111c-ChIP-RT-PCR) at all 9 Cdc48-dependent Ub-hotspots.
(D) Endogenously expressed Ymr111c is required for reporter gene activation by SUMO and Yfr006w (as a Gal4 transcription-activation domain fusion, AD) in the yeast-one-hybrid system. The *HIS3* reporter gene activation by an empty vector (pGAD-HA) AD-Ymr111c$^{174-462}$, AD-SUMO, and AD-Yfr006w$^{38-535}$ was analysed in the bait strain of the yeast-one-hybrid screen (*YM4271 ubx5Δ* 3x DNA motif) and a mutant variant that lacks *YMR111C* (*YM4271 ubx5Δ ymr111cΔ* 3x DNA motif). Shown are spottings of serial dilutions (1:8) of the indicated strains on a control plate (Sc-Leu, only selecting for plasmid presence) and plates that additionally lack histidine (Sc-Leu-His, containing 20 mM 3-aminotriazol to supress *HIS3* background activity). Cell growth on plates lacking histidine indicates interaction between the AD-protein and the bait DNA motifs upstream of the *HIS3* reporter. Plates were incubated at 30°C for 3 (control) or 4 days (Sc-Leu-His 20 mM 3-AT), respectively.

ChIP experiments demonstrated that Ymr111c but not Yfr0006w plays an important role in the formation of Cdc48-dependent Ub-hotspots that contain the conserved DNA sequence motif. However, initial yeast-one-hybrid studies suggested that despite Ymr111c also Yfr006w and SUMO are linked to the DNA sequence motif. To test if endogenously expressed Ymr111c bridges SUMO or Yfr006w interaction with the DNA motif, a new yeast-one-hybrid bait strain that lacks *YMR111C* was generated. Spotting assays using this strain revealed that AD-Yfr006w and AD-SUMO could only confer growth on media lacking histidine, if endogenous *YMR111C* was expressed (see Figure 15D). This finding suggests that Ymr111c indeed bridges the DNA interactions of Yfr006w and SUMO. Yfr0006w is probably a binding partner of Ymr111c, given that an interaction between both proteins could be detected in yeast-two-hybrid analysis (data not shown). In contrast, the DNA interaction of SUMO is most likely triggered by SUMO conjugation to Ymr111c or a binding partner.

3.8 Ymr111c Is SUMOylated on Lysine-231

The yeast-one-hybrid screens and their verification by ChIP-RT-PCR analysis revealed that Ymr111c plays a crucial role in formation of 7 Cdc48-dependent Ub-hotspots. Ymr111c is a previously uncharacterised protein that contains a Gcr1 and a coiled-coiled domain (see Figure 16A). The Gcr1 domain is a conserved domain that has also been identified in 4 other *S. cerevisiae* proteins. 3 of these proteins (Gcr1, Msn1, and Hot1) have been implicated as transcription factors. A study on the DNA binding capacity of the Gcr1 transcription factor suggests that the Gcr1 domain might mediate DNA binding[150]. Coiled-coiled domains are typically short structural features that often mediate protein-protein interactions.

Given that the transcription activation potential of AD-SUMO in the yeast-one-hybrid assay depends on Ymr111c (see Figure 15D), it appeared very likely that Ymr111c is SUMOylated. Indeed, Ymr111c has been identified as a SUMO substrate in several high-throughput screens[47,151-153], including an unpublished mass-spectrometry based screen performed in the Jentsch lab (unpublished, Ivan Psakhye). The screen of the Jentsch lab suggests that Ymr111c can be SUMOylated by both DNA-bound SUMO E3 ligases Siz1 and Siz2.

To confirm that Ymr111c is SUMOylated, directed yeast-two-hybrid assays with Ymr111c and SUMO were performed (see Figure 16B). As indicated by cell growth on media lacking histidine, Ymr111c strongly interacts with the conjugatable SUMO-GG but

not with the non-conjugatable SUMO-AA variant (see Figure 16B). In line with SUMOylation of Ymr111c by Siz1 or Siz2, a rather weak but reproducible interaction between Ymr111c and both SUMO E3 ligases, as well as with the SUMO E2 enzyme Ubc9 was detected in a yeast-two-hybrid assay (see Figure 16B).

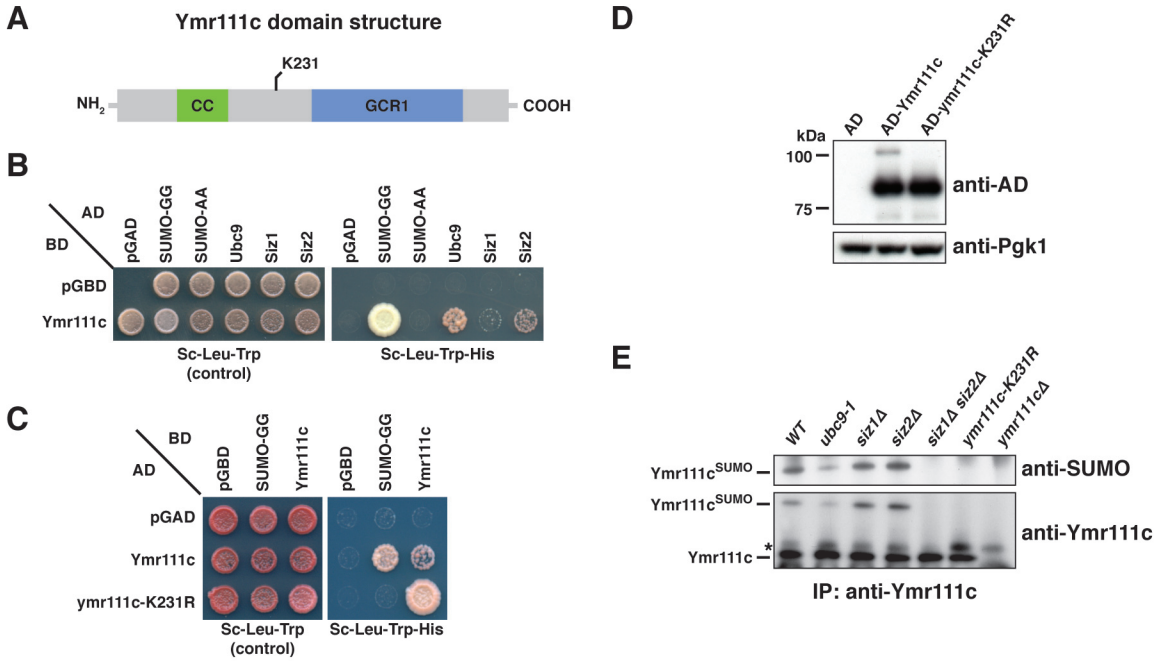

Figure 16: Ymr111c Is SUMOylated on Lysine-231 by Ubc9 and Siz1 or Siz2.
(A) Scheme depicting the protein domain structure of Ymr111c. Ymr111c contains a coiled-coiled (CC) and a Gcr1 domain. The position of the SUMO acceptor lysine residue (K231) is indicated.
(B) Ymr111c interacts with conjugatable SUMO, the SUMO E2 enzyme Ubc9, and the SUMO E3 ligases Siz1 and Siz2. Yeast-two-hybrid analysis of Ymr111c (as a Gal4 DNA-binding domain fusion, BD) with conjugatable SUMO (SUMO-GG), non-conjugatable SUMO (SUMO-AA), Ubc9, Siz1, and Siz2 (as Gal4 transcription-activation domain fusions, AD) is shown. Growth on plates lacking histidine (Sc-Leu-Trp-His) indicates binding. Plates were incubated at 30°C for 3 (control) or 6 days (Sc-Leu-Trp-His), respectively.
(C) Ymr111c but not its mutant variant ymr111c-K231R interacts with conjugatable SUMO, suggesting that Ymr111c is SUMOylated on lysine-231. Self-self interaction of ymr111c-K231 with WT Ymr111c is enhanced. Yeast-two-hybrid analysis of Ymr111c or its mutant variant ymr111c-K231R (as a Gal4 transcription-activation domain fusion, AD) with conjugatable SUMO (SUMO-GG) and Ymr111c (as a Gal4 DNA-binding domain fusion, BD) is shown. Growth on plates lacking histidine (Sc-Leu-Trp-His) indicates binding. Plates were incubated at 30°C for 3 (control) or 5 days (Sc-Leu-Trp-His), respectively.
(D) Expression levels of Ymr111c and ymr111c-K231R (as a Gal4 transcription-activation domain fusion, AD) in the yeast-two-hybrid reporter strain are similar. A slower migrating band that probably correlates to SUMOylated AD-Ymr111c is lost in cells expressing AD-ymr111c-K231R. Western blotting of whole cell extracts from cells expressing AD, AD-Ymr111c, or AD-ymr111c-K231R using an anti-AD antibody was performed. Equal loading was verified Pgk1-directed western blotting.
(E) Ymr111c is SUMOylated on lysine-231 by Ubc9 and Siz1 or Siz2. Immunoprecipitations (IPs) of Ymr111c (using a polyclonal anti-Ymr111c antibody) from the indicated cells was analysed by western blotting with anti-Ymr111c (lower panel) and anti-SUMO (upper panel) antibodies. A slower migrating band corresponds to $Ymr111c^{SUMO}$, because it was detected with both antibodies in western blotting. The asterisk marks a cross-reacting band.

SUMO is typically attached to one or several lysine residues of proteins. Frequently, SUMOylation targets lysine residues that are embedded in so-called SUMO consensus sites. Interestingly, Ymr111c contains 4 SUMO consensus sites (K123; K130; K131; K231) that are potential SUMO attachment sites. To test if SUMOylation indeed occurs on one of these lysine residues, I performed directed yeast-two-hybrid assays with mutant variants of Ymr111c, in which individual lysine residues in the SUMO consensus motifs were replaced by arginines (see Figure 16C and data not shown). Notably, a mutant variant of Ymr111c in which lysine-231 was replaced by arginine (ymr111c-K231R) completely lost its ability to interact with SUMO in a yeast-two-hybrid assay (see Figure 16C). Western blot analysis demonstrated that the expression levels of the WT and ymr111c-K231R Gal4 transcription-activation domain (AD) fusion proteins are nearly identical (see Figure 16D), thereby excluding that the observed effect is caused by alterations in protein expression. Strikingly, in cells expressing AD-Ymr111c, a second slower migrating band was detected. Notably, the observed size shift corresponds to the attachment of a single SUMO moiety to Ymr111c (see Figure 16D). In line with SUMOylation of Ymr111c on lysine-231 the slower migrating band was lost in cells expressing the ymr111c-K231R mutant variant (see Figure 16B). The structural integrity of the AD-ymr111c-K231R variant was verified by testing Ymr111c self-self interaction (see Figure 16C) that has been observed in previous high-throughput studies[154]. Surprisingly the AD-ymr111c-K231R variant interacts much stronger with BD-Ymr111c than the WT protein, suggesting that the SUMOylation of Ymr111c might inhibit Ymr111c oligomerisation (see Figure 16C).

To confirm by different means that Ymr111c is indeed SUMOylated on lysine-231, immunoprecipitation with a Ymr111c-specific antibody in different genetic backgrounds was performed (see Figure 16E). As already observed for AD-Ymr111c (see Figure 16D), a fraction of immunoprecipitated Ymr111c migrates slower in SDS-gel electrophoresis (see Figure 16E). Western blotting with a SUMO-directed antibody confirmed that this slower migrating band corresponds to SUMOylated Ymr111c (Ymr111c^{SUMO}; see Figure 16E). In line with the yeast-two-hybrid data, Ymr111c SUMOylation was completely abolished in *siz1Δ siz2Δ* as well as *ymr111c-K231R* cells (see Figure 16E). Siz1 and Siz2 apparently have a redundant function in Ymr111c SUMOylation since neither Siz1 nor Siz2 single deletions affected Ymr111C SUMOylation (see Figure 16E). As expected, SUMOylation was also significantly reduced in a yeast strain that expresses a temperature-sensitive mutant of Ubc9 (*ubc9-1*; see Figure 16E).

Both yeast-two-hybrid assays and Ymr111c immunoprecipitation clearly demonstrate that Ymr111c is SUMOylated on lysine-231. Interestingly, yeast-two-hybrid analysis also suggests that SUMOylation might negatively impact Ymr111c oligomerisation.

3.9 SUMOylation of Ymr111c Is Required for Formation of Ymr111c-dependent Ub-hotspots

To test if Ymr111c SUMOylation influences the accumulation of K48-linked ubiquitin conjugates at Ymr111c-dependent Ub-hotspots, K48-Ub-ChIP-RT-PCR experiments in strains that are impaired in Ymr111c SUMOylation were performed (see Figure 17A). Strikingly, interference with Ymr111c SUMOylation on lysine-231 in *ubx5Δ* cells (*ubx5Δ siz1Δ siz2Δ*, *ubx5Δ ubc9-1, and ubx5Δ ymr111c-K231R*) completely blocked or strongly reduced the accumulation of K48-linked ubiquitin chains at all tested Ymr111c-dependent Ub-hotspots (see Figure 17A). Likewise, the milder ubiquitin conjugate accumulation that was observed in *WT* cells was also completely blocked in cells that are impaired in Ymr111c SUMOylation (*siz1Δ siz2Δ*, *ubc9-1*, and *ymr111c-K231R*). Importantly, the ymr111c-K231R steady-state levels are even slightly increased compared to the WT protein, suggesting that the protein is efficiently expressed and probably structurally intact (see Figure 17B). In contrast to Ymr111c-dependent Ub-hotspots, ubiquitylation at a Ymr111c-independent Ub-hotspot (Hotspot 4) was not decreased in cells that were impaired in Ymr111c SUMOylation (see Figure 17A). Instead, the accumulation of K48-linked ubiquitin chains at the Ymr111c-independent Ub-hotspot (hotspot 4) was even increased in cells that are deficient in the SUMO E2 Ubc9 (*ubc9-1* and *ubx5Δ ubc9-1)* or the SUMO E3 ligases Siz1 and Siz2 (*siz1Δ siz2Δ* and *ubx5Δ siz1Δ siz2Δ*) (see Figure 17A). However, neither the deletion of *YMR111C* (*ymr111cΔ* and *ubx5Δ ymr111cΔ*) nor the mutation of the Ymr111c SUMO acceptor lysine (*ymr111c-K231R* and *ubx5Δ ymr111c-K231R*) increased ubiquitin conjugate enrichment at Ymr111c-dependent Ub-hotspots (see Figure 17A). Thus, this finding suggests that Ubc9, Siz1, and Siz2-dependent SUMOylation of another protein might negatively regulate ubiquitylation at Ymr111c-independent Ub-hotspots.

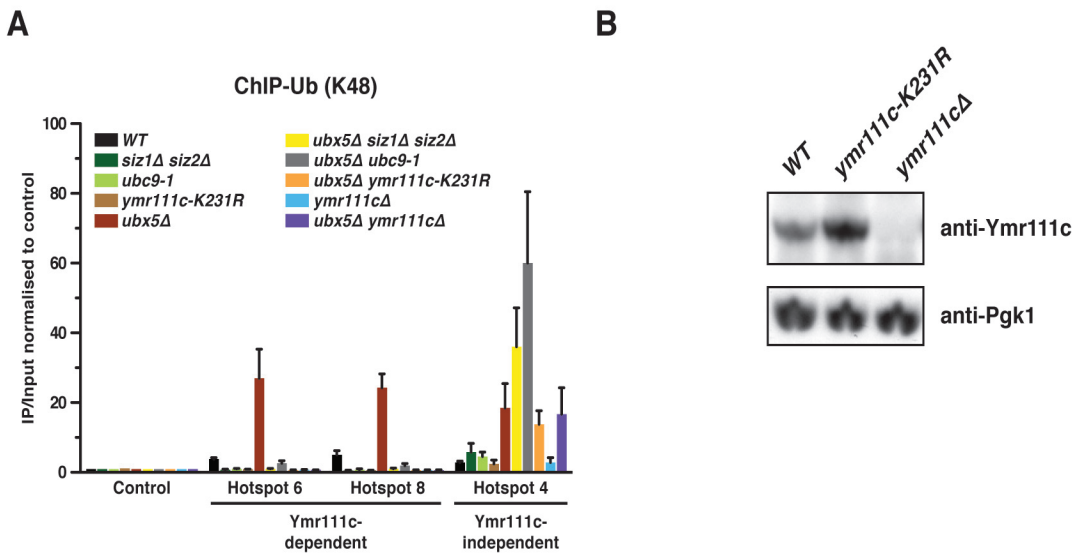

Figure 17: SUMOylation of Ymr111c on Lysine-231 Is Required for Ubiquitylation at Ymr111c-dependent Ub-hotspots.

(A) Interference with Ymr111c SUMOylation on lysine-231 abolishes ubiquitylation at Ymr111c-dependent Ub-hotspots. Shown are K48-Ub-ChIP-RT-PCR experiments with *WT* or *ubx5Δ* cells and mutant variants that are impaired in Ymr111c SUMOylation by mutation of the SUMO E2 enzyme Ubc9 (*ubc9-1* and *ubx5Δ ubc9-1*), deletion of the SUMO E3 ligases Siz1 and Siz2 (*siz1Δ siz2Δ* and *ubx5Δ siz1Δ siz2Δ*), or mutation of the SUMO acceptor lysine in Ymr111c (*ymr111cΔ* and *ubx5Δ ymr111cΔ*). For comparison, also *YMR111C* deletion cells (*ymr111cΔ and ubx5Δ ymr111cΔ*) were analysed. Ubiquitin abundance was detected at a control region on chromosome II (control), two Ymr111c-dependent Ub-hotspots (Hotspots 5 and 6), and the Ymr111c-independent Ub-hotspot 4. Shown are IP/Input ratios that were normalised to the control region (IP/Input at control regions is set to 1). Data represents the mean (and the standard deviation) of three independent experiments.

(B) Steady-state expression levels of the mutant ymr111c-K231R protein are slightly increased. Western blot analysis using a Ymr111c-directed antibody was performed with whole cell extracts (WCEs) from *WT* and *ymr111c-K231R* cells (same cells that were subjected to ChIP analysis in A). Equal loading of samples was verified by Pgk1-directed western blotting.

3.10 Slx5-Slx8 Mediates Ubiquitylation at Ymr111c-dependent Ub-hotspots in a Ymr111c SUMOylation-dependent Manner

Ubiquitylation at Ymr111c-dependent Ub-hotspots critically depends on SUMOylation of Ymr111c (see Figure 17A). Moreover, the Slx5 subunit of the heterodimeric SUMO-targeted ubiquitin ligase (STUbL) Slx5-Slx8 has been identified as a potential binding partner of the conserved DNA sequence motif at these genomic positions (see Figure 14D). Together these findings implicated that SUMOylated Ymr111c recruits Slx5-Slx8 to Ymr111c-dependent Ub-hotspots, where Slx5-Slx8 acts as an E3 ubiquitin ligase. To support this model, I first tested if Ymr111c interacts with Slx5-Slx8. Indeed, yeast-two-hybrid analysis with Slx5 (as Gal4 binding domain fusion, BD) and Ymr111c (as Gal4 transcription-activation domain fusion, AD) suggests that Ymr111c robustly interacts with Slx5 (see Figure 18A). Notably, binding between AD-Ymr111c and BD-Slx5 appears to

critically depend on SUMOylation of Ymr111c, because a mutant variant of Ymr111c that lacks the SUMO acceptor site (AD-ymr111c-K231R) is nearly defective in Slx5 binding (see Figure 18A). In contrast to Slx5 binding, the self-self interaction of AD-ymr111c-K231R with BD-Ymr111c is even increased, indicating that the mutant protein is properly expressed and structurally intact (see Figure 18A).

Given that Ymr111c appears to interact with Slx5-Slx8 in a SUMO-dependent manner, I next tested if Slx5-Slx8 is recruited to Ymr111c-dependent Ub-hotspots *in vivo*. To this end, Slx8-directed ChIP-RT-PCR experiments were conducted with cells that express carboxy-terminally 9Myc-tagged Slx8 (Slx8-9myc) from the endogenous locus (see Figure 18B, Figure 18C). Notably, in contrast to the deleterious phenotype of *SLX5-9MYC* cells (data not shown), epitope tagging of Slx8 affected neither ubiquitin accumulation at Ymr111c-dependent Ub-hotspots nor cell growth (data not shown). In line with the interaction between Ymr111c and Slx8, ChIP-RT-PCR experiments using a Myc-specific antibody demonstrated that Slx8-9myc is recruited to all tested Ymr111c-dependent but not -independent Ub-hotspots (see Figure 18C). Importantly, the association between Slx8-9myc and these genomic loci was strongly reduced in cells that either lack Ymr111c (*SLX8-9MYC ymr111cΔ*) or are impaired in Ymr111c SUMOylation (*SLX8-9MYC siz1Δ siz2Δ*, *SLX8-9MYC ubc9-1*, and *SLX8-9MYC ymr111c-K231R;* see Figure 18C). These findings suggest that the heterodimeric STUbL Slx5-Slx8 is recruited to Ymr111c-dependent Ub-hotspots in a Ymr111c^{SUMO}-dependent manner. Notably, the levels of Slx8-9myc enrichments vary dramatically between individual Ymr111c-dependent Ub-hotspots, indicating that different amounts of Slx8 are recruited (see Figure 18C). Strikingly, the enrichments of Slx8-9myc and Ymr111c strongly correlate at all tested Ymr111c-dependent Ub-hotspots (compare Figure 15B and Figure 18C), suggesting that both proteins are bound in a stoichiometric ratio. However, similar to Ymr111c, Slx8-9myc levels do not correlate with the enrichment of ubiquitin at Ymr111c-dependent Ub-hotspots (compare Figure 10A and Figure 10B with Figure 18C). A possible explanation for this observation is that Ymr111c is not directly ubiquitylated but rather involved in Slx5-Slx8 recruitment (see 4.3 for further discussion).

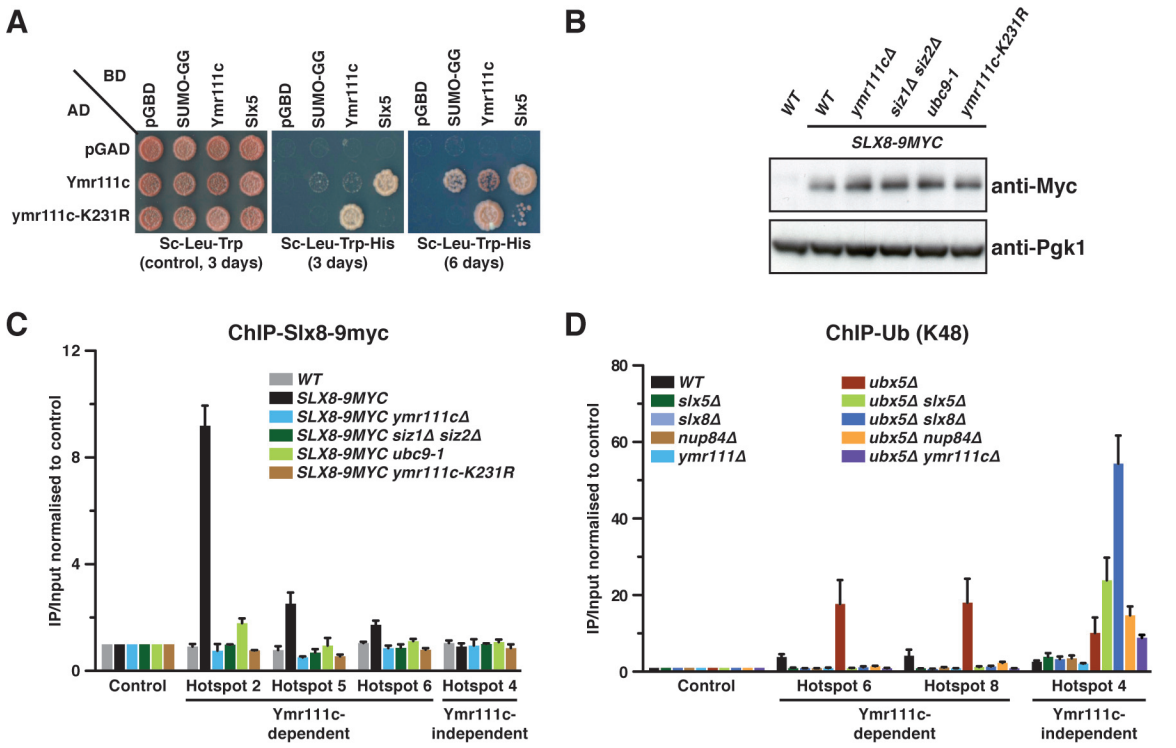

Figure 18: Ubiquitylation at Ymr111c-dependent Ub-hotspots Is Mediated by the SUMO-targeted Ubiquitin E3 Ligase Slx5-Slx8 in a Ymr111c SUMOylation-dependent Manner.

(A) Slx5 interacts with Ymr111c in a SUMOylation-dependent manner. Yeast-two-hybrid analysis of Ymr111c or its mutant variant ymr111c-K231R (as Gal4 transcription-activation domain fusions, AD) with conjugatable SUMO (SUMO-GG), Ymr111c, and Slx5 (as Gal4 DNA-binding domain fusions, BD) is shown. Growth on plates lacking histidine (Sc-Leu-Trp-His) indicates binding. Plates were incubated at 30°C for 3 (left and middle) or 6 days (right), respectively.

(B) Steady-state expression levels of 9Myc-tagged Slx8 are similar in all genetic backgrounds used for ChIP analysis (see Figure 18C). Western blot analysis using an anti-Myc antibody was performed with whole cell extracts (WCEs) from the indicated cells (same cells that were subjected to ChIP analysis in C). Equal loading of samples was verified by Pgk1-directed western blotting.

(C) Slx8-9myc accumulates at Ymr111c-dependent Ub-hotspots in a Ymr111c SUMOylation-dependent manner. ChIP-RT-PCR using anti-Myc antibody was performed with *WT* cells (*WT* and *SLX8-9MYC*), cells lacking Ymr111c (*SLX8-9MYC ymr111cΔ*), and cells that were impaired in Ymr111c SUMOylation (*SLX8-9MYC siz1Δ siz2Δ*, *SLX8-9MYC ubc9-1*, and *SLX8-9MYC ymr111c-K231R*). Slx8-9myc abundance was analysed at a control region on chromosome II (control), three Ymr111c-dependent Ub-hotspots (Hotspots 2, 5, and 6), and the Ymr111c-independent Ub-hotspot 4. Shown are IP/Input ratios that were normalised to the control region (IP/Input at control regions is set to 1). Data represents the mean (and the standard deviation) of three independent experiments.

(D) Enrichment of K48-linked ubiquitin conjugates at Ymr111c-dependent Ub-hotspots depends on the E3 ubiquitin ligase Slx5-Slx8 and the nuclear pore component Nup84. K48-Ub-ChIP-RT-PCR analysis was performed with *WT, ubx5Δ*, and isogenic cells that lacked Slx5 (*slx5Δ* and *ubx5Δ slx5Δ*), Slx8 (*slx8Δ and ubx5Δ slx8Δ*), or Nup84 (*nup84Δ* and *ubx5Δ nup84Δ*). For comparison, also *YMR111C* deletion cells (*ymr111cΔ and ubx5Δ ymr111cΔ*) were analysed. Ubiquitin abundance was analysed at a control region on chromosome II (control), two Ymr111c-dependent Ub-hotspots (Hotspots 6 and 8), and the Ymr111c-independent Ub-hotspot 4. Shown are IP/Input ratios that were normalised to the control region (IP/Input at control regions is set to 1). Data represents the mean (and the standard deviation) of three independent experiments.

The recruitment of Slx8 to Ymr111c-dependent Ub-hotspots strongly suggested that the E3 ubiquitin ligase Slx5-Slx8 catalyses ubiquitylation at these genomic loci. In line with this idea, K48-Ub-ChIP-RT-PCR experiments revealed that deletion of Slx5 or Slx8 in *WT* (*slx5Δ* and *slx8Δ*) or *ubx5Δ* cells (*ubx5Δ slx5Δ* and *ubx5Δ slx8Δ*) completely abolished the enrichment of K48-linked ubiquitin conjugates at Ymr111c-dependent Ub-hotspots (see Figure 18D).

A previous study demonstrated that a large fraction of the Slx5-Slx8 protein pool localises to the nuclear pore complex and physically interacts with the nuclear pore component Nup84[67]. Given that the enrichment of K48-linked ubiquitin conjugates at Ymr111c-dependent Ub-hotspots was completely lost in cells lacking Nup84 (*nup84Δ* and *ubx5Δ nup84Δ*), the interaction between Slx5-Slx8 and Nup84 appears to be crucial for efficient ubiquitylation at these genomic positions. The critical importance of Nup84 for the ubiquitylation reaction at Ymr111c-dependent Ub-hotspots strongly suggests that these loci are at least transiently associated with the nuclear pore or the nuclear periphery.

In contrast to Ymr111c-dependent Ub-hotspots, ubiquitin accumulation at the tested Ymr111c-independent Ub-hotspot (Hotspot 4) was not reduced but rather increased in cells that lack Slx5 or Slx8 (compare *slx5Δ* and *slx8Δ* with *WT,* or *ubx5Δ slx5Δ* and *ubx5Δ slx8Δ* with *ubx5Δ*; see Figure 18D). A mild increase in the enrichment of K48-linked ubiquitin conjugates at the Ymr111c-independent Ub-hotspot was also observed in Nup84-deficient cells (compare *nup84Δ* with *WT*, or *ubx5Δ nup84Δ* with *ubx5Δ*; see Figure 18D). Notably, an increase in ubiquitin conjugate enrichment at Ymr111c-independent Ub-hotspots was already observed in cells that were impaired in Ubc9 or Siz1 and Siz2 function, but not in Ymr111c-deficient cells (see Figure 17A). A possible explanation for this phenomenon is that SUMOylation and SUMO-dependent protein degradation by Slx5-Slx8 might negatively regulate ubiquitylation at Ymr111c-independent Ub-hotspots.

All together, several lines of evidence support a model in which SUMOylated Ymr111c recruits Slx5-Slx8 to Ymr111c-dependent Ub-hotspots, where Slx5-Slx8 ubiquitylates either Ymr111c or more likely another protein.

3.11 Cdc48 Is Recruited to Ymr111c-dependent Ub-hotspots by Ubiquitylation but Does not Seem to Extract Ymr111c

Cdc48 is typically targeted to its substrates in a ubiquitin-dependent manner. To investigate if Cdc48 is also recruited to its substrate(s) at Ymr111c-dependent Ub-hotspots by ubiquitylation, Cdc48-directed ChIP experiments were performed with cells that were impaired in ubiquitylation at Ymr111c-dependent Ub-hotspots by deletion of *SLX8* (*slx8Δ* and *cdc48-6 slx8Δ*; see Figure 19A). As demonstrated before, Cdc48 is mildly enriched at both Ymr111c-dependent and -independent Ub-hotspots (see Figure 9C and Figure 19A). The mild enrichment of Cdc48 (in *WT* cells) was specifically lost at Ymr111c-dependent but not -independent Ub-hotspots in Slx8-deficient cells (*slx8Δ*; see Figure 19A). The mutant cdc48-6 variant binds substrates more robustly, thus resulting in a significantly increased Cdc48 enrichment at all tested Ymr111c-dependent and -independent Ub-hotspots (see Figure 9C and Figure 19A). In line with a critical dependence of Cdc48 recruitment on ubiquitylation, the stronger enrichment of the cdc48-6 protein at Ymr111c-dependent Ub-hotspots was also lost in cells that lack Slx8 (*cdc48-6 slx8Δ*; see Figure 19A). In contrast, the enrichment of the mutant cdc48-6 protein at the analysed Ymr111c-independent Ub-hotspot (Hotspot 4) was even slightly increased in the absence of Slx8 (*cdc48-6 slx8Δ*; see Figure 19A). This mild increase in Cdc48 enrichment might result from the enhanced ubiquitylation at the Ymr111c-independent Ub-hotspot in Slx8-deficient cells (see Figure 18D).

The ubiquitin-dependent physical interaction between Cdc48 and Ymr111c-dependent Ub-hotspots suggest that Cdc48 extracts one or several ubiquitylated proteins from chromatin at these genomic positions. On the one hand, based on the findings that Ymr111c binds to Ymr111c-dependent Ub-hotspots and recruits the ubiquitin E3 ligase Slx5-Slx8, it appeared attractive to assume that Ymr111c itself is ubiquitylated and extracted by Cdc48. On the other hand, Ymr111c and ubiquitin enrichments at Ymr111c-dependent Ub-hotspots do not correlate, indicating that Ymr111c is not the ubiquitylated Cdc48 substrate. To address if Ymr111c is a direct target of Cdc48, ChIP of Ymr111c was performed with *WT* and Cdc48-deficient cells *(cdc48-6)*. Interestingly, in *cdc48-6* cells the enrichment of Ymr111c was similar or even mildly decreased compared to *WT* cells at all tested Ymr111c-dependent Ub-hotspots (see Figure 19B). Assuming that Cdc48 indeed acts as a segregase at Ymr111c-dependent Ub-hotspots, this finding suggests that Ymr111c is not the direct target of ubiquitylation and Cdc48 extraction. In line with this idea, first experiments that aimed to detect a ubiquitylated form of Ymr111c were not

successful, even if cells in which ubiquitylation at Ymr111c-dependent Ub-hotspots accumulates (e.g. *cdc48-6* cells) were analysed (data not shown).

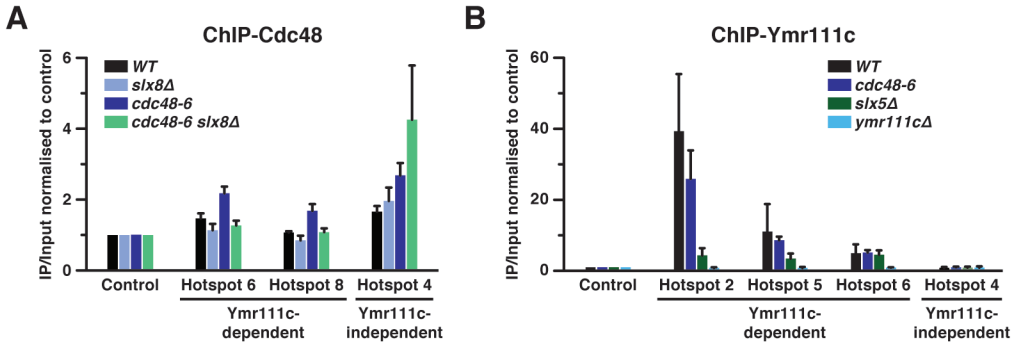

Figure 19: Cdc48 Is Recruited to Ymr111c-dependent Ub-hotspots by Ubiquitylation but Does not Seem to Extract Ymr111c.
(A) Cdc48 recruitment to Ymr111c-dependent Ub-hotspots depends on ubiquitylation by Slx5-Slx8. Cdc48-directed ChIP-RT-PCR was performed with *WT*, *cdc48-6*, and isogenic strains that lack Slx8 (*slx8Δ* and *cdc48-6 slx8Δ*). Cdc48 enrichment was analysed at a control region on chromosome II (control), two Ymr111c-dependent Ub-hotspots (Hotspots 6 and 8), and one Ymr111c-independent Ub-hotspot (Hotspot 4). Shown are IP/Input ratios that were normalised to the control region (IP/Input at control regions is set to 1). Data represents the mean (and the standard deviation) of three independent experiments. Notably, the data of *WT* and *cdc48-6* cells is the same as presented in Figure 9C.
(B) Ymr111c does not accumulate at Ymr111c-dependent Ub-hotspots in Cdc48-deficient cells. Ymr111c-directed ChIP (Ymr111c-ChIP) was performed with *WT*, *ymr111cΔ* (to control for antibody specificity), Cdc48-deficient *(cdc48-6)*, and *slx5Δ* cells. Ymr111c abundance was analysed at a control region on chromosome II (control), three Ymr111c-dependent Ub-hotspots (Hotspots 2, 5, and 6), and one Ymr111c-independent Ub-hotspot (Hotspot 4). Shown are IP/Input ratios that were normalised to the control region (IP/Input at control regions is set to 1). Data represents the mean (and the standard deviation) of three independent experiments. Notably, the data of *WT* and *ymr111cΔ* cells is the same as presented in Figure 15B.

Ymr111c-directed ChIP-RT-PCR experiments conducted with cells that lack one subunit of the Slx5-Slx8 E3 ubiquitin ligase (*slx5Δ*) revealed that Ymr111c enrichment at 2 out of 3 tested Ymr111c-dependent Ub-hotspots was strongly reduced in the absence of Slx5 (see Figure 19B). Despite the fact that this finding also argues against a ubiquitin-dependent chromatin extraction of Ymr111c, the dramatic reduction of Ymr111c abundance in cells lacking Slx5 could indicate that the interaction between Ymr111c and Slx5-Slx8 promotes the binding of Ymr111c to Ymr111c-dependent Ub-hotspots.

All together, Ymr111c-directed ChIP-RT-PCR experiments provide first evidence that Ymr111c is not a direct Cdc48 substrate, but rather facilitates the ubiquitylation of another protein in close proximity by recruitment of the SUMO-targeted E3 ubiquitin ligase Slx5-Slx8. However, to finally proof this model further experiments are required. Most importantly, another protein that is indeed ubiquitylated and extracted by Cdc48 has to be identified.

3.12 Gene Expression Profiling Suggests That Ymr111c Does not Regulate Gene Transcription

Ymr111c plays an important role in ubiquitylation at 7 out of 9 Cdc48-dependent Ub-hotspots (Ymr111c-dependent Ub-hotspots). First evidence suggests that Ymr111c is not ubiquitylated but rather recruits the ubiquitylation machinery to another protein that is associated with Ymr111c-dependent Ub-hotspots. Nevertheless, Ymr111c is closely linked to the physiological role of Ymr111c-dependent Ub-hotspots. Therefore studying the cellular function of Ymr111c is crucial to understand the physiological relevance of Ymr111c-dependent Ub-hotspots.

Given that all 7 Ymr111c-dependent Ub-hotspots peak in intergenic regions, which are typically very small in *S. cerevisiae*, these genomic features could be involved in transcription regulation of neighbouring genes. Interestingly, in line with this idea Ymr111c contains a Gcr1 domain that has also been identified in 3 yeast transcription factors (Gcr1, Msn1, and Hot1). To address if Ymr111c affects gene transcription (in particular of genes next to Ymr111c-dependent Ub-hotspots), genome-wide gene expression profiling using microarrays was performed in cells lacking (*ymr111cΔ*) or overexpressing (from a galactose-inducible *GAL1* promoter; *pGAL-YMR111C*) Ymr111c, and the corresponding *WT* controls[§]. Bioinformatic analysis of the data[**] revealed that deletion of *YMR111C* did not significantly affect the expression level of any gene except for *YMR111C* compared to *WT* cells (with a $\log_2$ fold change cut-off of 1; see Figure 20A). In contrast, overexpression of Ymr111c in a galactose-inducible system (*pGAL-YMR111C*) changed the expression of 211 genes (98 up- and 113 down-regulated with a $\log_2$ fold change cut-off of 1) compared to a *WT* control (*pGAL-empty*; see Figure 20B). However, none of the genes with a promoter in close proximity (approximately 1000 base pairs) to the Ymr111c-dependent Ub-hotspots was affected (see Figure 20B). Given that in *S. cerevisiae* transcription regulators typically bind in close proximity of the affected genes (typically in the range of several hundred base pairs)[155], it appeared rather unlikely that Ymr111c that is bound to Ub-hotspots directly affects gene transcription. The effect on transcription of 211 genes by Ymr111c overexpression might be rather indirectly caused by the toxicity of Ymr111c overexpression that impairs cell growth (see Figure 20C).

[§] Experiments were performed with the help of Kerstin Mair (Cramer laboratory, Gene Center, LMU Munich).
[**] Bioinformatic analysis was performed by Assa Yeroslaviz (Bioinformatic Core Facility, MPI of Biochemistry).

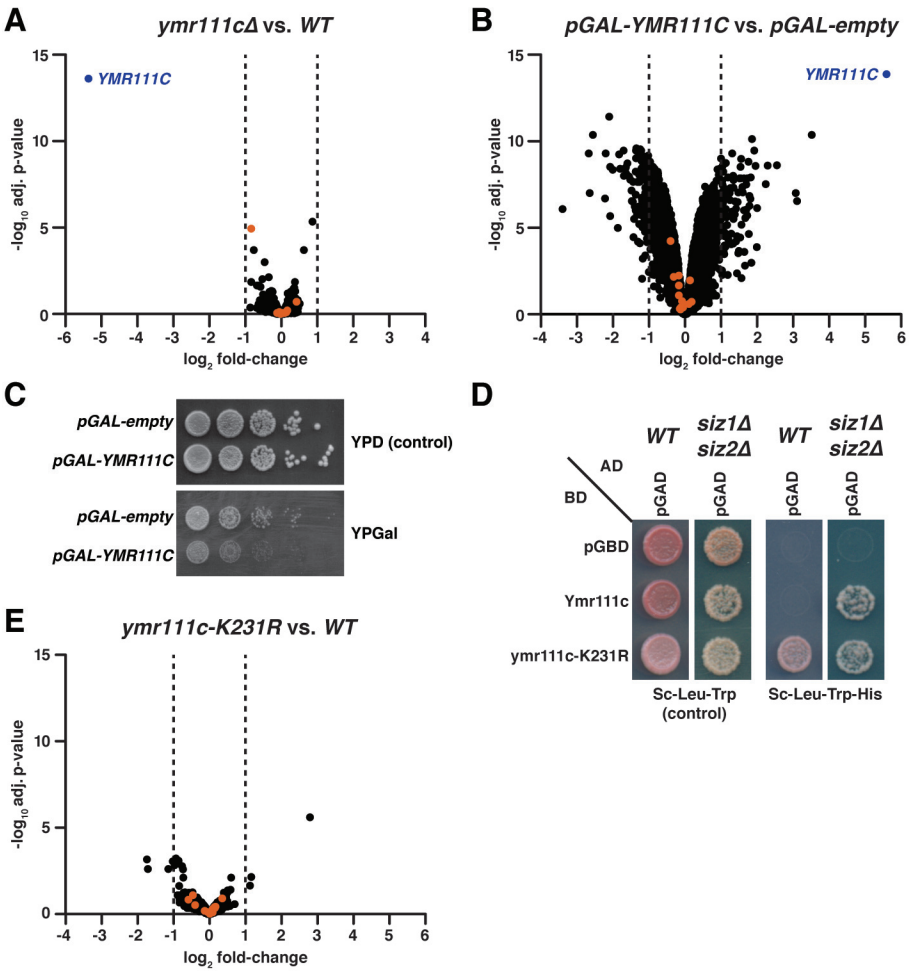

Figure 20: Ymr111c Does not Seem to Regulate Gene Transcription.
(A) Expression of genes close to Ymr111c-dependent Ub-hotspots is unaffected by *YMR111C* deletion. Shown is a volcano plot (plotting of $\log_2$ value of adjusted p-value against $\log_{10}$ value of fold change for all genes) that summarises the results of genome-wide gene expression profiling of cells lacking Ymr111c (*ymr111cΔ*) in comparison to *WT* cells. Each dot represents one gene. Genes with a promoter in close proximity of Ymr111c-dependent Ub-hotspots are highlighted in orange. The data point for *YMR111C* is depicted in blue. Dashed lines indicate the fold change cut-off. Gene expression was measured in three biological replicates per condition using microarrays (GeneChip Yeast Genome 2.0, Affimetrix). Further details on the bioinformatical analysis are described in section 5.4.
(B) Expression of genes close to Ymr111c-dependent Ub-hotspots is unaffected by Ymr111c overexpression. Shown is a volcano plot that summarises the results of genome-wide gene expression profiling of cells overexpressing Ymr111c (from a galactose-inducible *GAL1* promoter; *pGAL-YMR111C*) in comparison to *WT* cells (*pGAL-empty*). See A for further descriptions on the microarray and data visualisation.
(C) Overexpression of Ymr111c interferes with cell growth. 5-fold series dilutions of cells carrying an additional copy of *YMR111C* under control of a *GAL1* promoter (*pGAL-YMR111C*) and control cells (*pGAL-empty*) were spotted on control plates (YPD; *pGAL* "off") and galactose containing plates (YPGal; *pGAL* "on").
(D) Gal4 binding domain (BD) fusions of Ymr111c that are not SUMOylated are auto-activating in the yeast-two-hybrid assay. Yeast-two-hybrid analysis (using a *WT* or siz1*Δ* *siz2Δ* reporter strain) of Ymr111c or its mutant variant ymr111c-K231R (as Gal4 binding domain fusions, BD) with an empty pGAD-C1 vector (expressing free AD) is shown. Growth on plates lacking histidine (Sc-Leu-Trp-His) indicates auto-activation. Plates were incubated at 30°C for 3 days.
(E) Expression of genes close to Ymr111c-dependent Ub-hotspots is unaffected in cells expressing a SUMOylation-deficient mutant variant of Ymr111c *(ymr111c-K231R)*. Shown is a volcano plot that summarises the results of genome-wide gene expression profiling of *ymr111c-K231R* in comparison to *WT* cells. See A for further descriptions on the microarray and data visualisation.

Although gene expression profiling with cells lacking or overexpressing Ymr111c suggested that Ymr111c is not a transcription regulator, an observation in the yeast-two-hybrid analysis of the mutant ymr111c-K231R variant (as a Gal4 DNA binding domain fusion, BD) that cannot be SUMOylated challenged this view (see Figure 20D). In contrast to BD-Ymr111c, the mutated BD-ymr111c-K231R protein confers cell growth on media lacking histidine without the presence of a binding partner that is fused to the Gal4 transcription-activation domain (AD) in a *WT* yeast-two-hybrid reporter strain (*WT;* see Figure 20D). This effect, which is referred to as auto-activation, indicates that SUMOylation-deficient Ymr111c (ymr111c-K231R), triggers *HIS3* reporter gene activation without an AD-binding partner. In line with the idea that Ymr111c SUMOylation interferes with *HIS3* reporter gene activation, BD-Ymr111c triggered auto-activating in a mutated reporter strain that is deficient in Ymr111c SUMOylation by deletion of the SUMO E3 ligases Siz1 and Siz2 (*siz1Δ siz2Δ*) but not in a WT control (see Figure 20D). Mechanistically, unmodified Ymr111c could either directly trigger transcription activation, or recruit an endogenously expressed transcription factor.

To address if Ymr111c that is not SUMOylated indeed activates transcription, genome-wide gene expression profiling using microarrays was performed with cells that express the mutant ymr111c-K231R variant as the only source of Ymr111c. In total, 6 genes (with a $\log_2$ fold change cut-off of 1) were differentially expressed in *ymr111c-K231R* cells compared to *WT* cells (see Figure 20E). However, the expression of genes in close proximity of Ymr111c-dependent Ub-hotspots was unaffected in *ymr111c-K231R* cells (see Figure 20E). Therefore, despite the evidence provided by the yeast-two-hybrid auto-activation, this data suggests that SUMOylation-deficient Ymr111c (ymr111c-K231R) does not affect transcription of genes in close proximity to Ymr111c-dependent Ub-hotspots. Given that it appears rather unlikely that Ymr111c and Ub-hotspots regulate gene transcription, alternative models for the physiological role of Ymr111c and Ub-hotspots have to be investigated in future. Some cellular processes that might be regulated by the complex Cdc48-dependent protein extraction pathway at Ymr111c-dependent Ub-hotspots are discussed in section 4.4.

4 Discussion

4.1 Identification of 9 Cdc48-dependent Ub-hotspots

Many chromatin-associated proteins are modified with ubiquitin either to target them for proteasomal degradation or to trigger non-proteolytic functions. Recently, the role of the segregase Cdc48 (p97 in humans) in extraction of ubiquitylated proteins from chromatin has arisen to one of the major research fields in chromatin-related functions of the ubiquitin system[124]. A number of studies demonstrated that Cdc48/p97 extracts ubiquitylated proteins that are important for cellular processes such as mitosis[125], DNA replication[127,128], transcription[140,142], and the DNA damage response[132,133] from chromatin. However, despite the identification of individual Cdc48 substrates on chromatin, it has not been addressed if Cdc48 action is limited to few substrates or might rather be of general importance for chromatin extraction and proteasomal degradation of chromatin-bound proteins.

To globally address the role of Cdc48 in chromatin extraction of ubiquitylated proteins, I established ubiquitin-directed chromatin immunoprecipitation (ChIP) in combination with genome-wide tiling microarrays (Ub-ChIP-chip). This experimental setup enabled for the first time the detection of the relative distribution of ubiquitylated proteins on chromatin in *S. cerevisiae*. Applying this technique to yeast strains with different genetic backgrounds allowed studying the relative distribution of ubiquitylated proteins on chromatin, and the impact of Cdc48 function on this distribution.

First, the analysis of wild-type *(WT)* yeast cells identified that the vast majority of ubiquitin-enriched genomic positions is tightly linked to monoubiquitylation of the core histone H2B (H2B-Ub; see Figure 7). H2B-Ub-independent enrichment of ubiquitin conjugates was only detected at very few chromosomal locations (referred to as Ub-hotspots), even in cells that were impaired in H2B-Ub (see Figure 7).

Second, experiments with Cdc48-deficient yeast cells suggest that Cdc48 dysfunction globally affects the relative distribution of ubiquitylated proteins on chromatin, probably resulting from an increase in steady-state chromatin ubiquitylation (see Figure 8). Together with previous studies that identified individual Cdc48 substrates on chromatin[124], my data suggests that ubiquitin-dependent chromatin extraction by Cdc48 is a frequently used mechanism in cells. Even more importantly, my ubiquitin-directed ChIP-chip experiments using Cdc48-deficient cells led to the identification of 9 genomic positions at which ubiquitin conjugates strongly accumulated compared to WT cells

(referred to as Cdc48-dependent Ub-hotspots; see Figure 9). Cdc48-dependent Ub-hotspots are genome-wide the chromosomal locations with the by far highest ubiquitin enrichment in Cdc48-deficient cells, underlining the critical importance of Cdc48 at these genomic positions. Strikingly, 8 out of 9 Cdc48-dependent Ub-hotspots were identical with the H2B-Ub-independent Ub-hotspots in *WT* cells, indicating that ubiquitylation and chromatin extraction take constantly place at these genomic positions. Subsequent analysis revealed that Cdc48-dependent Ub-hotspots are mainly enriched in K48-linked ubiquitin conjugates that probably trigger protein degradation (see Figure 10). The predominant accumulation of K48-linked ubiquitin conjugates at Cdc48-dependent Ub-hotspots in Cdc48-deficient cells suggests that Cdc48 extracts K48-ubiquitylated proteins from chromatin, which are subsequently targeted for proteasomal degradation (see Figure 10).

Notably, detailed analysis of the 9 Cdc48-dependent Ub-hotpots revealed that 7 of these genomic features contain a conserved DNA sequence motif, which is sufficient to trigger ubiquitin accumulation at an artificial ectopic genomic locus (see Figure 12 and Figure 13). Subsequent yeast-one-hybrid screens and ChIP experiments revealed that the previously uncharacterised *S. cerevisiae* protein Ymr111c associates with this conserved DNA sequence motif (see Figure 14 and Figure 15). Ymr111c is strictly required for ubiquitin accumulation at all 7 Cdc48-dependent Ub-hotspots that contain the conserved DNA motif (referred to as Ymr111c-dependent Ub-hotspots), but not at the two remaining Cdc48-dependent Ub-hotspots (referred to as Ymr111c-independent Ub-hotspots; see Figure 15). Based on this finding this study revealed important principles of Cdc48-dependent chromatin extraction and protein ubiquitylation. First, given that ubiquitin-directed ChIP detects two subgroups of Cdc48-dependent Ub-hotspots, the systematic analysis of Cdc48 co-factor mutants (see Figure 11) has provided first evidence that chromatin extraction of different substrates involves the same set of Cdc48 co-factors. Second, a SUMO-dependent ubiquitylation mechanism at Ymr111c-dependent Ub-hotspots was identified, and shed new light on the mechanism of the SUMO-targeted E3 ubiquitin ligase (STUbL) Slx5-Slx8. Both the existence of a chromatin-specific Cdc48 complex, and the newly identified multi-step ubiquitylation mechanism and its implications to the mechanism of STUbLs will be discussed in detail in the next sections. Lastly, also speculative models for the currently unknown physiological function of Ymr111c-dependent Ub-hotspots will be discussed.

4.2 Cdc48-dependent Chromatin Extraction of Ubiquitylated Proteins Involves a Distinct Cdc48 Co-factor Subset

To act as a segregase in different cellular contexts, Cdc48/p97 requires a large number of co-factors, which mediate substrate recruitment and substrate processing[73]. At most cellular compartments Cdc48/p97 function appears to involve a rather distinct subset of Cdc48/p97 co-factors. For instance, in endoplasmic-reticulum-associated degradation (ERAD) Cdc48/p97 acts together with the major substrate-recruiting co-factor Ufd1-Npl4[108-110], the membrane-bound Ubx2/Ubxd8[91,98], and the substrate processing co-factors Ufd2[102] and Otu1/Yod1[103,156]. In contrast to ERAD, Cdc48/p97 co-factors that are important for Cdc48/p97-dependent chromatin extraction have not been studied intensively except for Ufd1-Npl4 that acts as the major substrate-recruiting co-factor for all currently studied chromatin substrates of Cdc48/p97[124].

Given that only 7 out of 9 Cdc48-dependent Ub-hotspots that have been identified in this study depend on Ymr111c and the SUMO-targeted ubiquitin ligase Slx5-Slx8 (see Figure 15 and Figure 18), ubiquitin-directed ChIP experiments monitored at least two prominent Cdc48 substrates on chromatin. Interestingly, chromatin extraction of ubiquitylated proteins at both Ymr111c-dependent and -independent Ub-hotspots involved the Cdc48 co-factors Ufd1-Npl4, Ubx4 and Ubx5 (see Figure 11), suggesting that this set of co-factors might be of general importance in Cdc48-dependent chromatin extraction. Notably, all other tested co-factors, including almost all currently described Cdc48 co-factors in yeast, did not significantly influence chromatin extraction, but might still be involved in substrate processing or proteasome delivery.

The identification of Ufd1-Npl4, Ubx4, and Ubx5 as crucial components of the chromatin extraction at both Ymr111c-dependent and –independent Ub-hotspots suggested that these co-factors might form a complex with Cdc48 that is generally important for chromatin extraction (see Figure 21). Whereas Ufd1-Npl4 has been previously described as major substrate-recruiting Cdc48/p97 co-factor in chromatin extraction by several independent studies[125,127,128,132,133,140,142], Ubx4 and Ubx5 have so far only been implicated in degradation of the largest subunit of irreversibly stalled RNA polymerase II (Rpb1) in yeast[142]. In contrast to the previous study on Rpb1 degradation[142], the ChIP experiments performed in this thesis indicate at which step of the Cdc48-dependent chromatin extraction Ubx4 and Ubx5 act. Whereas previously only defects in proteasomal degradation downstream of Cdc48 function have been assayed[142], ChIP

experiments performed in this thesis demonstrated that Ubx4 and Ubx5 are required prior to or during substrate extraction (see Figure 11).

Mechanistically, Ubx5 might assist Ufd1-Npl4 in substrate recruitment, because it contains two ubiquitin-binding domains (UBA and UIM domain)[89]. Recent studies suggested that Ubx5 and its human homologue Ubxd7 directly couple Cdc48/p97 to ubiquitin E3 ligases of the cullin family[104,157]. Therefore it is tempting to speculate that Ubx5 facilitates Cdc48 substrate recognition on chromatin by spatially linking ubiquitylation and substrate binding. Given that ubiquitylation at Ymr111c-dependent Ub-hotspots is not mediated by cullin-based E3 ligases but Slx5-Slx8, this model requires that Ubx5 physically links Cdc48 also to other E3 ubiquitin ligases such as Slx5-Slx8. Interestingly, in ERAD, Ubx2, another member of the UBX domain containing protein family, also spatially links substrate ubiquitylation and Cdc48-substrate recruitment[91]. This correlation suggests that the physical coupling of ubiquitylation and substrate recognition might be conserved for Cdc48 functions in all cellular contexts.

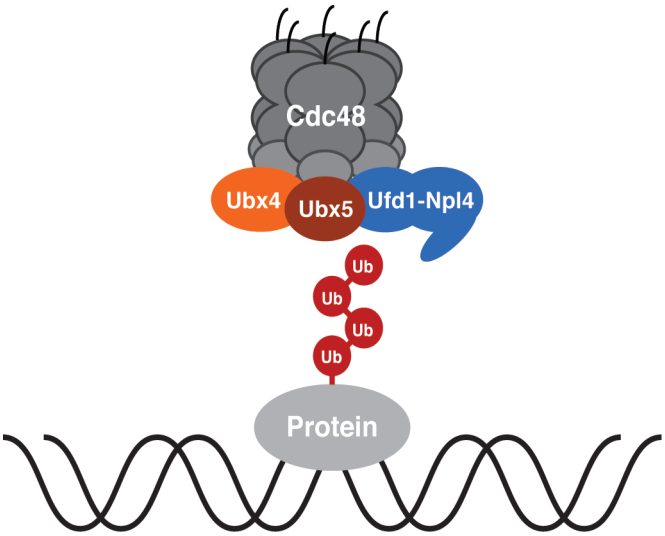

Figure 21: Ubiquitin-dependent Chromatin Extraction by Cdc48 Involves the Co-factors Ufd1-Npl4, Ubx4, and Ubx5.
To extract ubiquitylated proteins from chromatin, yeast Cdc48 seems to form a compartment-specific complex with its co-factors Ufd1-Npl4 (blue), Ubx4 (orange), and Ubx5 (dark red). It is still unclear if all three co-factors bind simultaneously to the same Cdc48 hexamer as depicted in this cartoon. Moreover, also the binding stoichiometry unknown and only depicted schematically.

Ubx4 is the only member of the UBX protein family in *S. cerevisiae* that does not contain a ubiquitin-binding domain[89]. Therefore it appears rather unlikely that Ubx4 is involved in the recruitment of Cdc48 substrates on chromatin. Evidence from studies on ERAD suggests that Ubx4 somehow facilitates Cdc48 segregase function[158]. In particular, it has been speculated that Ubx4, which contains two ubiquitin-like-domains (UBL domains), might facilitate proteasome delivery in ERAD and potentially other Cdc48-dependent degradation pathways[158]. However, given that our study demonstrates that Ubx4 acts upstream or during chromatin extraction (see Figure 11), it appears very likely that Ubx4

triggers Cdc48 segregase activity more directly, for instance by facilitating the Cdc48 ATPase activity.

Together, the results obtained in this study strongly suggest that besides Ufd1-Npl4, Ubx4 and Ubx5 are important components of the Cdc48 machinery that mediates ubiquitin-dependent chromatin extraction. Most importantly, the data indicates that both Ubx4 and Ubx5 are mechanistically important prior to or during substrate extraction. Using the identified Cdc48-dependent Ub-hotspots as a tool, it might be possible to mechanistically characterise both proteins in more detail in the future. For instance, Cdc48-dependent Ub-hotspots could serve as “model substrates” in a classical structure-function analysis of Ubx4 and Ubx5. Compared to the other chromatin-bound substrates of Cdc48/p97, using the Cdc48-dependent Ub-hotspots for structure-function analysis has the great advantage that chromatin extraction can be robustly and quantitatively monitored by ChIP experiments.

4.3 Ubiquitylation Mechanism and Substrate(s) at Ymr111c-dependent Ub-hotspots

In this study 9 Cdc48-dependent Ub-hotspots were identified and subsequently classified into Ymr111c-dependent and –independent Ub-hotspots (see Figure 9 and Figure 15). Whereas the information on Ymr111c-independent Ub-hotspots is still limited to the fact that Cdc48 extracts ubiquitylated proteins at these genomic positions, Ymr111c-dependent Ub-hotspots were characterised in detail. A number of experiments on Ymr111c-dependent Ub-hotspots discovered a complex two-step ubiquitylation reaction that involves ubiquitin and the ubiquitin-like modifier SUMO. This section will not only discuss the ubiquitylation mechanism and its implications for the understanding of SUMO-targeted ubiquitylation reactions, but also the identity of the ubiquitylation substrate(s).

A series of experiments in this study consistently demonstrated that ubiquitylation at Ymr111c-dependent Ub-hotspots is mediated by a two-step mechanism that involves multiple components (see Figure 22). First, Ymr111c is modified with the ubiquitin-like modifier SUMO on lysine-231 (see Figure 16). Second, SUMOylated Ymr111c recruits the heterodimeric SUMO-targeted E3 ubiquitin ligase (STUbL) Slx5-Slx8, which subsequently catalyses protein ubiquitylation (see Figure 18). In line with Slx5-Slx8 acting as a STUbL, several lines of evidence suggest that Slx5-Slx8 recruitment to Ymr111c strongly depends on SUMOylation, which is achieved by the SUMO conjugating enzyme Ubc9 in combination with the SUMO E3 ligases Siz1 or Siz2 (see Figure 17 and Figure 18). Both

Siz1 and Siz2 are normally bound to chromatin via their SAP domains[48,49], indicating that Ymr111c SUMOylation and subsequent Slx5-Slx8 recruitment occurs on chromatin.

Notably, prior to this study *in vivo* evidence on the SUMO-dependent recruitment of Slx5-Slx8 to its substrates was rather limiting. So far only the transcription regulators Matα2[64] and Mot1[159] have been identified as *in vivo* Slx5-Slx8 substrates. Given that Slx5-Slx8 targets Matα2 in a SUMO-independent manner[64], and that the contribution of SUMO to the physical interaction between Slx5-Slx8 and Mot1 has not been directly analysed[159], the importance of SUMO for Slx5-Slx8 substrate binding *in vivo* has not been formally proven. By demonstrating that both ubiquitylation at Ymr111c-dependent Ub-hotspots and the interaction between Ymr111c and Slx5-Slx8 critically depend on SUMOylation of Ymr111c (see Figure 17 and Figure 18), my study not only expands the list of identified Slx5-Slx8 substrates, but also provides *in vivo* evidence that SUMOylation is crucial for binding of some Slx5-Slx8 substrates. However, to gain a more comprehensive picture of Slx5-Slx8 and STUbL substrate recognition, the list of Slx5-Slx8 and STUbL substrates needs to be further expanded in future.

Previous studies have suggested that STUbLs like Slx5-Slx8 are preferentially targeted to polySUMOylated substrates[65,69,70]. However, Ymr111c efficiently recruits Slx5-Slx8 to Ymr111c-dependent Ub-hotspots, despite the fact that it appears to be mainly mono-SUMOylated (see Figure 16). This finding suggests that mono-SUMOylation is sufficient to facilitate Slx5-Slx8 recruitment *in vivo*. In line with this idea, initial experiments using a mutant SUMO variant that is defective in SUMO chain formation (by replacement of all lysine residues by arginine), revealed that ubiquitylation at Ymr111c-dependent Ub-hotspots does not depend on SUMO chain formation (data not shown).

Interestingly, Slx5-Slx8 function has been recently linked to the nuclear periphery and nuclear pore[67]. Both Slx5 and Slx8 partially co-localise with nuclear pore proteins, and physically interact with the nuclear pore component Nup84[67]. Functionally, the nuclear pore association of Slx5-Slx8 seems to be particularly important for a DNA repair pathway that deals with irreparable DNA double-strand breaks (DSBs) and collapsed replication forks[67]. Despite these implications, it has not been analysed if the interaction between Slx5-Slx8 and nuclear pore components is important for ubiquitylation of Slx5-Slx8 substrates. The strict dependence of ubiquitylation at Ymr111c-dependent Ub-hotspots on the expression of Nup84 (see Figure 18) suggests that the physical interaction between Slx5-Slx8 and the nuclear pore is indeed critical for substrate ubiquitylation. Based on this finding it is tempting to speculate that more or even all Slx5-Slx8 substrates might be ubiquitylated at the nuclear pore. In addition, this finding strongly suggests that Ymr111c-

dependent Ub-hotspots at least transiently localise to the nuclear periphery. Given that irreparable DSBs relocate to the nuclear periphery in a SUMO-dependent manner[160], it is attractive to assume that SUMOylation of Ymr111c triggers relocation of Ymr111c-dependent Ub-hotspots to nuclear pores.

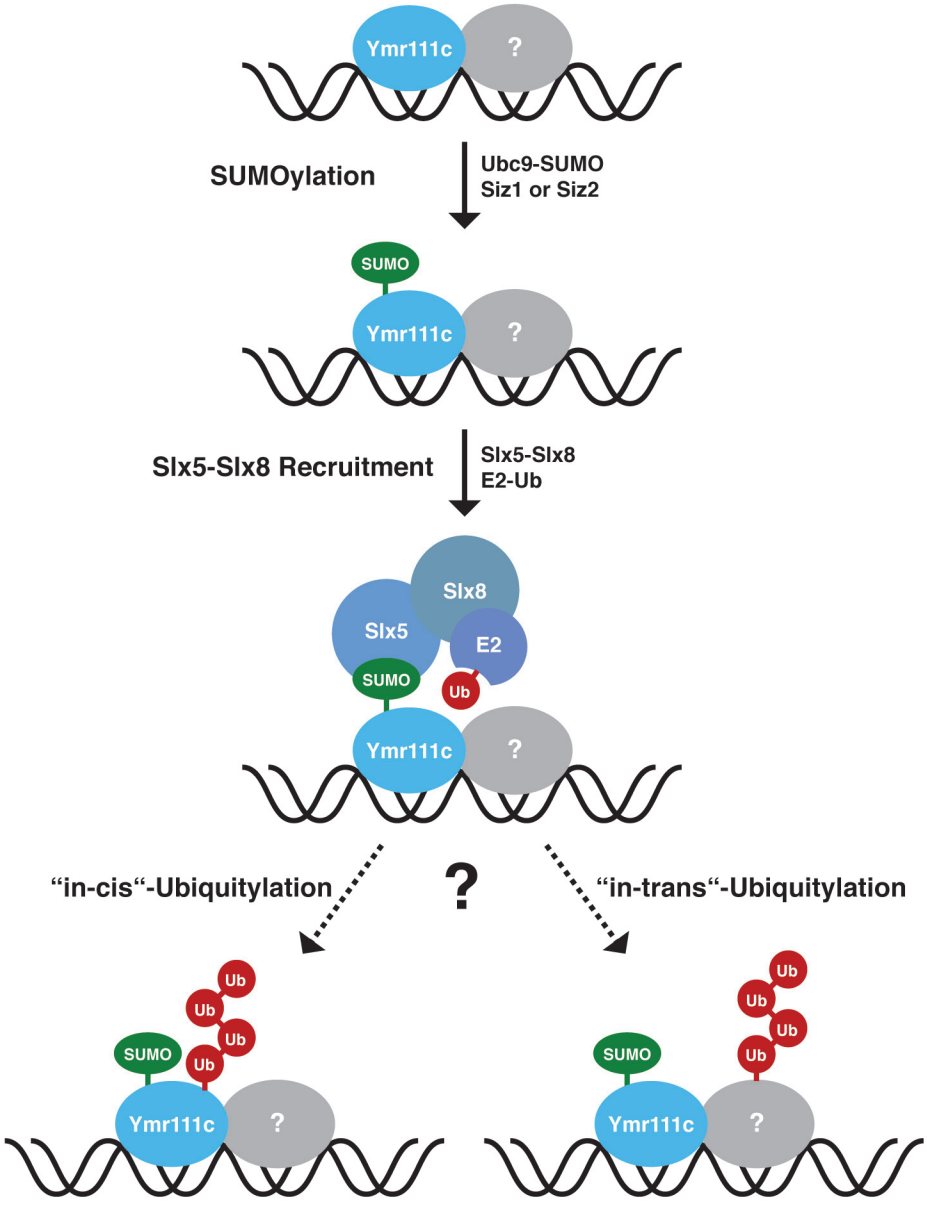

Figure 22: Two-step Ubiquitylation at Ymr111c-dependent Ub-hotpots.
Ubiquitylation at Ymr111c-dependent Ub-hotspots is mediated in a two-step mechanism, involving the heterodimeric SUMO-targeted E3 ubiquitin ligase (STUbL) Slx5-Slx8. First, SUMO-charged Ubc9 (Ubc9-SUMO) and either Siz1 or Siz2 (SUMO E3 ligases) attach SUMO to lysine-231 of Ymr111c. Second, the STUbL Slx5-Slx8 is recruited to Ymr111c in a SUMOylation-dependent manner by the SUMO-interaction motifs (SIMs) of Slx5. And lastly, the RING domain of Slx8 triggers ubiquitylation at Ymr111c-dependent Ub-hotspots by bringing a ubiquitin-charged E2 enzyme (E2-Ub) in close proximity to the ubiquitylation target. Given that the ubiquitylation substrate has not been identified so far, ubiquitin (Ub) could be either attached "in-cis" to Ymr111c or "in-trans" to a currently unknown binding partner of Ymr111c.

In this study, a detailed view on the mechanism of ubiquitylation at Ymr111c-dependent Ub-hotspots by the STUbL Slx5-Slx8 was obtained. Despite these mechanistic insights, the exact identity of the ubiquitylation substrate at Ymr111c-dependent Ub-hotpots is still unclear. Given that Slx5-Slx8 physically interacts with SUMOylated Ymr111c, it appears attractive to assume that Ymr111c is also ubiquitylated ("in-cis"; see Figure 22). However, first approaches to identify a ubiquitylated species of Ymr111c failed. In addition, other experimental evidences argue against Ymr111c as a ubiquitylation target. First, ubiquitin conjugates but not Ymr111c itself strongly accumulated at Ymr111c-dependent Ub-hotspots in Cdc48-deficient cells (see Figure 19). Second, at individual Ymr111c-dependent Ub-hotspots, the relative enrichments of the protein Ymr111c and ubiquitin conjugates did not correlate (see Figure 15). And lastly, in cells lacking Slx5 or Slx8, the enrichment of Ymr111c at Ymr111c-dependent Ub-hotspots was strongly decreased (see Figure 19). Thus, several lines of evidence argue against Ymr111c as a direct ubiquitylation target.

Assuming that Ymr111c is indeed not the target of Slx5-Slx8-dependent ubiquitylation, it seems very likely that SUMOylated Ymr111c recruits Slx5-Slx8, which subsequently ubiquitylates a binding partner of Ymr111c "in-trans" (see Figure 22). In line with the idea that STUbLs like Slx5-Slx8 might also be capable of ubiquitylation "in-trans", a recent study demonstrated that the yeast STUbL Rad18 can ubiquitylate all three subunits of a PCNA trimer, even if only one subunit is SUMOylated[68]. In order to proof this model in the context of Ymr111c-dependent Ub-hotspots, future experiments should aim to identify ubiquitylated interaction partners of Ymr111c. An attractive strategy to identify proteins that are ubiquitylated in a Ymr111c-dependent manner is to compare the abundance of ubiquitylated proteins in *WT* and *YMR111C*-deleted cells by mass-spectrometry. Alternatively, ubiquitylated proteins that are extracted from Ymr111c-dependent Ub-hotspots by Cdc48 could also be identified by a mass-spectrometry-based analysis of co-immunoprecipitating interaction partners of Ymr111c in *WT* and Cdc48-deficient cells.

4.4 Speculative Models for the Physiological Role of Cdc48-dependent Chromatin Extraction at Ymr111c-dependent Ub-hotspots

Ymr111c-dependent Ub-hotspots are among the chromosomal locations with the highest ubiquitin enrichment in *WT S. cerevisiae* cells. The accumulation of ubiquitin conjugates at Ymr111c-dependent Ub-hotspots is strongly enhanced in Cdc48-deficient cells (see

Figure 15), suggesting that Cdc48 constantly extracts ubiquitylated proteins at these genomic positions. Given that ubiquitylation and Cdc48-dependent chromatin extraction are both energy-consuming processes, it is tempting to speculate that extraction of ubiquitylated proteins from Ymr111c-dependent Ub-hotspots has important cellular relevance, although its precise physiological function has not been identified so far. In this section, speculative models for the physiological roles of Cdc48-dependent chromatin extraction at Ymr111c-dependent Ub-hotspots will be discussed.

First evidence for the physiological role of the extraction of ubiquitylated proteins from Ymr111c-dependent Ub-hotspots is provided by the domain structure of the Ymr111c protein. Interestingly, Ymr111c contains a Gcr1 domain, which has also been identified in three yeast transcription factors (Gcr1, Msn1, and Hot1). Together with the intergenic localisation of Ymr111c-dependent Ub-hotspots, the presence of a Gcr1 domain suggests that Ymr111c might be a transcription regulator. However, genome-wide gene expression profiling experiments revealed that neither the deletion and overexpression of *YMR111C*, nor the mutation of the Ymr111c SUMO acceptor site affected the expression levels of genes in short distance to the Ymr111c-dependent Ub-hotspots (see Figure 20). Considering that in *S. cerevisiae* transcription regulators typically bind in close proximity of the affected genes[155], it seems rather unlikely that the extraction of ubiquitylated proteins from Ymr111c-dependent Ub-hotspots regulates gene expression. However, the performed experiments cannot fully rule out that Ymr111c-dependent Ub-hotspots function in transcription regulation. On the one hand, a second pathway might act in parallel to the Cdc48-dependent chromatin extraction, thereby compensating defects caused by deletion, overexpression or mutation of *YMR111C*. In such a case, only the interference with both pathways might significantly alter transcription of genes in close proximity to Ymr111c-dependent Ub-hotspots. On the other hand, given that in the microarray analysis only the expression levels of genes were measured, the extraction of ubiquitylated proteins at Ymr111c-dependent Ub-hotspots could also regulate the transcription of non-coding RNA. Keeping in mind that deficiency in SUMOylation of the Gal4 DNA-binding domain fusion of Ymr111c lead to auto-activation in yeast-two-hybrid analysis (see Figure 20), it is very interesting to study both scenarios in future.

Instead of transcription regulation also other cellular processes might be regulated by chromatin extraction of ubiquitylated proteins at Ymr111c-dependent Ub-hotspots. Evidence pointing to a transcription-independent role of these genomic features was provided by the recent identification of so-called centromere-like regions (CLRs) in *S. cerevisiae*[161]. CLRs are chromosomal locations that do not overlap with centromeres, but

are associated with the centromeric histone variant Cse4 (also called CENP-A) and other kinetochore components (Ndc10, Ndc80, and Mif2)[161]. Interestingly, 1 out of 2 CLRs, for which centromere-like activity could be confirmed in plasmid-based assays[161], partially overlaps with a Ymr111c-dependent Ub-hotspot (Hotspot 1). Notably, a centromere-like activity of CLRs was only observed in cells that overexpress the centromere-specific histone variant Cse4, indicating that the assembly of CLRs is negatively regulated under normal conditions[161]. In line with a negative regulation, it has been previously observed that ubiquitylation and proteasomal degradation of Cse4 is important to restrict Cse4 binding to centromeres[162]. Based on this evidence, it is an attractive hypothesis that all 7 Ymr111c-dependent Ub-hotspots might be CLRs at which Cdc48 constantly extracts ubiquitylated Cse4 from chromatin in order to negatively regulate CLR assembly. To test this model, it needs to be addressed first if all 7 Ymr111c-dependent Ub-hotspots can indeed function as CLRs, and second Cse4 extraction needs to be monitored by ChIP experiments.

Given that the STUbL Slx5-Slx8 mediates ubiquitylation at Ymr111c-dependent Ub-hotspots, chromatin extraction by Cdc48 at these genomic loci could also be linked to known Slx5-Slx8 function. Notably, Slx5-Slx8 has been tightly linked to a DNA repair pathway that acts on DNA double-strand breaks (DSBs) or collapsed replication forks, which cannot be repaired by homologous recombination[67,163]. Interestingly, this repair pathway is linked to the nuclear periphery, where a significant pool of Slx5-Slx8 is localised and physically interacts with the nuclear pore component Nup84[67]. Since both the DNA repair pathway and the ubiquitylation at Ymr111c-dependent Ub-hotspots require not only Slx5-Slx8 but also the nuclear pore component Nup84 (see Figure 18)[67], it seems possible that both pathways are functionally linked. For instance, Ymr111c-dependent Ub-hotspots could be genomic positions that are particularly frequently targeted by the Slx5-Slx8-dependent DNA repair pathway. However, this model is highly speculative, considering that it implies that DNA damage occurs extremely frequently at Ymr111c-dependent Ub-hotspots compared to other genomic loci.

Alternatively, as discussed before (see 4.3), Nup84 association of Slx5-Slx8 might play a much broader role in ubiquitylation of Slx5-Slx8 substrates, and could be also functionally important for other pathways than DNA repair. Given that the list of known Slx5-Slx8 substrates is very limited, it is currently difficult to speculate about other cellular functions. However, independent of the physiological role of such a pathway, it is a very interesting molecular concept that ubiquitylation by Slx5-Slx8 and Cdc48 extraction regulates the association of Ymr111c-dependent Ub-hotspots with the nuclear periphery.

Notably, such a pathway would represent an attractive possibility to regulate local nuclear architecture by fine-tuning the association of genomic positions with the nuclear periphery. The importance of the positioning of DNA loci relative to the nuclear envelope has been illustrated by its functional link to cellular pathways such as DNA replication, transcription, and DNA repair[164].

Based on the current data, the physiological relevance of ubiquitylation and Cdc48-dependent chromatin extraction at Ymr111c-dependent Ub-hotspots still remains enigmatic. Nevertheless, many potential links to known cellular pathways exist and are a good starting point for future studies, which will eventually lead to a model why ubiquitylation and Cdc48-dependent chromatin extraction seem to constantly take place at Ymr111c-dependent Ub-hotspots under normal growth conditions.

5 Materials and Methods

Unless otherwise mentioned, chemicals (analytical pure), reagents, and materials were purchased from Agilent, Applied Biosystems, BD, Biomol, Bioneer, Bio-Rad, GE Healthcare, Kodak, Life Technologies, Merck, New England Biolabs, PeqLab, Promega, Qiagen, Roth, Roche, Serva, Sigma, or Thermo Scientific. For all procedures described, sterile flasks, solutions, and deionised water were used. Basic microbiological, molecular biological, and biochemical techniques followed standard protocols[165,166].

5.1 Microbiological Techniques

5.1.1 *Escherichia Coli (E. Coli)* Techniques

E. Coli Strains

Strain	Genotype	Source
XL1-Blue	*recA1 endA1 gyrA96 thi-1 hsdR17(r_K^- m_K^+) supE44 relA1 lac [F´ proAB lacIqZΔM15 Tn10 (Tetr)]*	Agilent
Mach1^{TM} T1^{R}	*F´ϕ80(lacZ)ΔM15 ΔlacX74 hsdR(r_K^- m_K^+) ΔrecA1398 endA1 tonA*	Life Technologies

E. Coli Media

LB Medium/Plates

1% (w/v) trypton
0.5% (w/v) yeast extracts
1% (w/v) NaCl
1.5% (w/v) agar (only for plates)
sterilised by autoclaving

For plasmid selection, ampicillin (100 µg/ml), kanamycin (30 µg/ml), or chloramphenicol (34 µg/ml) were added.

Competent *E. Coli* Cells

For the preparation of electro-competent *E. coli* cells, 1 l liquid LB medium was inoculated from a fresh overnight culture (inoculated from a single bacterial colony) and grown to a final OD_{600} of 0.6-0.8 at 37°C. Subsequently, the culture was chilled in ice-cold water for 30 min, and cells were harvested by centrifugation (10 min, 5000 *g*, 4°C). The sedimented cells were carefully resuspended in 1 l of pre-chilled water, harvested by centrifugation, and washed three times with 0.5 l of a pre-chilled 10% (v/v) glycerol solution. After a final

washing step with 50 ml of 10% (v/v) glycerol, the bacterial pellet was resuspended in 3 ml 10% (v/v) glycerol, frozen in 50 µl aliquots with liquid nitrogen, and stored at -80°C.

Transformation of *E. Coli* Cells

Transformation of plasmid DNA into *E. coli* cells was achieved by electroporation. Shortly before transformation, 50 µl of electro-competent cells were thawed on ice and mixed with 1-500 ng plasmid DNA or 1-5 µl of a dialysed ligation reaction (see 5.2.3, "Ligation"). Electroporation was performed in a pre-chilled cuvette (0.1 cm electrode gap; Bio-Rad) with a pulse of 1.8 kV and 25 µF at a resistance of 200 Ω using a Gene Pulser X-cell (Bio-Rad). After electroporation, cells were recovered in 1 ml LB medium and incubated on a shaker (800 rpm) at 37°C for 1 h. For selection of transformants, the cells were plated on LB plates containing the appropriate antibiotics (mostly ampicillin) and incubated overnight at 37°C.

5.1.2 *Saccharomyces Cerevisiae (S. Cerevisiae)* Techniques

S. Cerevisiae Strains

All yeast strains used in this study were isogenic to DF5, W303, PJ69-7, or YM4271. Genetic manipulation was performed as described below (see "Genetic Manipulation of *S. Cerevisiae*"). Some of the genetic manipulations were initially performed in diploid cells, and the listed haploid strains were generated by sporulation and tetrad dissection (see "Mating, Sporulation, and Tetrad Analysis"). For the construction of most yeast strains with multiple gene deletions or chromosomal taggings, respective haploid *S. cerevisiae* cells of opposite mating type were crossed, diploid cells were sporulated, and tetrads were dissected (see "Mating, Sporulation, and Tetrad Analysis").

Strain	Genotype	Source
DF5	*trp1-1 ura3-52 his3Δ200 leu2-3,11 lys2-801*	Ref.167
MJK183	*DF5, MATa htb2Δ::hphNT1; Htb1-K123R-tADH::kanMX6*	I. Psakhye
Y0066	*DF5, MATa rad6Δ::HIS3*	Ref.37
Y0649	*DF5, MATa cdc48-6*	Ref.120
Y0650	*DF5, MATα cdc48-6*	Ref.120
MJK503	*DF5, MATa cdc48-3::LEU2*	This study
Y2305	*DF5, MATa ump1Δ::hphNT1*	Jentsch strain collection
Y1912	*DF5, MATa rad23Δ::kanMX6 dsk2::kanMX6*	Ref.102
Y0472	*DF5, MATa ufd1-2*	Ref.120
Y0802	*DF5, MATa npl4-1*	Ref.120
YAB1729	*DF5, MATa shp1-7*	Ref.168
MJK100	*DF5, MATa ubx2Δ::kanMX6*	A. Buchberger
MJK101	*DF5, MATa ubx3Δ::kanMX6*	A. Buchberger
Y0845	*DF5, MATa ubx4Δ::hisMX6*	Jentsch strain collection
MJK102	*DF5, MATa ubx5Δ::kanMX6*	A. Buchberger
MJK103	*DF5, MATa ubx6Δ::kanMX6*	A. Buchberger
MJK104	*DF5, MATa ubx7Δ::kanMX6*	A. Buchberger
Y3387	*DF5, MATα vms1Δ::kanMX6*	Jentsch strain collection
Y0597	*DF5, MATa ufd2Δ::LEU2*	Ref.6
Y0578	*DF5, MATa ufd3Δ::HIS3*	Ref.103
Y1908	*DF5, MATa otu1Δ::kanMX4*	Ref.103
MJK253	*DF5, MATα cdc48-6 YIplac128-empty::LEU2*	This study
MJK256	*DF5, MATα cdc48-6 YIplac128-Hotspot 5::LEU2*	This study
MJK257	*DF5, MATα cdc48-6 YIplac128-Hotspot 5-F1::LEU2*	This study
MJK258	*DF5, MATα cdc48-6 YIplac128-Hotspot 5-F2::LEU2*	This study
MJK259	*DF5, MATα cdc48-6 YIplac128-Hotspot 5-F3::LEU2*	This study
MJK260	*DF5, MATα cdc48-6 YIplac128-Hotspot 5-F4::LEU2*	This study
MJK303	*DF5, MATα cdc48-6 YIplac128-Hotspot 5-F5::LEU2*	This study
MJK325	*DF5, MATα cdc48-6 YIplac128-Hotspot 5-F6::LEU2*	This study
MJK354	*DF5, MATα cdc48-6 YIplac128-Hotspot 5-F7::LEU2*	This study
MJK355	*DF5, MATα cdc48-6 YIplac128-Hotspot 5-F7-Mut::LEU2*	This study
MJK337	*DF5, MATα cdc48-6 YIplac128-Hotspot 5-F8::LEU2*	This study
YM4271	*MATa, ura3-52, his3-200, ade2-101, ade5, lys2-801, leu2-3, 112, trp1-901, tyr1-501, gal4D, gal8D, ade5::hisG*	Clontech
MJK377	*YM4271, ubx5Δ::hphNT1*	This study
MJK391	*MJK377, YIplac211-3xHotspot 5-F7-min.promoter-HIS3::URA3*	This study
MJK409	*MJK377, YIplac211-3xHotspot 5-F7-Mut-min.promoter-HIS3::URA3*	This study
MJK392	*MJK377, YIplac211-min.promoter-HIS3::URA3*	This study
MJK447	*MJK391, ymr111cΔ::natMT2*	This study
MJK407	*DF5, MATa ubx5Δ::kanMX6 yfr006wΔ::natNT2*	This study

Strain	Genotype	Source
MJK450	*DF5, MATa ubx5Δ::kanMX6 ymr111cΔ::natNT2*	This study
MJK448	*DF5, MATa ymr111cΔ::natNT2*	This study
PJ69-7A	*trp-901-, leu2-3,112 ura3-53 his3-200 gal4 gal80 GAL1::HIS GAL2-ADE2 met2::GAL7-lacZ*	Ref.169
MJK531	*DF5, MATa siz1Δ::HIS3*	I. Psakhye
MJK532	*DF5, MATa siz2Δ::HIS3*	I. Psakhye
Y0439	*DF5, MATa ubc9-1::URA3*	Jentsch strain collection
Y3061	*DF5, MATa siz1Δ::HIS3 siz2Δ::HIS3*	Jentsch strain collection
MJK612	*DF5, MATa ymr111c-K231R::URA3*	This study
MJK460	*DF5, MATa siz1Δ::HIS3 siz2Δ::HIS3 ubx5Δ::hphNT1*	This study
MJK611	*DF5, MATa ubc9-1::URA3 ubx5Δ::natNT2*	This study
MJK616	*DF5, MATa ymr111c-K231R::URA3 ubx5Δ::natNT2*	This study
MJK567	*DF5, MATa SLX8-9MYC::kanMX6*	This study
MJK569	*DF5, MATa SLX8-9MYC::kanMX6 ymr111cΔ::natNT2*	This study
MJK590	*DF5, MATa SLX8-9MYC::kanMX6 siz1Δ::HIS3 siz2Δ::HIS3*	This study
MJK609	*DF5, MATa SLX8-9MYC::kanMX6 ubc9-1::URA3*	This study
MJK617	*DF5, MATa SLX8-9MYC::kanMX6 ymr111c-K231R::URA3*	This study
MJK622	*DF5, MATa slx5Δ::natNT2*	This study
MJK595	*DF5, MATa slx8Δ::hphNT1*	This study
MJK619	*DF5, MATa nup84Δ::kanMX6*	This study
MJK624	*DF5, MATa slx5Δ::natNT2 ubx5Δ::kanMX6*	This study
MJK610	*DF5, MATa slx8Δ::hphNT1 ubx5Δ::kanMX6*	This study
MJK620	*DF5, MATa nup84Δ::kanMX6 ubx5Δ::natNT2*	This study
MJK605	*DF5, MATa cdc48-6 slx8Δ::hphNT1*	This study
W303a	*MATa RAD5 leu2-3,112 ade2-1 can1-100 his3-11,15 ura3-1 trp1-1*	Jentsch strain collection
MJK347	*W303a, YIplac211-pGAL1-tADH::URA3*	This study
MJK534	*W303a, YIplac211-pGAL1-YMR111C-tADH::URA3*	This study
MJK589	*PJ69-7A, siz1Δ::kanMX6 siz2Δ::natNT2*	This study

S. Cerevisiae Vectors

Type	Name (marker)	Reference
Integrative	*YIplac211* (*URA3*)	Ref.170
	YIplac128 (*LEU2*)	Ref.170
Yeast-two-hybrid	*pGAD-C1*	Ref.169
	pGAD424	Clontech
	pGBD-C1	Ref.169
	pGBT9	Clontech
Yeast-one-hybrid	*pGAD-HA*	Dualsystems
	pHISi-1	Clontech

S. Cerevisiae Plasmids

If not otherwise indicated plasmids were generated either by molecular cloning (see 5.2.3) or site-directed mutagenesis (see 5.2.3, “Site-directed Mutagenesis”).

Name	Plasmid (marker)	Source
pMax114	*YIplac128-Hotspot 5 (LEU2)*	This study
pMax115	*YIplac128-Hotspot 5-F1 (LEU2)*	This study
pMax116	*YIplac128-Hotspot 5-F2 (LEU2)*	This study
pMax117	*YIplac128-Hotspot 5-F3 (LEU2)*	This study
pMax118	*YIplac128-Hotspot 5-F4 (LEU2)*	This study
pMax125	*YIplac128-Hotspot 5-F5 (LEU2)*	This study
pMax135	*YIplac128-Hotspot 5-F6 (LEU2)*	This study
pMax144	*YIplac128-Hotspot 5-F7 (LEU2)*	This study
pMax145	*YIplac128-Hotspot 5-F7-Mut (LEU2)*	This study
pMax138	*YIplac128-Hotspot 5-F8 (LEU2)*	This study
pMax197	*YIplac211-min.promotor-HIS3 (URA3)*	This study
pMax193	*YIplac211-3xHotspot 5-F7-min.promotor-HIS3 (URA3)*	This study
pMax196	*YIplac211-3xHotspot 5-F7-Mut-min.promoter-HIS3 (URA3)*	This study
V0001	*YIplac211-pGAL1-tADH (URA3)*	Jentsch DNA collection
pMax230	*YIplac211-pGAL1-YMR111C-tADH (URA3)*	This study
pMax218	*pGAD-HA-5’UTR-SUMO (LEU2)*	This study*
pMax219	*pGAD-HA-YFR006W$^{38\text{-}535}$ (LEU2)*	This study*
pMax223	*pGAD-HA-YMR111C$^{174\text{-}462}$ (LEU2)*	This study*
pMax209	*pGAD-C1-YMR111C (LEU2)*	This study
pMax198	*PGBD-C1-YMR111C (TRP1)*	This study
pMax242	*pGAD-C1-ymr111c-K231R (LEU2)*	This study
pMax241	*pGBD-C1- ymr111c-K231R (TRP1)*	This study
D1097	*pGAD424-SUMO-GG (LEU2)*	Jentsch DNA collection
D1099	*pGAD424-SUMO-AA (LEU2)*	Jentsch DNA collection
D1096	*pGBT9-SUMO-GG (TRP1)*	Jentsch DNA collection
pMax90	*pGAD-C1-UBC9 (LEU2)*	This study
D1674	*pGAD-C1-SIZ1 (LEU2)*	Jentsch DNA collection
pMax122	*pGAD-C1-SIZ2 (LEU2)*	This study
D3559	*pGBD-C1-SLX5 (TRP1)*	Jentsch DNA collection

* Plasmids were isolated during the yeast-one-hybrid screen

S. Cerevisiae Media

YPD / YPGal Medium/Plates:
1% (w/v) yeast extract
2% (w/v) bacto-peptone
2% (w/v) carbon source (glucose or galactose)
2% (w/v) agar (only for plates)
sterilised by autoclaving

YP-Lactate Medium:	1% (w/v) yeast extract 2% (w/v) bacto-peptone 3% (w/v) lactic acid adjust pH to 5.5 with NaOH (ca. 12 g/l final) sterilised by autoclaving
YPD G418/NAT/Hph Plates:	after autoclaving, YPD medium with 2% (w/v) agar was cooled to 50°C, and 200 mg/l G418 (geneticine disulphate, PAA Laboratories), 100 mg/l NAT (nourseothricin, HK Jena) or 500 mg/l Hph (hygromycin B, PAA Laboratories) was added.
Sc Medium/Plates**:**	0.67% (w/v) yeast nitrogen base 0.2% (w/v) amino acid drop-out mix (lacking one or more amino acids if indicated) 2% (w/v) glucose 2% (w/v) agar (for plates) sterilised by autoclaving
Amino Acid Drop-out Mix:	20 mg Ade, Ura, Trp, His 30 mg Arg, Tyr, Leu, Lys 50 mg Phe 100 mg Glu, Asp 150 mg Val 200 mg Thr 400 mg Ser
Sporulation Medium:	2% (w/v) KAc, sterilised by autoclaving
SORB Buffer:	100 mM LiOAc 10 mM Tris-HCl, pH 8.0 1 mM EDTA, pH 8.0 1 M sorbitol sterilised by filtration
PEG Solution:	100 mM LiOAc 10 mM Tris-HCl, pH 8 1 mM EDTA, pH 8.0 40% (w/v) PEG-3350 sterilised by filtration stored at 4°C

Cultivation and Storage of *S. Cerevisiae*

Yeast cells were grown either on agar plates or in liquid cultures. For growth on agar pates yeast cells were typically streaked with a sterile toothpick or an inoculation loop. To grow liquid yeast cultures, 5-25 ml of growth medium was inoculated with cells from freshly streaked plates (typically a single colony) and grown overnight. From this preculture the main culture was inoculated to an OD_{600} of 0.1-0.2 and incubated in baffle-flask (size ≥ 5x liquid culture volume) on a shaking platform (150-220 rpm) until mid-log phase growth had been reached (equals OD_{600} of 0.6-1.0). Plates and liquid cultures were typically incubated at 30ºC for all yeast strains except for temperature-sensitive mutants. Plates and precultures of temperature-sensitive mutants were cultivated at 25°C (permissive temperature), and main cultures were shifted to 30°C (semi-permissive temperature) during experiments. Notably, all temperature-sensitive mutants used in this study show already phenotypes at this semi-permissive temperature. Therefore a temperature shift to 37°C was not necessary. The cell density of liquid yeast cultures was determined photometrically (OD_{600} of 1 corresponds to $1.5x10^7$ cells/ml). For short-term storage of yeast, agar plates were sealed with parafilm and stored at 4°C up to 2-4 weeks. For long-term storage, stationary cultures (OD_{600} ≥ 3) were frozen in 15% (v/v) glycerol solutions at –80°C.

Competent *S. Cerevisiae* Cells

To generate competent *S. cerevisiae* cells for DNA transformation, 50 ml YPD were inoculated to an OD_{600} of 0.1-0.2 with a fresh overnight culture. The culture was grown to mid-log phase, and cells were harvested by centrifugation (5 min, 500 *g*, room temperature). Subsequently, cells were washed with 25 ml sterile water and 10 ml SORB solution, and resuspended in 360 µl SORB and 40 µl carrier DNA (salmon sperm DNA, 10 mg/ml, Invitrogen). Competent cells were either directly used for transformation or stored in 50 *µ*l aliquots at -80°C.

Transformation of *S. Cerevisiae* Cells

For transformation with plasmid DNA or linear DNA fragments, competent yeast cells (10 *µ*l for transformation of circular plasmid DNA, or 50 *µ*l for transformation of PCR products and linearised plasmids) were mixed with DNA (100-500 ng of circular plasmid DNA, 1-3 *µ*g PCR product, or 1 *µ*g of linearised plasmid DNA) and 6 volumes of PEG solution in a sterile 1.5 ml reaction tube. After incubation for 30 min at room temperature, DMSO was

added to a final concentration of 10%, and cells were heat shocked in a 42°C water bath for 8-15 min. Finally, cells were pelleted by centrifugation (5 min, 500 *g*, room temperature) and plated on agar plates containing the respective selection media. For selection of *kanMX6*, *natNT2*, or *hphNT1* marker genes, the transformation was resuspended in 3 ml YPD and incubated on a shaker at 25°C (for temperature-sensitive mutants) or 30°C for 2-3 h prior to plating. Agar plates were incubated at 25°C or 30°C for 2-3 days, and if necessary transformants were replica plated onto the respective selection plate using sterile velvet.

Genetic Manipulation of *S. Cerevisiae*

Chromosomal tagging and gene deletions in *S. cerevisiae* were achieved with a PCR-based strategy[171,172]. Briefly, PCR products that contained selection markers and were flanked by targeting sequences (of 50 base pairs) on both sites (homologous to targeting region) were generated (see 5.2.2; “Targeting Cassette Amplification”) and transformed in competent yeast cells. For chromosomal tagging, PCR fragments not only contained a marker gene but also an epitope tag. Transformants that integrated the PCR product by homologous recombination were selected on respective agar plates. For gene deletions, the integration of the PCR products at the correct chromosomal locations and the absence of the open reading frame were confirmed by yeast colony PCR using specific primers (see 5.2.2, “Yeast Colony PCR”). If feasible, gene deletions were additionally confirmed by western blot analysis of cell extracts (see 5.3.1, “Western Blot Analysis”). Chromosomal taggings were typically exclusively verified by western blot analysis using whole cell extracts gained from fresh overnight cultures (see 5.3.1, “TCA-Precipitation”).

To create cells that express a mutant variant of histone H2B, in which lysine-123 was replaced by arginine *(h2B-K123R)*, *HTB2* was deleted as described above. Subsequently, the second H2B encoding allele *HTB1* was mutated by integration of a PCR fragment that carried the respective mutation in its homologous 5’ flanking sequence. In addition to the mutation, the integration of the PCR fragment introduced an *ADH1* terminator and a *kanMX6* marker gene. Correct integration and mutation in G418 selected transformants was confirmed by yeast colony PCR (see 5.2.2, “Yeast Colony PCR”) and sequencing of colony PCR products.

Chromosomal mutations of *CDC48 (cdc48-3)* and *YMR111C (ymr111c-K231R)* were also achieved by a PCR-based strategy. In both cases, PCR products containing the mutated genes and a marker gene (*LEU2* for *CDC48* and *URA3* for *YMR111C)* were generated by Fusion-PCR (see 5.2.2, “Fusion of DNA fragments by PCR”) and

transformed in competent yeast cells. Correct integration and mutation in transformants was verified by yeast colony PCR and sequencing of colony PCR products.

Integrative plasmids (*YIplac211*, and *YIplac128*) were linearised by restriction digest (see 5.2.3, "Restriction Digest") in the marker gene and subsequently transformed in competent yeast cells. Plasmid integration at the correct chromosomal location was confirmed by yeast colony PCR using specific primers (see 5.2.2, "Yeast Colony PCR"). Strains with multiple plasmid integrations (tested by yeast colony PCR) were excluded.

Mating, Sporulation and Tetrad Analysis

To mate yeast strains of opposite mating type (*MATa* and *MATα*), equal amounts of cell material from freshly streaked agar plates were mixed on a YPD plate and incubated for 4 h or overnight at 30ºC. For diploid selection, a patch of cells was restreaked on double-selection plates. If one of the yeast strains did not carry a selectable marker, diploids were identified by the lack of a mating type on mating type test plates (see 5.1.2, "Mating Type Analysis").

For sporulation a single colony of diploid cells was inoculated in YPD and grown overnight. Cells were harvested from 300 µl of the saturated overnight culture (5 min, 500 *g*, room temperature) and subsequently washed 4 times with sterile water. After washing cells were resuspended in 4 ml of sporulation medium and incubated for 3-6 days on a shaker at room temperature. Sporulation efficiency was verified microscopically.

To dissect tetrads, equal volumes of the sporulation culture (typically 10 µl) and a zymolyase solution (1 Unit of Zymolyase 20T per ml) were mixed and incubated for 6 min at room temperature. After transferring the mixture on a YPD plate, tetrads were dissected with a micromanipulator (Singer MSM Systems). Germination and growth of the spores were carried out on non-selective YPD plates for 2-4 days. Tetrad genotypes were analysed by replica plating on selection plates and/or incubation at restrictive temperatures.

Mating Type Analysis

For mating type identification of haploid *S. cerevisiae* cells, the tester strains RC634a and RC75-7α were used[173]. These strains are hypersensitive to the mating pheromone secreted by yeast cells of the opposite mating type. To prepare mating type test plates with either RC634a or RC75-7α cells, 300 µl of a dense cell suspension was mixed with 1% (w/v) molten agar, which has been cooled to 45°C before. Subsequently, 8 ml of this

mixture was poured on top of YPD agar plates, forming a top agar layer. To test the mating of yeast strains, cells were either replica plated or streaked on both types of mating type test plates. After incubation for 1-2 days at 30°C, the mating type test plates were analysed. Given that cell growth of the tester strains is inhibited by the mating pheromone secreted by cells of the opposite mating types, a so-called “halo” on one of the two mating type test plates indicates the mating type of the analysed cells. Diploid cells form neither “halos” on RC634a nor on RC75-7α mating type test plates, because they do not secret mating type pheromones.

Spotting Assays

To analyse and compare growth of different *S. cerevisiae* strains under various conditions, equal amounts (approximately 5 µl) of serial dilutions were spotted on respective agar plates using a custom-made stamping device. Prior to spotting, yeast strains were diluted to an OD_{600} of 0.5, and 3-5 serial dilutions (1:5, or 1:8) in sterile PBS (10 mM phosphate, 137 mM NaCl, 2.7 mM KCl, pH 7.4) were prepared. Plates were incubated 2-5 days depending on the growth medium and temperature.

Directed Yeast-two-hybrid Assay

Directed yeast-two-hybrid assays were used to analyse protein-protein interactions. First, plasmids encoding for Gal4 transcription-activation (AD) and DNA-binding domain (BD) fusions of the assessed proteins were co-transformed in the yeast-two-hybrid tester strain (PJ69-7a[169]). Second, several colonies of freshly transformed cells were transferred to 1 ml of sterile water, diluted to an OD_{600} of 0.2, and spotted on selection plates using a custom-made stamping device. Plates were typically incubated for 3-7 days. Protein-protein interaction results in the reconstitution of the Gal4 transcription activator, which then drives the expression of reporter genes under the control of Gal4 (*HIS3* and *ADE2*). The activation of the reporter genes enables cell growth on Sc media lacking histidine or adenine, respectively. Auto-activation activity of AD- and BD-fusion proteins was analysed by co-expression with isolated BD (by transformation with *pGAD-C1*) and AD (by transformation of *pGBD-C1*) domains, respectively.

Yeast-one-hybrid Screen

A Yeast-one-hybrid screen was performed to identify proteins that potentially interact with a defined DNA sequence (bait DNA sequence). Initially, a yeast strain (in YM4271 genetic

background) that contains a reporter gene *(HIS3)* under the control of a minimal promoter and three copies of the bait DNA sequence was generated by plasmid integration (using *YIplac211* as a plasmid backbone; *HIS3* gene with its minimal promoter was cloned from *pHISi-1*). This bait strain was subsequently transformed with a *S. cerevisiae* c-DNA library (cloned in a *pGAD-HA* vector, Dualsystems) that encodes for Gal4 transcription-activation domain (AD) fusion proteins. Transformation was performed with 50 µl of competent cells and 1 µg of c-DNA library plasmid DNA (see 5.1.2, "Transformation of *S. Cerevisiae* Cells"), giving rise to approximately 7-8x10^5 transformants. Transformation efficiency was verified by plating a small aliquot of the transformation reaction on plates selecting for plasmid containing cells (Sc-Leu plates). To perform a saturated screen, in which optimally all of the approximately 1x10^7 constructs of the c-DNA library were analysed, 38 transformations were conducted simultaneously, resulting in approximately 3x10^7 transformants. Interaction between an expressed AD-fusion protein and the bait DNA sequence typically results in *HIS3* transcription, thus conferring growth on media lacking histidine. Therefore each transformation reaction was plated on a Sc-Leu-His agar plate (145 mm diameter) that was supplemented with 50 mM 3-aminotriazol (3-AT) in order to supress auto-activation of the *HIS3* reporter gene in the bait strain (3-AT concentration was determined by titration experiments before the screen). Transformation plates were incubated for 5-7 days at 30°C and subsequently transformants were restreaked on Sc-Leu-His (50 mM 3-AT) plates. Next, the AD-fusion protein encoding plasmids were isolated from all selected transformants, amplified by transformation in *E. coli*, and sequenced. To verify that growth on Sc-Leu-His (50 mM 3-AT) plates was conferred by expression of the respective AD-fusion proteins, the isolated plasmids were re-transformed into the bait strain and subjected to directed yeast-one-hybrid assays (see 5.1.2, "Directed Yeast-one-hybrid Assay"). The bait sequence specificity of *HIS3* activation was verified by performing directed yeast-one-hybrid assays using a control bait strain that either lacked a bait DNA sequence or contained a mutated version of the bait DNA sequence upstream of the *HIS3* reporter.

Directed Yeast-one-hybrid Assay

For directed yeast-one-hybrid assays, yeast-one-hybrid bait strains were transformed with plasmids encoding for the Gal4 transcription-activation domain (AD) fusion proteins of interest. Several colonies of freshly transformed cells were transferred from plate to 1 ml of sterile water, diluted to an OD_{600} of 0.5, and spotted in 8-fold series dilutions on Sc-Leu-His plates containing various amounts of 3-AT (10 mM, 20 mM, or 50 mM), as well as on

control plates (Sc-Leu). Protein-DNA interaction results in *HIS3* activation, which confers better growth on Sc-Leu-His plates with 3-AT. For comparison a bait strain transformed with a plasmid that expresses the isolated AD (typically *pGAD-HA*) was spotted.

5.2 Molecular Biological Techniques

5.2.1 DNA Purification and Analysis

Purification of Plasmid DNA from *E. Coli*

Single *E. coli* colonies (derived from transformation of plasmid DNA) were inoculated in 5 ml of liquid LB medium (containing the respective antibiotics) and grown overnight at 37°C. Plasmid DNA was isolated using a commercially available kit (AccuPrep Plasmid Mini Extraction Kit, Bioneer) according to the manufacturer's instructions.

Purification of Genomic DNA from *S. Cerevisiae*

Isolation of genomic DNA from *S. cerevisiae* (e.g. as a template for the amplification of specific genes or chromosomal elements by PCR) was conducted with the commercially available Master Pure Yeast DNA Purification Kit (Epicentre) according to the manufacturer's instructions. Typically one or several colonies from freshly streaked yeast plates were used.

Purification of Plasmid DNA from *S. Cerevisiae*

Isolation of plasmids DNA from yeast was performed as described for *E. coli* cells with the only difference that yeast cells were initially lysed by glass bead lysis. For glass bead lysis cells from 1.5 ml of a dense overnight culture were harvested, resuspended in 250 µl buffer 1 (of the AccuPrep Plasmid Mini Extraction Kit, Bioneer), and mixed with 250 µl acid washed glass beads (diameter of 425-600 nm, Sigma). Subsequently cells were lysed for 4 min using a cell disruptor (Disruptor Genie, Scientific Industries) at maximum speed. Since plasmids were afterwards typically used for transformation in electro-competent *E. coli* cells, the final elution from the spin columns was performed with 35 µl water instead of elution buffer.

Purification of Linear DNA Fragments

Linear DNA fragments, resulting from PCR were purified with the QIAquick PCR Purification Kit (Qiagen) according to the manufacturer's instructions.

Separation of DNA Fragments by Agarose Gel Electrophoresis

For analytical or preparative separation of DNA fragments, 0.7-2.0% (w/v) agarose gels prepared in TBE buffer (89 mM Tris, 89 mM boric acid, 2 mM EDTA) were used. To allow visualisation of double stranded DNA using an UV transilluminator (Raytest), agarose gels were supplemented with ethidium bromide. DNA samples were mixed with 5-fold DNA loading buffer (Qiagen) and were electrophoretically separated at 120 volts in TBE buffer. The size of DNA fragments was estimated with a standard size marker (1kB ladder, Invitrogen) migrating on the same gel.

Purification of DNA Fragments from Agarose Gels

For preparative isolation of DNA fragments from agarose gels, the desired band was excised from the gel using a sterile razor blade. Subsequently, DNA was purified from the agarose block using the QIAquick Gel Extraction Kit (Qiagen) according to the manufacturer's instructions.

Measurement of DNA Concentration

DNA concentration was determined photometrically using a NanoDrop ND-1000 spectrophotometer (PeqLab). Measured was the absorbance at a wavelength of 260 nm (A_{260}). An A_{260} of 1 is equal to a concentration of 50 µg/ml double-stranded DNA.

DNA Sequencing

DNA sequencing was performed by the core facility of the MPI of Biochemistry using an ABI 3730 DNA analyser (Applied Biosystems) and ABI Big Dye 3.1 sequencing chemistry.

5.2.2 Polymerase Chain Reaction (PCR)

PCR was used to amplify DNA fragments for molecular cloning, to amplify targeting cassettes for chromosomal gene disruption and epitope tagging, to fuse linear DNA fragments, and to verify genomic recombination events. Oligonucleotides (primers) for PCRs were designed manually and purchased from MWG. PCR reactions were performed in a Thermo Cycler (Applied Biosystems).

Amplification of DNA Fragments for Molecular Cloning

For subsequent cloning into vectors, DNA fragments were amplified from plasmid (10 ng) or genomic yeast DNA (200 ng) using the high fidelity Phusion polymerase (Thermo) and primers with restriction sites as 5' overhangs. PCR reactions were typically performed in a total volume of 50 µl, containing the respective template DNA, 0.6 µM of forward and reverse primer, 0.2 mM deoxynucleotide triphosphates, 1x Phusion HF buffer, and 2 Units of Phusion High-Fidelity DNA-polymerase (Thermo Scientific). The reaction was run in a PCR cycler (Biometra), using an amplification program adjusted to primer melting temperatures and target sequence length according to the instructions of the DNA-polymerase manufacturer.

Targeting Cassette Amplification

Targeting cassettes for chromosomal gene deletions and epitope tagging (see 5.1.2, "Genetic Manipulation of *S. Cerevisiae*") were amplified with a Taq/Vent DNA-polymerase mixture as described previously[171,172]. Primers for targeting cassette amplification contained 50 base pairs overhangs, which are homologous to the respective targeting regions. PCR reactions were typically performed in a 100 µl volume, containing 100 ng template DNA (plasmids from the pYM collection[171,172]), 0.64 µM of both primers, 0.35 mM deoxynucleotide triphosphates, 1x ThermoPol buffer (New England Biolabs), 2.4 µl of Taq DNA-polymerase (self-made by a former group member), and 4 Units of Vent DNA-polymerase (New England Biolabs). The amplification program was adopted from Janke and co-workers[172]. Prior to transformation, the PCR products were typically purified using the QIAquick PCR Purification Kit (Qiagen).

Fusion of DNA Fragments by PCR

To fuse two DNA fragments by PCR, first two individual DNA fragments were produced by PCR amplification using Phusion High-Fidelity DNA-polymerase (Thermo) as described above (see 5.2.2, "Amplification of DNA Fragments for Molecular Cloning"). The primers used for these reactions were designed in a way that the 3'-end of one PCR product shares a 25-30 base pairs overlap with the 5'-end of the other PCR product. After the PCR products were purified from agarose gels, 30-100 ng of both PCR products were mixed and used as template for a second PCR reaction. In this second PCR reaction, which also contained the forward primer of the 5'-DNA fragment and the reverse primer of the 3'-DNA fragment, the PCR fragments were fused (due to the overlap) and the fusion product was

amplified (by the primers). The second PCR reaction was performed with Phusion High-Fidelity DNA-polymerase (Thermo) as described above (see 5.2.2, “Amplification of DNA Fragments for Molecular Cloning”). The annealing temperature in the amplification program for the second PCR reaction was typically set to 55°C independent of the primer melting temperatures.

Yeast Colony PCR

To confirm integration of plasmids and targeting cassettes to the correct chromosomal locations, yeast colony PCRs using specific primers were performed. As DNA template for colony PCR, crude genomic yeast DNA was generated. To this end, a single yeast colony was resuspended in 20 µl of NaOH (0.02 M), mixed with 10 µl acid washed glass beads (diameter of 425-600 nm, Sigma), and shaken (1400 rpm) in a thermomixer at 99°C for 5 min. Subsequently, the sample was briefly centrifuged and the supernatant was used as template for colony PCR. The PCR reactions were typically carried out in a volume of 20 µl, containing 1.6 µl template DNA, 0.65 µM of both primers, 0.35 mM deoxynucleotide triphosphates, 1x ThermoPol buffer (New England Biolabs), and 0.2 µl of Taq DNA-polymerase (self-made by former group member). Amplification was performed in a Thermo Cycler (Applied Biosystems) using the following amplification protocol:

Denaturation	94°C	5 min
Amplification (30x)	94°C	30 sec
	55°C	30 sec
	72°C	1 min (or longer if required)
Final Extension	72°C	5 min
Cooling	4°C	∞

5.2.3 Molecular Cloning

Restriction Digest

For sequence specific cleavage of vector DNA and linear PCR products, restriction enzymes (New England Biolabs) were used according to the manufacturer’s instructions. For molecular cloning usually 2 µg of vector DNA or purified PCR products were digested in a 40 µl reaction for 2-5 h at 37°C. For molecular cloning, DNA fragments were typically purified from gel after restriction digest.

Dephosphorylation of Linearised Plasmid DNA

In order to avoid re-ligation of linearised vector DNA, the 5'-end of vector DNA was dephosphorylated prior to ligation. For dephosphorylation, 1-2 μg of gel purified vector DNA was incubated with 2 Units of rAPid Alkaline Phosphatase (Roche) in the provided buffer at 37°C for 10-60 min. For cloning reactions that only involved one restriction site, dephosphorylation was typically performed overnight at 37°C. After dephosphorylation the rAPid Alkaline Phosphatase was heat-inactivated by incubation for 5 min at 75°C.

Oligonucleotide Annealing

To generate double stranded DNA fragments with a size of 25-80 base pairs as inserts for cloning reactions, two complementary oligonucleotides with sticky end overhangs (as they would arise by restriction digest) were annealed. For annealing, a mixture containing 50 μM of both oligonucleotides (in 50 mM Tris-HCl, pH 8.0, 100 mM NaCl, 1 mM EDTA) was heated to 95°C for 90 sec and subsequently slowly cooled down in a rate of 1°C per 20 sec. For subsequent cloning, either 1 μl of the undiluted or 1 μl of a 10-fold dilution was used.

Ligation

For ligation, linearised and dephosphorylated vector DNA (heat inactivated after dephosphorylation) was mixed with digested PCR product (purified from gel) or double stranded DNA with sticky ends that was generated by oligonucleotide annealing. The 20 µl ligation reaction contained 50-150 ng of vector DNA, a 3 to 10-fold molar excess of insert DNA, and 400 Units T4 DNA ligase (New England Biolabs). The ligation reaction was incubated either for 10 min at 25°C or overnight at 16°C. After ligation, the T4 DNA ligase was heat inactivated for 10 min at 65°C and the sample was dialysed for 20 min against deionised water with a nitrocellulose filter (pore size of 0.05 µm, Millipore) prior to transformation in electro-competent *E. coli* cells.

Site-directed Mutagenesis

Point mutations were introduced into plasmids by following the PCR-based quick change site-directed mutagenesis approach[174]. For this approach, two complementary primers containing the mutated nucleotide(s) with 18-22 nucleotides wild-type flanking-sequence on each side were designed. The PCR was performed with Pfu Turbo DNA-polymerase (Agilent Technologies) according to the user manual of the QuikChange Site-Directed

Mutagenesis Kit (Agilent Technologies), using 1-10 ng Dam-methylated plasmid DNA as template. Subsequent to the PCR, the template plasmid was digested by incubation with 20 Units of the Dpn1 restriction enzyme (New England Biolabs) at 37°C for 3 h. Finally, the reaction was dialysed against deionised water with a nitrocellulose filter (pore size of 0.05 µm, Millipore) for 20 min, and 5 µl were transformed in electro-competent *E. coli* cells. Plasmids from individual transformants were isolated and the incorporation of the desired mutation and the absence of unwanted second-site mutations was confirmed by DNA sequencing.

5.3 Biochemical and Cell Biological Techniques

5.3.1 Protein Methods

Buffers and Solutions

HU Buffer	200 mM Tris, pH 6.8 8 M urea 5% (w/v) SDS 1 mM EDTA 0.1% (w/v) bromophenol blue before use 100 mM DTT were added
2x SDS Loading Buffer	125 mM Tris pH 6.8 4% (w/v) SDS 20% (w/v) glycerol 0.01% (w/v) bromophenol blue before use 100 mM DTT were added
MOPS Buffer	50 mM MOPS 50 mM Tris base 3.5 mM SDS 1 mM EDTA
Blotting Buffer (self-made)	250 mM Tris base 1.92 M glycine 0.1% (w/v) SDS 20% (v/v) methanol
Swift Blotting Buffer	5% (v/v) 20x Swift buffer (G-Bioscience) 10% (v/v) Methanol

TBS-T Solution	25 mM Tris, pH 7.5 137 mM NaCl 2.6 mM KCl 0.1% (v/v) Tween 20
PBS	10 mM phosphate, pH 7.4 137 mM NaCl 2.7 mM KCl
IP Lysis Buffer	50 mM Tris, pH 7.5 150 mM NaCl 10% (v/v) glycerol 2 mM $MgCl_2$ 0.5% (v/v) NP-40

TCA-Precipitation

Yeast whole cell protein extracts (WCE) for SDS-PAGE and Western blot analysis were prepared by trichloroacetic acid (TCA) precipitation. To this end, 1-2 OD_{600} of a yeast culture (for most experiments in mid-log phase) were harvested by centrifugation, resuspended in 1 ml ice-cold water, and mixed with 150 µl of 1.85 M NaOH/7.5% (v/v) β-mercaptoethanol. After incubation on ice for 15 min, 150 µl of ice-cold 55% (w/v) trichloroacetic acid (TCA) was added, and the mixture was incubated for 10 min on ice. Precipitated proteins were collected by centrifugation (20 min, 14000 rpm, 4°C) and the supernatant was discarded. After a second centrifugation step (5 min, 14000 rpm, 4°C), the remaining supernatant was removed by aspiration and the protein pellet was resuspended in 30-100 µl of HU-buffer and denatured for 10 min at 65°C.

SDS-Polyacrylamide Gel Electrophoresis (SDS-PAGE)

SDS-PAGE was performed with pre-cast 4-12% NuPage Bis-Tris gels (Invitrogen), using MOPS buffer at a constant voltage of 140-200 V. Protein samples were prepared in HU buffer or SDS loading buffer and denatured at 65°C for 10 min or at 99°C for 5 min, respectively. To estimate protein size, the standard size marker Precision Plus Protein All Blue Standard (Bio-Rad) was loaded next to the analysed samples.

Western Blot (WB) Analysis

For Western blot analysis, proteins were separated by SDS-PAGE and subsequently transferred to a pre-activated (with methanol) polyvinylidene fluoride (PVDF) membrane (Millipore), using a tank blot system (Hoefer). The protein transfer was performed in self-

made or Swift blotting buffer at a constant voltage of 75 V at 4°C for 2 h or at a constant amperage of 200 mA at 4°C for 100 min, respectively. Thereafter, the membrane was blocked for 10-30 min in TBS-T + 5% milk powder at room temperature, and incubated overnight at 4°C with a primary antibody diluted in TBS-T + 5% milk powder (containing 0.02% sodium azide). Then, the membrane was washed 4 times for 5 min at room temperature with TBS-T and was subsequently incubated with a 1:5000 dilution (in TBS-T) of a horseradish peroxidase (HRP)-coupled secondary antibody (Dianova). After incubation for 1 h at room temperature, the membrane was washed again 4 times for 10 min with TBS-T, and protein detection was carried out with the chemiluminescence kits ECL, ECL-plus or ECL advanced (GE Healthcare) following the manufacturer's instructions. Signals were detected by exposure of the membrane to a chemiluminescence film (Amersham Hyperfilm ECL, GE Healthcare) with variable exposure times and subsequent automated film development.

To detect multiple proteins, membranes were either cut into pieces that were incubated with different primary antibodies at the same time, or sequentially incubated with different antibodies. For sequential incubation, membranes were stripped with Restore Western Blot Stripping Buffer (Piercenet) according to the manufacturer's instructions.

Immunoprecipitation

For immunoprecipitation experiments, native yeast extracts were prepared. To avoid protein degradation, all steps were performed at 4°C and the IP lysis buffer was freshly supplemented with protease inhibitors: 1 mg/ml Pefabloc SC (Roche) and 1x EDTA-free complete cocktail (Roche). If modifications with ubiquitin or SUMO were analysed, the lysis buffer was additionally supplemented with 20 mM N-ethylmaleimide (NEM), which inhibits deubiquitylating enzymes and SUMO isopeptidases.

Typically, 50-200 OD_{600} cells were harvested from mid-log phase yeast cultures, washed once in ice-cold PBS, and transferred to 2 ml reaction tubes. Cell pellets were either shock frozen in liquid nitrogen and stored at -80°C for some days or directly used for cell extract preparation. To prepare cell extracts, cell pellets were resuspended in 600-800 μl of ice-cold lysis buffer (with inhibitors), an equal volume zirconia/silica beads (BioSpec Inc.) was added, and cells were lysed on a multi-tube bead-beater (MM301, Retsch GmbH) in 6 intervals of 1 min shaking (frequency 30/s) and 3 min cooling (bead-beater was used in a 4°C room). Upon cell lysis, samples were separated from the beads and transferred to a new tube (by piggyback method). Since in this study typically

chromatin-bound proteins were analysed, the DNA in the lysate was subsequently sheared by a 10 min water/ice bath sonication (output 200W; 10 cycles with 30 sec sonication and 30 sec break) using the Bioruptor UCD-200 sonication system (Diagenode). After DNA shearing, the cell lysates were cleared from insoluble cell debris by centrifugation (8 min, 20000 *g*, 4°C) and were subsequently used as input material for immunoprecipitation experiments. For immunoprecipitation, a defined volume of antibody (in this study 1.5 µl anti-Ymr111c antibody) was added and the samples were incubated for 1.5 h at 4°C on a rotating wheel. Subsequently, 35 µl of a prewashed Protein A agarose bead slurry (Roche) was added and the samples were incubated again for 30 min at 4°C on a rotating wheel. Next, the beads were pelleted by centrifugation (1 min, 500 *g*, 4°C), the supernatant was removed by aspiration, and the beads were washed 5 times with 500 µl of lysis buffer. After a final washing step with detergent-free lysis buffer, the beads were dried by aspiration, and the immunoprecipitated material was eluted by incubation with 35 µl of 2x SDS loading buffer for 5 min at 99°C in a shaking thermomixer (1400 rpm). Both the input material and the immunoprecipitatied material were subsequently analysed by SDS PAGE and western blot analysis.

Antibodies

Primary Antibodies

Name	Use	Type	Source
anti-ubiquitin (FK2)	ChIP (4 µl)	monoclonal (mouse IgG_1)	Millipore
anti-ubiquitin (K48, Apu2)	ChIP (4 µl)	monoclonal (rabbit IgG)	Millipore
anti-ubiquitin (P4D1)	WB (1:1000)	monoclonal (mouse IgG_1)	Santa Cruz
anti-Myc (9E10)	WB (1:2000) ChIP (3 µl)	monoclonal (mouse IgG_1)	Sigma
anti-Pgk1	WB (1:10000)	monoclonal (mouse IgG_1)	Life Technologies
anti-H2B-Ub (D11)	WB (1:1000)	monoclonal (rabbit IgG)	Cell Signaling
anti-Gal4-BD (RK5C1)	WB (1:1000)	monoclonal (mouse IgG_2)	Santa Cruz
anti-Gal4-AD (C10)	WB (1:1000)	monoclonal (mouse IgG_2)	Santa Cruz
IgG (rabbit)	ChIP (1 µl)	polyclonal (rabbit IgG)	Bethyl Laboratories Inc.
IgG (mouse)	ChIP (1.5 µl)	monoclonal (mouse IgG_1)	Bethyl Laboratories Inc.
anti-Smt3	WB (1:5000)	polyclonal (rabbit IgG)	Ref. 37
anti-Cdc48 (clone 63)	WB (1:10000) ChIP (3 µl)	polyclonal (rabbit IgG)	Self-made (Alexander Strasser)
anti-Ymr111c	WB (1:10000) IP (1.5 µl) ChIP (1.5 µl)	polyclonal (rabbit IgG)	Self-made (Alexander Strasser)

The anti-Cdc48 (raised against His_6-Cdc48) and the anti-Ymr111c (raised against His_6-Ymr111c$^{292-462}$) antibodies were raised and affinity-purified by Alexander Strasser (technical assistant of the Jentsch group) according to standard protocols. Antibody specificity was demonstrated by western blot analysis (see Figure 17B and data not shown).

Secondary Antibodies

Name	Use	Type	Source
goat anti-mouse	WB (1:5000)	HRP-coupled	Dianova
goat anti-rabbit	WB (1:5000)	HRP-coupled	Dianova

5.3.2 Chromatin Immunoprecipitation (ChIP)

Buffers and Solutions

FA Lysis Buffer	50 mM Hepes, pH 7.5 150 mM NaCl 1 mM EDTA 1% (v/v) Triton X-100 0.1% (w/v) Deoxycholic acid, Na-salt 0.1% (w/v) SDS
FA Lysis Buffer HS	50 mM Hepes, pH 7.5 500 mM NaCl 1 mM EDTA 1% (v/v) Triton X-100 0.1% (w/v) Deoxycholic acid, Na-salt 0.1% (w/v) SDS
ChIP Wash Buffer	10 mM Tris, pH 8 250 mM LiCl 1 mM EDTA 0.5% (v/v) NP-40 0.5% (w/v) Deoxycholic acid, Na-salt
ChIP Elution Buffer	50 mM Tris, pH 7.5 10 mM EDTA 1% (w/v) SDS
TE	10 mM Tris, pH 8 1 mM EDTA

Chromatin Immunoprecipitation

Chromatin immunoprecipitation (ChIP) experiments were in most parts performed as described previously[160,175]. For all ChIP experiments shown in this study, 200 ml yeast cultures were grown to mid-log phase in YPD media at 30°C (also temperature-sensitive mutants) and subsequently cross-linked by the addition of 1% (final concentration) formaldehyde (37% solution, Roth) for 16 min at 25°C. The cross-linking reaction was terminated and quenched by the addition of 30 ml 2.5 M glycine solution and subsequent incubation for at least 15 min at 25°C. Next, 160 OD_{600} of cross-linked cells were pelleted by centrifugation (5 min, 5000 *g*, 4°C), washed once with ice-cold PBS, and transferred to a 2 ml reaction tube. Cells were frozen in liquid nitrogen, and generally stored overnight or for some days at -80°C.

For chromatin preparation, the frozen cell pellet was immediately resuspended in 800 µl FA lysis buffer that was freshly complemented with protease inhibitors (1 mg/ml Pefabloc SC (Roche) and EDTA-free complete cocktail (Roche)). Subsequently the cell suspension was supplemented with an equal amount of zirconia/silica beads (BioSpec Inc.) and cell lysis was performed with a multi-tube bead-beater (MM301, Retsch GmbH) in 6 intervals of 3 min shaking (30/s frequency) and 3 min cooling (bead-beater was used in a 4°C room). Upon cell lysis, the sample was separated from the beads (by piggyback method) and transferred to a 2 ml reaction tube. Chromatin was sedimented by centrifugation (15 min, 20000 *g*, 4°C), resuspended in 1 ml ice-cold FA lysis buffer (complemented with protease inhibitors), and transferred to hard plastic Sumilon 15 ml centrifuge tubes (Sumitomo Bakelite Co.). In this tube, chromatin was sheared by water/ice bath sonication using the Bioruptor UCD-200 sonication system (Diagenode). Generally, 40 times 30 sec cycles (with 30 sec breaks in between) at an output of 200 W were performed with the aim to shear the DNA to an average length of 250-500 base pairs. To assure efficient cooling the water/ice bath was supplemented wit fresh ice every 10 cycles. Notably, the sonication protocol was slightly modified during this study. The chromatin pellet was initially resuspended in 2 ml instead of 1 ml, but it turned out that shearing in 1 ml is more efficient. The differences in DNA shearing also affected the relative differences in individual experiments, which can therefore not be directly compared.

The sheared and thus solubilised chromatin (if sonication was performed in 1 ml, 1 ml of FA Lysis buffer with protease inhibitors was added) was purified from cell debris by centrifugation (30 min, 20000 *g*, 4°C). Subsequently, 20 µl of the supernatant was removed as “input sample”, and 800 µl of the supernatant was used for

immunoprecipitation (IP). For the IP, the respective antibody (see 5.3.1, “Antibodies”) was added to the chromatin solution and the mixture was incubated for 90 min on a rotating wheel. Thereafter, a final volume of 25 µl pre-swollen Protein A Sepharose CL-4B beads (GE Healthcare) dissolved in 50-100 *µ*l FA lysis buffer (complemented with protease inhibitors) was added and the mixture was incubated for 30 min at 25°C on a rotating wheel. Then, beads were washed three times with 400 µl FA lysis buffer, once with 400 µl FA lysis buffer HS, once with 400 µl ChIP wash buffer, and once with TE (beads were sedimented by centrifugation; 1 min, 300 *g*, room temperature). For subsequent elution of bound protein-DNA complexes, the beads were dried by aspiration and incubated with 120 µl ChIP elution buffer for 10 min at 65°C (shaking at 1400 rpm). Upon brief centrifugation, 100 µl of the eluate was removed as “IP sample”. Input and IP samples were subjected to Proteinase K (Sigma) digest in a volume of 200 *µ*l with a final SDS concentration of 0.5% for 2 h at 42°C, and subsequently incubated at 65°C for 6 h to revert formaldehyde cross-links. Finally, the input and IP DNA samples were purified using the QIAquick PCR Purification Kit (Qiagen), and either used for Real-Time PCR (see 5.3.2, “Quantitative Real-Time PCR Analysis of ChIP Experiments”) or ChIP-chip analysis (see 5.3.2, “ChIP-chip Analysis”).

Quantitative Real-Time PCR Analysis of ChIP Experiments

Quantitative Real-Time PCR (RT-PCR) analysis of ChIP experiments was performed with the LightCycler 480 system (Roche), using the LightCycler 480 SYBR Green I Master hot-start reaction mix (Roche). All input and IP samples were analysed with different primer pairs in PCR reactions that contained 18 *µ*l of a master mix and 2 *µ*l of the respective IP (undiluted) or input (1:10 dilution) material (see below). All reactions were assembled in 384-well LightCycler plates (Roche), using a CAS-1200 PCR setup robot (Corbett Life Science).

To quantify the template DNA concentration, a dilution series of one input sample (1:5, 1:50, 1:500, an 1:5000) was measured as a standard curve with every primer pair. The resulting LightCycler PCR amplification curves were quantified from their second derivate maximum using the LightCycler 480 software. As a quality control for primer specificity (only one PCR product should be amplified), a melting curve analysis was performed. For data presentation the IP/input ratios were calculated and subsequently normalised to the IP/input ratios of the control primer pair. The control primer pair measured the levels of a locus on chromosome II (see primer list) that was selected based on the ChIP-chip experiments.

RT-PCR Reaction Mix

SYBR Green I Master Mix	10 µl
Primer 1 (100 µM)	0.12 µl
Primer 2 (100 µM)	0.12 µl
Water (PCR grade)	7.76 µl
Sample (Input or IP)	2 µl

LightCycler Program

Initial Denaturation	
95°	10 min
Amplification/Detection (45 cycles)	
95°C	10 sec
57°C	10 sec
72°C	16 sec
Melting Curve Analysis	
95°C	30 sec
65°C	30 sec
65°C-95°C	0.11°C/sec
4°C	∞

Primers Used for RT-PCR Analysis of ChIP Experiments

Name	Sequence	Position	Feature
MaxP420_fwd	TTTCTGCCAGTAGCGACACCACACAT	*ChrIII_123537bp*	Hotspot 1
MaxP421_rev	ATGACGATGGCAGGGAAAATAGGGCTGT	*ChrIII_123719bp*	Hotspot 1
MaxP769_fwd	CCTTGTCAGATAATGTATGGGTGGTGTG	*ChrIV_358238bp*	Hotspot 2
MaxP770_rev	TATTCTTTGTGTTCGCATTCGCTTCCC	*ChrIV_358367bp*	Hotspot 2
MaxP698_fwd	AACAATAGAAAAACGCGGGACTCGAT	*ChrIV_1087121bp*	Hotspot 3
MaxP699_rev	TGCTAATTTTCAGCCACATCACATGC	*ChrIV_1087280bp*	Hotspot 3
MaxP371_fwd	GCATCTATCGTATTCTTGAGTTATTGCGAC	*ChrIV_1116954bp*	Hotspot 4
MaxP372_rev	ATGTCAATACCATCAGGATCTTGCATGA	*ChrIV_1117151bp*	Hotspot 4
MaxP373_fwd	TGGAAGCATCACATCGTATGCTACTAGA	*ChrXIII_309445bp*	Hotspot 5
MaxP374_rev	TATGTATGCGGCAATGAACTACTCCGA	*ChrXIII_309647bp*	Hotspot 5
MaxP437_fwd	AACGACGTACCCACTACGCGTTTGAA	*ChrXIII_413843bp*	Hotspot 6
MaxP438_rev	AACTGTTGGAATGTGAGGGCGACCTAGT	*ChrXIII_414033bp*	Hotspot 6
MaxP717_fwd	TCTTTGCACAATGCATTACGTGGGAG	*ChrXIII_433645bp*	Hotspot 7
MaxP718_rev	GAGAAATAGATTCAATGCCGTGGCGA	*ChrXIII_433789bp*	Hotspot 7
MaxP702_fwd	TGTTACGCGTTCCATTTGAGAAGCAA	*ChrXV_168011bp*	Hotspot 8
MaxP703_rev	CGGCTTTAAACACCCGTGCCTATATT	*ChrXV_168209bp*	Hotspot 8
MaxP422_fwd	AGTCGTCGCAAGCGACAAATCTCAACT	*ChrXVI_899848bp*	Hotspot 9
MaxP423_rev	AGCGGTTGTTTTGCCTGCTTTGCCAT	*ChrXVI_900025bp*	Hotspot 9
MaxP342_fwd	ACCGACTAATGCGGTCATGGAAAGC	*ChrII_564535bp*	Control region
MaxP343_rev	CTTTTCTCGCAAGAAGACTCCAGAATCA	*ChrII_564727bp*	Control region
MaxP433_rev	CATTAATGCAGCTGGCACGACAGGTT	*YI128* backbone	Ectopic Hotspot
MaxP434_fwd	ACAATTCCACACAACATACGAGCCGGA	*YI128* backbone	Ectopic Hotspot

ChIP-chip Analysis

To analyse ChIP experiments in a genome-wide manner, ChIP-chip was performed as described previously[160,175]. Briefly, input and IP DNA samples arising from ChIP experiments were RNase (DNase-free RNase, Sigma) treated and subsequently amplified in two steps using the GenomePlex Whole Genome Amplification (WGA) and re-amplification kits (Sigma), as described in the Farnham lab protocol for WGA amplification[176]. Labelling of input and IP samples (with either Cy3 or Cy5), hybridisation to custom-made high-density whole *S. cerevisiae* genome NimbleGen arrays, array scanning, and raw data extraction were performed by the NimbleGen ChIP-chip service of SourceBioSource (former imaGenes). In this study custom-deigned c12plex NimbleGen custom arrays with 84 base pairs median genomic probe spacing and only unique oligonucleotides have been used. Typically, ChIP-chip experiments were performed in duplicates, involving a hybridisation dye swap of input and IP material. ChIP-chip data processing is described in section 5.4 ("ChIP-chip Analysis").

5.3.3 Gene Expression Profiling

Isolation of *S. Cerevisiae* Total RNA

Total RNA from *S. cerevisiae* cells was isolated with the RNeasy Mini Kit (Qiagen) according to the manufacturer's instructions. Typically, RNA was isolated from 1.5 OD_{600} of mid-log phase yeast cells that were lysed by bead lysis using zirconia/silica beads (BioSpec Inc.) and a multi-tube bead-beater (MM301, Retsch GmbH). As recommended by the manufacturer's instruction, DNA digest was performed on column using the RNase-free DNase Set (Qiagen). RNA concentration was determined photometrically with a NanoDrop ND-1000 spectrophotometer (PeqLab). The absorbance at a wavelength of 260 nm (A_{260}) was measured. An A_{260} of 1 is equal to a concentration of 40 µg/ml RNA. RNA quality was assessed using a Bioanalyzer 2100 (Agilent) with an RNA 6000 Nano Assay (Agilent) at the laboratory of Prof. Cramer (LMU Munich).

Gene Expression Profiling with Microarrays

Gene expression profiling was performed with GeneChIP Yeast Genome 2.0 arrays (Affimetrix) at the laboratory of Prof. Cramer (LMU Munich) with the help of Kerstin Maier according to the standard Affimetrix procedures. In brief, biotin labelled antisense RNA (aRNA) was produced from 300 ng total yeast RNA using the GeneChip 3' IVT Express Kit (Affimetrix) and fragmented according to the manufacturer's instructions.

Subsequently, 5 μg of labelled and fragmented aRNA was hybridised on a GeneChIP Yeast Genome 2.0 array (Affimetrix) using the GeneChip Hybridization Wash and Stain Kit (Affimetrix). Array washing and staining procedures were performed with a GeneChip Fluidics Station 450 using the GeneChip Hybridization Wash and Stain Kit (Affimetrix). Finally, array scanning was performed with a GeneChip scanner 3000 (Affymetrix) and data was processed as described in section 5.4 ("Microarray Data Analysis"). To ensure high data quality all experiments were performed in biological triplicates.

5.4 Bioinformatic Analysis, Online Resources, and Computer Programs

ChIP-chip Data Analysis

Quality control, normalisation, averaging, and analysis of ChIP-chip data were performed with R/Bioconductor (www.Rproject.org; www.bioconductor.org) as previously described (Tobias Straub, Epigenome project PROT43, http://www.epigenesys.eu/). All ChIP-chip data are presented as $\log_2$ of the IP/input ratio. Peak identification and comparison of ChIP-chip profiles was performed manually.

MEME DNA Motif Prediction

To predict DNA sequence motifs that are enriched at Cdc48-dependent Ub-hotspots, the online tool MEME[149] (http://meme.nbcr.net/meme) was used. The calculation was performed with the standard settings except for the number of allowed repetitions, which was set to "any number". The following sequences were used as data input: Hotspot 1 (*ChrIII-122730-127260 bp*), Hotspot 2 (*ChrIV-357600-358500 bp*), Hotspot 3 (*ChrIV-1086750-1087512 bp*), Hotspot 4 (*ChrIV-1116160-1117800 bp*), Hotspot 5 (*ChrXIII-307620-311540 bp*), Hotspot 6 (*ChrXIII-412050-415500 bp*), Hotspot 7 (*ChrXIII-433200-434120 bp*), Hotspot 8 (*ChrXV-167470-169080 bp*), and Hotspot 9 (*ChrXVI-899700-900630 bp*).

Microarray Data Analysis

Microarray data was analysed by Assa Yeroslaviz (Bioinformatic Core Facility, MPI of Biochemistry) using the R/Bioconducter software. Raw gene expression intensities were first normalised by the Robust Multiarray Analysis (RMA) at the probe level[177]. Quality control was performed using the R/Bioconductor packages affyPLM[178] and simpleaffy[179]. The low-level analysis of the microarray data was performed in the R/Bioconductor environment using the limma[178] and affy[180] microarray packages.

Gene annotation for the used arrays (GeneChIP Yeast Genome 2.0 arrays, Affimetrix) was obtained from R/Bioconductor metadata packages[181] as well as from the biomaRt repository[182,183].

The differential expression analysis for the data sets in the present study was investigated by functions and methods that are implemented in R/Bioconductor[178,181]. In brief, a fixed effects linear model was fitted for each individual feature to estimate expression differences between the two groups of normalised expression levels from the mutant and the corresponding *WT* samples. Next, an empirical Bayes approach was applied to moderate standard errors of M-values[178]. And finally, for each analysed feature a moderated t-statistics as well as the raw and adjusted p-values (FDR control by the Benjamini and Hochberg method[184]) were obtained. To identify biological significance, a $\log_2$ fold change cut-off of 1 between mutants and WT was used.

Online Resources and Computer Programs

For literature search, sequence search as well as protein sequence and domain analysis databases and tools provided by the *S. cerevisiae* Genome Database (http://www.yeastgenome.org/), the National Center for Biotechnology Information (http://www.ncbi.nlm.nih.gov/), and the UniProt Consortium (http://www.uniprot.org) were used. Protein structure files were downloaded from the protein databank (www.pdb.org) and structures were visualised using the PyMol software (www.pymol.org). DNA sequence analysis (DNA restriction enzyme maps, DNA sequencing analysis) was performed with the DNA-Star software package (DNA Star Inc.). For data statistics and representation of ChIP-RT-PCR experiments GraphPad Prism (http://www.graphpad.com/scientific-software/prism/) was used. Representation of ChIP-chip data was performed with the Integrated Genome Browser (http://bioviz.org/igb/). Contrast of western blot exposures was linearly adjusted using Adobe Photoshop (Adobe Systems Inc.). Figures were labelled and cartoons were created with the Adobe Illustrator software (Adobe Systems Inc.). For text and table generation, the Microsoft Office software package (Microsoft Corp.) was used.

6 References

1. Finley, D., Ulrich, H. D., Sommer, T. & Kaiser, P. The Ubiquitin-Proteasome System of Saccharomyces cerevisiae. *Genetics* **192,** 319–360 (2012).
2. Shimizu, Y., Okuda-Shimizu, Y. & Hendershot, L. M. Ubiquitylation of an ERAD substrate occurs on multiple types of amino acids. *Mol Cell* **40,** 917–926 (2010).
3. Breitschopf, K. A novel site for ubiquitination: the N-terminal residue, and not internal lysines of MyoD, is essential for conjugation and degradation of the protein. *The EMBO Journal* **17,** 5964–5973 (1998).
4. Pickart, C. M. & Eddins, M. J. Ubiquitin: structures, functions, mechanisms. *Biochimica et Biophysica Acta (BBA) - Molecular Cell Research* **1695,** 55–72 (2004).
5. Komander, D. & Rape, M. The ubiquitin code. *Annual review of biochemistry* **81,** 203–229 (2012).
6. Koegl, M. *et al.* A novel ubiquitination factor, E4, is involved in multiubiquitin chain assembly. *Cell* **96,** 635–644 (1999).
7. Scheffner, M., Nuber, U. & Huibregtse, J. M. Protein ubiquitination involving an E1-E2-E3 enzyme ubiquitin thioester cascade. *Nature* **373,** 81–83 (1995).
8. Deshaies, R. J. & Joazeiro, C. A. P. RING domain E3 ubiquitin ligases. *Annual review of biochemistry* **78,** 399–434 (2009).
9. Komander, D., Clague, M. J. & Urbé, S. Breaking the chains: structure and function of the deubiquitinases. *Nat Rev Mol Cell Biol* **10,** 550–563 (2009).
10. Dikic, I., Wakatsuki, S. & Walters, K. J. Ubiquitin-binding domains - from structures to functions. *Nat Rev Mol Cell Biol* **10,** 659–671 (2009).
11. Ye, Y. *et al.* Ubiquitin chain conformation regulates recognition and activity of interacting proteins. *Nature* **492,** 266–270 (2012).
12. Raasi, S., Varadan, R., Fushman, D. & Pickart, C. M. Diverse polyubiquitin interaction properties of ubiquitin-associated domains. *Nat Struct Mol Biol* **12,** 708–714 (2005).
13. Hershko, A. & Ciechanover, A. The Ubiquitin System. *Annual review of biochemistry* **67,** 425–479 (1998).
14. Varshavsky, A. The ubiquitin system. *Trends Biochem Sci* **22,** 383–387 (1997).
15. Thrower, J. S., Hoffman, L., Rechsteiner, M. & Pickart, C. M. Recognition of the polyubiquitin proteolytic signal. *The EMBO Journal* **19,** 94–102 (2000).
16. Kim, W. *et al.* Systematic and quantitative assessment of the ubiquitin-modified proteome. *Mol Cell* **44,** 325–340 (2011).
17. Xu, P. *et al.* Quantitative proteomics reveals the function of unconventional ubiquitin chains in proteasomal degradation. *Cell* **137,** 133–145 (2009).
18. Saeki, Y. *et al.* Lysine 63-linked polyubiquitin chain may serve as a targeting signal for the 26S proteasome. *The EMBO Journal* **28,** 359–371 (2009).
19. Matyskiela, M. E. & Martin, A. Design principles of a universal protein degradation machine. *J. Mol. Biol.* **425,** 199–213 (2013).
20. Elsasser, S. *et al.* Proteasome subunit Rpn1 binds ubiquitin-like protein domains. *Nat Cell Biol* **4,** 725–730 (2002).
21. Elsasser, S., Chandler-Militello, D., Müller, B., Hanna, J. & Finley, D. Rad23 and Rpn10 serve as alternative ubiquitin receptors for the proteasome. *J Biol Chem* **279,** 26817–26822 (2004).
22. Schreiner, P. *et al.* Ubiquitin docking at the proteasome through a novel pleckstrin-homology domain interaction. *Nature* **453,** 548–552 (2008).
23. Husnjak, K. *et al.* Proteasome subunit Rpn13 is a novel ubiquitin receptor. *Nature* **453,** 481–488 (2008).

24. Verma, R., Oania, R., Graumann, J. & Deshaies, R. J. Multiubiquitin chain receptors define a layer of substrate selectivity in the ubiquitin-proteasome system. *Cell* **118,** 99–110 (2004).
25. Verma, R. *et al.* Role of Rpn11 metalloprotease in deubiquitination and degradation by the 26S proteasome. *Science* **298,** 611–615 (2002).
26. Leggett, D. S. *et al.* Multiple associated proteins regulate proteasome structure and function. *Mol Cell* **10,** 495–507 (2002).
27. Bergink, S. & Jentsch, S. Principles of ubiquitin and SUMO modifications in DNA repair. *Nature* **458,** 461–467 (2009).
28. Chen, Z. J. & Sun, L. J. Nonproteolytic Functions of Ubiquitin in Cell Signaling. *Mol Cell* **33,** 275–286 (2009).
29. Emmerich, C. H., Schmukle, A. C. & Walczak, H. The emerging role of linear ubiquitination in cell signaling. *Science Signaling* **4,** re5 (2011).
30. Mukhopadhyay, D. & Riezman, H. Proteasome-independent functions of ubiquitin in endocytosis and signaling. *Science* **315,** 201–205 (2007).
31. Geng, F., Wenzel, S. & Tansey, W. P. Ubiquitin and proteasomes in transcription. *Annual review of biochemistry* **81,** 177–201 (2012).
32. Ulrich, H. D. Ubiquitin and SUMO in DNA repair at a glance. *J. Cell. Sci.* **125,** 249–254 (2012).
33. Kannouche, P. L., Wing, J. & Lehmann, A. R. Interaction of human DNA polymerase eta with monoubiquitinated PCNA: a possible mechanism for the polymerase switch in response to DNA damage. *Mol Cell* **14,** 491–500 (2004).
34. Jian Cao, Q. Y. Histone Ubiquitination and Deubiquitination in Transcription, DNA Damage Response, and Cancer. *Frontiers in Oncology* **2,** 1–9 (2012).
35. Fierz, B. *et al.* Histone H2B ubiquitylation disrupts local and higher-order chromatin compaction. *Nat Chem Biol* **7,** 113–119 (2011).
36. Braun, S. & Madhani, H. D. Shaping the landscape: mechanistic consequences of ubiquitin modification of chromatin. *EMBO Rep* **13,** 619–630 (2012).
37. Hoege, C., Pfander, B., Moldovan, G.-L., Pyrowolakis, G. & Jentsch, S. RAD6-dependent DNA repair is linked to modification of PCNA by ubiquitin and SUMO. *Nature* **419,** 135–141 (2002).
38. Kirisako, T. *et al.* A ubiquitin ligase complex assembles linear polyubiquitin chains. *The EMBO Journal* **25,** 4877–4887 (2006).
39. van der Veen, A. G. & Ploegh, H. L. Ubiquitin-like proteins. *Annual review of biochemistry* **81,** 323–357 (2012).
40. Geiss-Friedlander, R. & Melchior, F. Concepts in sumoylation: a decade on. *Nat Rev Mol Cell Biol* **8,** 947–956 (2007).
41. Gareau, J. R. & Lima, C. D. The SUMO pathway: emerging mechanisms that shape specificity, conjugation and recognition. *Nat Rev Mol Cell Biol* **11,** 861–871 (2010).
42. Kevin A Wilkinson, J. M. H. Mechanisms, regulation and consequences of protein SUMOylation. *The Biochemical journal* **428,** 133–145 (2010).
43. Johnson, E. S. & Gupta, A. A. An E3-like factor that promotes SUMO conjugation to the yeast septins. *Cell* **106,** 735–744 (2001).
44. Hickey, C. M., Wilson, N. R. & Hochstrasser, M. Function and regulation of SUMO proteases. *Nat Rev Mol Cell Biol* **13,** 755–766 (2012).
45. Meulmeester, E. & Melchior, F. Cell biology: SUMO. *Nature* **452,** 709–711 (2008).
46. Ulrich, H. D. The SUMO system: an overview. *Methods Mol. Biol.* **497,** 3–16 (2009).
47. Hannich, J. T. *et al.* Defining the SUMO-modified proteome by multiple approaches in Saccharomyces cerevisiae. *J Biol Chem* **280,** 4102–4110 (2005).

48. Psakhye, I. & Jentsch, S. Protein group modification and synergy in the SUMO pathway as exemplified in DNA repair. *Cell* **151,** 807–820 (2012).
49. Jentsch, S. & Psakhye, I. Control of Nuclear Activities by Substrate-Selective and Protein-Group SUMOylation. *Annu Rev Genet* advanced online publication, (2013).
50. Song, J., Durrin, L. K., Wilkinson, T. A., Krontiris, T. G. & Chen, Y. Identification of a SUMO-binding motif that recognizes SUMO-modified proteins. *Proc Natl Acad Sci USA* **101,** 14373–14378 (2004).
51. Hecker, C.-M., Rabiller, M., Haglund, K., Bayer, P. & Dikic, I. Specification of SUMO1- and SUMO2-interacting motifs. *J Biol Chem* **281,** 16117–16127 (2006).
52. Stehmeier, P. & Muller, S. Phospho-regulated SUMO interaction modules connect the SUMO system to CK2 signaling. *Mol Cell* **33,** 400–409 (2009).
53. Ullmann, R., Chien, C. D., Avantaggiati, M. L. & Muller, S. An acetylation switch regulates SUMO-dependent protein interaction networks. *Mol Cell* **46,** 759–770 (2012).
54. Zhao, J. Sumoylation regulates diverse biological processes. *Cell. Mol. Life Sci.* **64,** 3017–3033 (2007).
55. Rosonina, E., Duncan, S. M. & Manley, J. L. SUMO functions in constitutive transcription and during activation of inducible genes in yeast. *Genes Dev* **24,** 1242–1252 (2010).
56. Rosonina, E., Duncan, S. M. & Manley, J. L. Sumoylation of transcription factor Gcn4 facilitates its Srb10-mediated clearance from promoters in yeast. *Genes Dev* **26,** 350–355 (2012).
57. Pfander, B., Moldovan, G.-L., Sacher, M., Hoege, C. & Jentsch, S. SUMO-modified PCNA recruits Srs2 to prevent recombination during S phase. *Nature* **436,** 428–433 (2005).
58. Golebiowski, F. *et al.* System-Wide Changes to SUMO Modifications in Response to Heat Shock. *Science Signaling* **2,** ra24 (2009).
59. Cremona, C. A. *et al.* Extensive DNA Damage-Induced Sumoylation Contributes to Replication and Repair and Acts in Addition to the Mec1 Checkpoint. *Mol Cell* **45,** 422–432 (2012).
60. Praefcke, G. J. K., Hofmann, K. & Dohmen, R. J. SUMO playing tag with ubiquitin. *Trends Biochem Sci* **37,** 23–31 (2012).
61. Zhang, Z. & Buchman, A. R. Identification of a member of a DNA-dependent ATPase family that causes interference with silencing. *Molecular and Cellular Biology* **17,** 5461–5472 (1997).
62. Cal-Bakowska, M., Litwin, I., Bocer, T., Wysocki, R. & Dziadkowiec, D. The Swi2-Snf2-like protein Uls1 is involved in replication stress response. *Nucleic Acids Research* **39,** 8765–8777 (2011).
63. Lescasse, R., Pobiega, S., Callebaut, I. & Marcand, S. End-joining inhibition at telomeres requires the translocase and polySUMO-dependent ubiquitin ligase Uls1. *The EMBO Journal* **32,** 805–815 (2013).
64. Xie, Y., Rubenstein, E. M., Matt, T. & Hochstrasser, M. SUMO-independent in vivo activity of a SUMO-targeted ubiquitin ligase toward a short-lived transcription factor. *Genes Dev* **24,** 893–903 (2010).
65. Uzunova, K. *et al.* Ubiquitin-dependent proteolytic control of SUMO conjugates. *J Biol Chem* **282,** 34167–34175 (2007).
66. Mullen, J. R., Kaliraman, V., Ibrahim, S. S. & Brill, S. J. Requirement for three novel protein complexes in the absence of the Sgs1 DNA helicase in Saccharomyces cerevisiae. *Genetics* **157,** 103–118 (2001).
67. Nagai, S. *et al.* Functional targeting of DNA damage to a nuclear pore-associated SUMO-dependent ubiquitin ligase. *Science* **322,** 597–602 (2008).

68. Parker, J. L. & Ulrich, H. D. A SUMO-interacting motif activates budding yeast ubiquitin ligase Rad18 towards SUMO-modified PCNA. *Nucleic Acids Research* **40,** 11380–11388 (2012).
69. Tatham, M. H. *et al.* RNF4 is a poly-SUMO-specific E3 ubiquitin ligase required for arsenic-induced PML degradation. *Nat Cell Biol* **10,** 538–546 (2008).
70. Lallemand-Breitenbach, V. *et al.* Arsenic degrades PML or PML-RARα through a SUMO-triggered RNF4/ubiquitin-mediated pathway. *Nat Cell Biol* **10,** 547–555 (2008).
71. Yin, Y. *et al.* SUMO-targeted ubiquitin E3 ligase RNF4 is required for the response of human cells to DNA damage. *Genes Dev* **26,** 1196–1208 (2012).
72. Galanty, Y., Belotserkovskaya, R., Coates, J. & Jackson, S. P. RNF4, a SUMO-targeted ubiquitin E3 ligase, promotes DNA double-strand break repair. *Genes Dev* **26,** 1179–1195 (2012).
73. Jentsch, S. & Rumpf, S. Cdc48 (p97): a 'molecular gearbox' in the ubiquitin pathway? *Trends Biochem Sci* **32,** 6–11 (2007).
74. Pye, V. E. *et al.* Going through the motions: the ATPase cycle of p97. *J. Struct. Biol.* **156,** 12–28 (2006).
75. Stolz, A., Hilt, W., Buchberger, A. & Wolf, D. H. Cdc48: a power machine in protein degradation. *Trends Biochem Sci* **36,** 515–523 (2011).
76. Bergink, S. *et al.* Role of Cdc48/p97 as a SUMO-targeted segregase curbing Rad51-Rad52 interaction. *Nat Cell Biol* **15,** 526–532 (2013).
77. Krick, R. *et al.* Cdc48/p97 and Shp1/p47 regulate autophagosome biogenesis in concert with ubiquitin-like Atg8. *J Cell Biol* **190,** 965–973 (2010).
78. Huyton, T. *et al.* The crystal structure of murine p97/VCP at 3.6A. *J. Struct. Biol.* **144,** 337–348 (2003).
79. Wang, Q., Song, C. & Li, C.-C. H. Molecular perspectives on p97-VCP: progress in understanding its structure and diverse biological functions. *J. Struct. Biol.* **146,** 44–57 (2004).
80. Briggs, L. C. *et al.* Analysis of nucleotide binding to P97 reveals the properties of a tandem AAA hexameric ATPase. *J Biol Chem* **283,** 13745–13752 (2008).
81. Song, C., Wang, Q. & Li, C.-C. H. ATPase activity of p97-valosin-containing protein (VCP). D2 mediates the major enzyme activity, and D1 contributes to the heat-induced activity. *J Biol Chem* **278,** 3648–3655 (2003).
82. Wang, Q., Song, C., Yang, X. & Li, C.-C. H. D1 ring is stable and nucleotide-independent, whereas D2 ring undergoes major conformational changes during the ATPase cycle of p97-VCP. *J Biol Chem* **278,** 32784–32793 (2003).
83. Davies, J. M., Brunger, A. T. & Weis, W. I. Improved structures of full-length p97, an AAA ATPase: implications for mechanisms of nucleotide-dependent conformational change. *Structure* **16,** 715–726 (2008).
84. DeLaBarre, B. & Brunger, A. T. Nucleotide dependent motion and mechanism of action of p97/VCP. *J. Mol. Biol.* **347,** 437–452 (2005).
85. Yeung, H. O. *et al.* Insights into adaptor binding to the AAA protein p97. *Biochem. Soc. Trans.* **36,** 62–67 (2008).
86. Mullally, J. E., Chernova, T. & Wilkinson, K. D. Doa1 is a Cdc48 adapter that possesses a novel ubiquitin binding domain. *Molecular and Cellular Biology* **26,** 822–830 (2006).
87. Allen, M. D., Buchberger, A. & Bycroft, M. The PUB domain functions as a p97 binding module in human peptide N-glycanase. *J Biol Chem* **281,** 25502–25508 (2006).
88. Böhm, S., Lamberti, G., Fernandez-Saiz, V., Stapf, C. & Buchberger, A. Cellular Functions of Ufd2 and Ufd3 in Proteasomal Protein Degradation Depend on Cdc48 Binding. *Molecular and Cellular Biology* **31,** 1528–1539 (2011).

89. Schuberth, C. & Buchberger, A. UBX domain proteins: major regulators of the AAA ATPase Cdc48/p97. *Cell. Mol. Life Sci.* **65,** 2360–2371 (2008).
90. Hänzelmann, P., Buchberger, A. & Schindelin, H. Hierarchical binding of cofactors to the AAA ATPase p97. *Structure* **19,** 833–843 (2011).
91. Schuberth, C. & Buchberger, A. Membrane-bound Ubx2 recruits Cdc48 to ubiquitin ligases and their substrates to ensure efficient ER-associated protein degradation. *Nat Cell Biol* **7,** 999–1006 (2005).
92. Li, G., Zhao, G., Schindelin, H. & Lennarz, W. J. Tyrosine phosphorylation of ATPase p97 regulates its activity during ERAD. *Biochemical and Biophysical Research Communications* **375,** 247–251 (2008).
93. Zhao, G. *et al.* Studies on peptide:N-glycanase-p97 interaction suggest that p97 phosphorylation modulates endoplasmic reticulum-associated degradation. *Proceedings of the National Academy of Sciences* **104,** 8785–8790 (2007).
94. Meyer, H. H. Direct binding of ubiquitin conjugates by the mammalian p97 adaptor complexes, p47 and Ufd1-Npl4. *The EMBO Journal* **21,** 5645–5652 (2002).
95. Meyer, H. H., Shorter, J. G., Seemann, J., Pappin, D. & Warren, G. A complex of mammalian ufd1 and npl4 links the AAA-ATPase, p97, to ubiquitin and nuclear transport pathways. *The EMBO Journal* **19,** 2181–2192 (2000).
96. Nie, M. *et al.* Dual Recruitment of Cdc48 (p97)-Ufd1-Npl4 Ubiquitin-selective Segregase by Small Ubiquitin-like Modifier Protein (SUMO) and Ubiquitin in SUMO-targeted Ubiquitin Ligase-mediated Genome Stability Functions. *Journal of Biological Chemistry* **287,** 29610–29619 (2012).
97. Schuberth, C., Richly, H., Rumpf, S. & Buchberger, A. Shp1 and Ubx2 are adaptors of Cdc48 involved in ubiquitin-dependent protein degradation. *EMBO Rep* **5,** 818–824 (2004).
98. Neuber, O., Jarosch, E., Volkwein, C., Walter, J. & Sommer, T. Ubx2 links the Cdc48 complex to ER-associated protein degradation. *Nat Cell Biol* **7,** 993–998 (2005).
99. Ritz, D. *et al.* Endolysosomal sorting of ubiquitylated caveolin-1 is regulated by VCP and UBXD1 and impaired by VCP disease mutations. *Nat Cell Biol* **13,** 1116–1123 (2011).
100. Bug, M. & Meyer, H. Expanding into new markets-VCP/p97 in endocytosis and autophagy. *J. Struct. Biol.* **179,** 78–82 (2012).
101. Meyer, H., Bug, M. & Bremer, S. Emerging functions of the VCP/p97 AAA-ATPase in the ubiquitin system. *Nat Cell Biol* **14,** 117–123 (2012).
102. Richly, H. *et al.* A series of ubiquitin binding factors connects CDC48/p97 to substrate multiubiquitylation and proteasomal targeting. *Cell* **120,** 73–84 (2005).
103. Rumpf, S. & Jentsch, S. Functional Division of Substrate Processing Cofactors of the Ubiquitin-Selective Cdc48 Chaperone. *Mol Cell* **21,** 261–269 (2006).
104. Alexandru, G. *et al.* UBXD7 binds multiple ubiquitin ligases and implicates p97 in HIF1alpha turnover. *Cell* **134,** 804–816 (2008).
105. Ossareh-Nazari, B. *et al.* Cdc48 and Ufd3, new partners of the ubiquitin protease Ubp3, are required for ribophagy. *EMBO Rep* **11,** 548–554 (2010).
106. Li, G. The AAA ATPase p97 links peptide N-glycanase to the endoplasmic reticulum-associated E3 ligase autocrine motility factor receptor. *Proceedings of the National Academy of Sciences* **103,** 8348–8353 (2006).
107. Meusser, B., Hirsch, C., Jarosch, E. & Sommer, T. ERAD: the long road to destruction. *Nat Cell Biol* **7,** 766–772 (2005).
108. Ye, Y., Meyer, H. H. & Rapoport, T. A. The AAA ATPase Cdc48/p97 and its partners transport proteins from the ER into the cytosol. *Nature* **414,** 652–656 (2001).

109. Braun, S., Matuschewski, K., Rape, M., Thoms, S. & Jentsch, S. Role of the ubiquitin-selective CDC48$^{UFD1/NPL4}$ chaperone (segregase) in ERAD of OLE1 and other substrates. *The EMBO Journal* **21,** 615–621 (2002).
110. Jarosch, E. *et al.* Protein dislocation from the ER requires polyubiquitination and the AAA-ATPase Cdc48. *Nat Cell Biol* **4,** 134–139 (2002).
111. Brandman, O. *et al.* A Ribosome-Bound Quality Control Complex Triggers Degradation of Nascent Peptides and Signals Translation Stress. *Mol Cell* **151,** 1042–1054 (2012).
112. Verma, R., Oania, R. S., Kolawa, N. J. & Deshaies, R. J. Cdc48/p97 promotes degradation of aberrant nascent polypeptides bound to the ribosome. *Elife* **2,** e00308 (2013).
113. Nishikori, S., Yamanaka, K., Sakurai, T., Esaki, M. & Ogura, T. p97 Homologs from Caenorhabditis elegans, CDC-48.1 and CDC-48.2, suppress the aggregate formation of huntingtin exon1 containing expanded polyQ repeat. *Genes Cells* **13,** 827–838 (2008).
114. Song, C., Wang, Q. & Li, C.-C. H. Characterization of the aggregation-prevention activity of p97/valosin-containing protein. *Biochemistry* **46,** 14889–14898 (2007).
115. Kobayashi, T., Manno, A. & Kakizuka, A. Involvement of valosin-containing protein (VCP)/p97 in the formation and clearance of abnormal protein aggregates. *Genes Cells* **12,** 889–901 (2007).
116. Fischer, F., Hamann, A. & Osiewacz, H. D. Mitochondrial quality control: an integrated network of pathways. *Trends Biochem Sci* **37,** 284–292 (2012).
117. Livnat-Levanon, N. & Glickman, M. H. Ubiquitin-proteasome system and mitochondria - reciprocity. *Biochim. Biophys. Acta* **1809,** 80–87 (2011).
118. Heo, J.-M. *et al.* A stress-responsive system for mitochondrial protein degradation. *Mol Cell* **40,** 465–480 (2010).
119. Xu, S., Peng, G., Wang, Y., Fang, S. & Karbowski, M. The AAA-ATPase p97 is essential for outer mitochondrial membrane protein turnover. *Mol Biol Cell* **22,** 291–300 (2011).
120. Rape, M. *et al.* Mobilization of Processed, Membrane-Tethered SPT23 Transcription Factor by CDC48$^{UFD1/NPL4}$, a Ubiquitin-Selective Chaperone. *Cell* **107,** 667–677 (2001).
121. Rape, M. & Jentsch, S. Taking a bite: proteasomal protein processing. *Nat Cell Biol* **4,** E113–6 (2002).
122. Hoppe, T. *et al.* Activation of a membrane-bound transcription factor by regulated ubiquitin/proteasome-dependent processing. *Cell* **102,** 577–586 (2000).
123. Vaz, B., Halder, S. & Ramadan, K. Role of p97/VCP (Cdc48) in genome stability. *Front. Genet.* **4**:60 1–14 (2013).
124. Dantuma, N. P. & Hoppe, T. Growing sphere of influence: Cdc48/p97 orchestrates ubiquitin-dependent extraction from chromatin. *Trends Cell Biol* **22,** 483–491 (2012).
125. Ramadan, K. *et al.* Cdc48/p97 promotes reformation of the nucleus by extracting the kinase Aurora B from chromatin. *Nature* **450,** 1258–1262 (2007).
126. Mouysset, J. *et al.* Cell cycle progression requires the CDC-48$^{UFD-1/NPL-4}$ complex for efficient DNA replication. *Proceedings of the National Academy of Sciences* **105,** 12879–12884 (2008).
127. Raman, M., Havens, C. G., Walter, J. C. & Harper, J. W. A genome-wide screen identifies p97 as an essential regulator of DNA damage-dependent CDT1 destruction. *Mol Cell* **44,** 72–84 (2011).
128. Franz, A. *et al.* CDC-48/p97 coordinates CDT-1 degradation with GINS chromatin dissociation to ensure faithful DNA replication. *Mol Cell* **44,** 85–96 (2011).

129. Remus, D. & Diffley, J. F. X. Eukaryotic DNA replication control: lock and load, then fire. *Curr Opin Cell Biol* **21,** 771–777 (2009).
130. Zhong, W., Feng, H., Santiago, F. E. & Kipreos, E. T. CUL-4 ubiquitin ligase maintains genome stability by restraining DNA-replication licensing. *Nature* **423,** 885–889 (2003).
131. Ramanathan, H. N. & Ye, Y. Revoking the cellular license to replicate: yet another AAA assignment. *Mol Cell* **44,** 3–4 (2011).
132. Meerang, M. *et al.* The ubiquitin-selective segregase VCP/p97 orchestrates the response to DNA double-strand breaks. *Nat Cell Biol* **13,** 1376–1382 (2011).
133. Acs, K. *et al.* The AAA-ATPase VCP/p97 promotes 53BP1 recruitment by removing L3MBTL1 from DNA double-strand breaks. *Nat Struct Mol Biol* **18,** 1345–1350 (2011).
134. Stewart, G. S. Solving the RIDDLE of 53BP1 recruitment to sites of damage. *Cell Cycle* **8,** 1532–1538 (2009).
135. Botuyan, M. V. *et al.* Structural basis for the methylation state-specific recognition of histone H4-K20 by 53BP1 and Crb2 in DNA repair. *Cell* **127,** 1361–1373 (2006).
136. Kalakonda, N. *et al.* Histone H4 lysine 20 monomethylation promotes transcriptional repression by L3MBTL1. *Oncogene* **27,** 4293–4304 (2008).
137. Mosbech, A. *et al.* DVC1 (C1orf124) is a DNA damage-targeting p97 adaptor that promotes ubiquitin-dependent responses to replication blocks. *Nat Struct Mol Biol* **19,** 1084–1092 (2012).
138. Davis, E. J. *et al.* DVC1 (C1orf124) recruits the p97 protein segregase to sites of DNA damage. *Nat Struct Mol Biol* **19,** 1093–1100 (2012).
139. Ghosal, G., Leung, J. W.-C., Nair, B. C., Fong, K.-W. & Chen, J. Proliferating cell nuclear antigen (PCNA)-binding protein C1orf124 is a regulator of translesion synthesis. *Journal of Biological Chemistry* **287,** 34225–34233 (2012).
140. Wilcox, A. J. & Laney, J. D. A ubiquitin-selective AAA-ATPase mediates transcriptional switching by remodelling a repressor-promoter DNA complex. *Nat Cell Biol* **11,** 1481–1486 (2009).
141. Laney, J. D. & Hochstrasser, M. Ubiquitin-dependent degradation of the yeast Matα2 repressor enables a switch in developmental state. *Genes Dev* **17,** 2259–2270 (2003).
142. Verma, R., Oania, R., Fang, R., Smith, G. T. & Deshaies, R. J. Cdc48/p97 mediates UV-dependent turnover of RNA Pol II. *Mol Cell* **41,** 82–92 (2011).
143. Wilson, M. D., Harreman, M. & Svejstrup, J. Q. Ubiquitylation and degradation of elongating RNA polymerase II: The last resort. *Biochimica et Biophysica Acta (BBA) - Gene Regulatory Mechanisms* **1829,** 151–157 (2013).
144. Woudstra, E. C. *et al.* A Rad26-Def1 complex coordinates repair and RNA pol II proteolysis in response to DNA damage. *Nature* **415,** 929–933 (2002).
145. Anindya, R., Aygün, O. & Svejstrup, J. Q. Damage-induced ubiquitylation of human RNA polymerase II by the ubiquitin ligase Nedd4, but not Cockayne syndrome proteins or BRCA1. *Mol Cell* **28,** 386–397 (2007).
146. Fujimuro, M., Sawada, H. & Yokosawa, H. Production and characterization of monoclonal antibodies specific to multi-ubiquitin chains of polyubiquitinated proteins. *FEBS Lett.* **349,** 173–180 (1994).
147. Schulze, J. M. *et al.* Splitting the task: Ubp8 and Ubp10 deubiquitinate different cellular pools of H2BK123. *Genes Dev* **25,** 2242–2247 (2011).
148. Robzyk, K. Rad6-Dependent Ubiquitination of Histone H2B in Yeast. *Science* **287,** 501–504 (2000).
149. Bailey, T. L. & Elkan, C. Fitting a mixture model by expectation maximization to discover motifs in biopolymers. *Proc Int Conf Intell Syst Mol Biol* **2,** 28–36 (1994).

150. Huie, M. A. *et al.* Characterization of the DNA-binding activity of GCR1: in vivo evidence for two GCR1-binding sites in the upstream activating sequence of TPI of Saccharomyces cerevisiae. *Molecular and Cellular Biology* **12,** 2690–2700 (1992).
151. Zhou, W., Ryan, J. J. & Zhou, H. Global analyses of sumoylated proteins in Saccharomyces cerevisiae. Induction of protein sumoylation by cellular stresses. *J Biol Chem* **279,** 32262–32268 (2004).
152. Denison, C. *et al.* A proteomic strategy for gaining insights into protein sumoylation in yeast. *Mol. Cell Proteomics* **4,** 246–254 (2005).
153. Albuquerque, C. P. *et al.* Distinct SUMO ligases cooperate with Esc2 and Slx5 to suppress duplication-mediated genome rearrangements. *PLoS Genet* **9,** e1003670 (2013).
154. Mariño-Ramírez, L. & Hu, J. C. Isolation and mapping of self-assembling protein domains encoded by the Saccharomyces cerevisiae genome using lambda repressor fusions. *Yeast* **19,** 641–650 (2002).
155. Dobi, K. C. & Winston, F. Analysis of transcriptional activation at a distance in Saccharomyces cerevisiae. *Molecular and Cellular Biology* **27,** 5575–5586 (2007).
156. Ernst, R., Mueller, B., Ploegh, H. L. & Schlieker, C. The Otubain YOD1 Is a Deubiquitinating Enzyme that Associates with p97 to Facilitate Protein Dislocation from the ER. *Mol Cell* **36,** 28–38 (2009).
157. Besten, den, W., Verma, R., Kleiger, G., Oania, R. S. & Deshaies, R. J. NEDD8 links cullin-RING ubiquitin ligase function to the p97 pathway. *Nat Struct Mol Biol* **19,** 511–516 (2012).
158. Alberts, S. M., Sonntag, C., Schäfer, A. & Wolf, D. H. Ubx4 modulates Cdc48 activity and influences degradation of misfolded proteins of the endoplasmic reticulum. *J Biol Chem* **284,** 16082–16089 (2009).
159. Wang, Z. & Prelich, G. Quality Control of a Transcriptional Regulator by SUMO-Targeted Degradation. *Molecular and Cellular Biology* **29,** 1694–1706 (2009).
160. Kalocsay, M., Hiller, N. J. & Jentsch, S. Chromosome-wide Rad51 spreading and SUMO-H2A.Z-dependent chromosome fixation in response to a persistent DNA double-strand break. *Mol Cell* **33,** 335–343 (2009).
161. Lefrançois, P., Auerbach, R. K., Yellman, C. M., Roeder, G. S. & Snyder, M. Centromere-like regions in the budding yeast genome. *PLoS Genet* **9,** e1003209 (2013).
162. Collins, K. A., Furuyama, S. & Biggins, S. Proteolysis Contributes to the Exclusive Centromere Localization of the Yeast Cse4/CENP-A Histone H3 Variant. *Current Biology* **14,** 1968–1972 (2004).
163. Nagai, S., Davoodi, N. & Gasser, S. M. Nuclear organization in genome stability: SUMO connections. *Cell Res.* **21,** 474–485 (2011).
164. Mekhail, K. & Moazed, D. The nuclear envelope in genome organization, expression and stability. *Nat Rev Mol Cell Biol* **11,** 317–328 (2010).
165. Ausubel, F. M. *et al. Current Protocols in Molecular Biology*. (Current Protocols, 1988).
166. Sambrook, J., Fritsch, E. F. & Maniatis, T. *Molecular Cloning*. (Cold Spring Harbor Laboratory Press, 1989).
167. Finley, D., Ozkaynak, E. & Varshavsky, A. The yeast polyubiquitin gene is essential for resistance to high temperatures, starvation, and other stresses. *Cell* **48,** 1035–1046 (1987).
168. Böhm, S. & Buchberger, A. The budding yeast Cdc48(Shp1) complex promotes cell cycle progression by positive regulation of protein phosphatase 1 (Glc7). *PLoS ONE* **8,** e56486 (2013).

169. James, P., Halladay, J. & Craig, E. A. Genomic libraries and a host strain designed for highly efficient two-hybrid selection in yeast. *Genetics* **144,** 1425–1436 (1996).
170. Gietz, R. D. & Akio, S. New yeast-Escherichia coli shuttle vectors constructed with in vitro mutagenized yeast genes lacking six-base pair restriction sites. *Gene* **74,** 527–534 (1988).
171. Knop, M. *et al.* Epitope tagging of yeast genes using a PCR-based strategy: more tags and improved practical routines. *Yeast* **15,** 963–972 (1999).
172. Janke, C. *et al.* A versatile toolbox for PCR-based tagging of yeast genes: new fluorescent proteins, more markers and promoter substitution cassettes. *Yeast* **21,** 947–962 (2004).
173. Dietzel, C. & Kurjan, J. Pheromonal regulation and sequence of the Saccharomyces cerevisiae SST2 gene: a model for desensitization to pheromone. *Molecular and Cellular Biology* **7,** 4169–4177 (1987).
174. Kunkel, T. A. Rapid and efficient site-specific mutagenesis without phenotypic selection. *Proc Natl Acad Sci USA* **82,** 488–492 (1985).
175. Renkawitz, J., Lademann, C. A., Kalocsay, M. & Jentsch, S. Monitoring homology search during DNA double-strand break repair in vivo. *Mol Cell* **50,** 261–272 (2013).
176. O'Geen, H., Nicolet, C. M., Blahnik, K., Green, R. & Farnham, P. J. Comparison of sample preparation methods for ChIP-chip assays. *BioTechniques* **41,** 577–580 (2006).
177. Irizarry, R. A. *et al.* Exploration, normalization, and summaries of high density oligonucleotide array probe level data. *Biostatistics* **4,** 249–264 (2003).
178. Gentleman, R. *Bioinformatics and Computational Biology Solutions Using R and Bioconductor*. (Springer Verlag, 2005).
179. Wilson, C. L. & Miller, C. J. Simpleaffy: a BioConductor package for Affymetrix Quality Control and data analysis. *Bioinformatics* **21,** 3683–3685 (2005).
180. Gautier, L., Cope, L., Bolstad, B. M. & Irizarry, R. A. affy--analysis of Affymetrix GeneChip data at the probe level. *Bioinformatics* **20,** 307–315 (2004).
181. Gentleman, R. C. *et al.* Bioconductor: open software development for computational biology and bioinformatics. *Genome Biol.* **5,** R80 (2004).
182. Durinck, S. *et al.* BioMart and Bioconductor: a powerful link between biological databases and microarray data analysis. *Bioinformatics* **21,** 3439–3440 (2005).
183. Durinck, S., Spellman, P. T., Birney, E. & Huber, W. Mapping identifiers for the integration of genomic datasets with the R/Bioconductor package biomaRt. *Nat Protoc* **4,** 1184–1191 (2009).
184. Benjamini, Y. & Hochberg, Y. Controlling the false discovery rate: a practical and powerful approach to multiple testing. *J. R. Stat. Soc.* **57,** 289–300 (1995).

7 Abbreviations

3-AT	3-aminotriazol
A	Ampere
A_x	absorbance at x nm
aa	amino acid(s)
aRNA	antisense RNA
AAA	ATPases associated with various cellular activities
Ac	acetate
AD	Gal4 transcription-activation domain
ADP	adenosine 5'-diphosphate
AMP	adenosine 5'-monophosphate
ATP	adenosine 5'-triphosphate
BD	Gal4 DNA-binding domain
bp	base pair(s)
°C	degree celcius
CC	coiled-coiled
Cdc	cell division cycle
cDNA	complementary DNA
ChIP	chromatin immunoprecipitation
ChIP-chip	ChIP analysed by genome-wide tiling microarrays
ChIP-RT-PCR	ChIP analysed by Real-Time PCR
CLR	centromere-like region
Cy3	cyanine dye 3
Cy5	cyanine dye 5
DMSO	dimethylsulfoxide
DNA	deoxyribonucleic acid
DUB	deubiquitylating enzyme
DSB	DNA double-strand break
DTT	dithiothreitol
E	glutamic acid
E. coli	Escherichia coli
e.g.	exempli gratia, for example
E1	activating enzyme
E2	conjugating enzyme
E3	ligase
E4	chain elongating ligase
EDTA	ethylenediaminetetraacidic acid
ER	endoplasmic reticulum
ERAD	ER-associated degradation
FDR	false discovery rate
G	glycine
g	gram
g	gravity
G1	gap 1 phase of the cell cylce
G418	geneticine disulfate
Gal	galactose
GFP	green fluorescent protein
Glu	glutamate
h	hour(s)
H2B	histone 2B
H2B-Ub	H2B monoubiquitylated on lysine-123
H4	histone 4
H4K20me$_2$	histone 4 lysine-20 dimethylation
HA	hemagglutinin epitope
HECT	homologous to the E6-AP carboxyl terminus
His	histidine
Hph	hygromycin B
hphNT1	gene conferring resistance to hygromycin
HRP	horse radish peroxidase
I	isoleucine
IF	in frame
IgG	immunoglobulin G
IP	immunoprecipitation
K	lysine
kanMX6	gene conferring resistance to G418
kb	kilo base pair(s)
kDa	kilo Dalton
kV	kilo Volt
l	liter(s)
LB	Luria-Bertani
Leu	leucine
LMU	Ludwig-Maximilians-University Munich
Log	logarithmic
m	milli (x10^{-3})
µ	micro (x10^{-6})
M	molar
*µ*m	micrometre(s)
MAT	mating-type locus
MATα	*MAT* locus containing α information
MATa	*MAT* locus containing a information
min	minute(s)
MPI	Max-Planck-Institute
Myc	epitope from c-Myc

n	nano (x10^{-9})
NAT	nourseothricin
natNT2	gene conferring resistance to nourseothricin
NEM	N-ethylmaleimide
nm	nanometre(s)
NFκB	nuclear factor kappa-light-chain-enhancer of activated B cells
NP-40	nonidet p-40
OD_x	optical density at x nm
ORF	open reading frame
Ω	Ohm
p-value	probability value
PAGE	polyacrylamide gel electrophoresis
PBS	phosphate buffered saline
PCNA	proliferating cell nuclear antigen
PCR	polymerase chain reaction
PDB ID	protein databank (www.pdb.org) identification number
PE	phosphatidylethanolamine
PEG	polyethylene glycol
Pgk1	phospho-glycerate kinase 1
PML	promyelocytic leukaemia
PNGase	peptide:N-glycanase
PP_i	pyrophosphate
PUB	PNGase/ubiquitin-associated
PUL	PLAP, Ufd3 and Lub1
PVDF	polyvinylidene fluoride
R	arginine
Rad	radiation
RING	really interesting new gene
RMA	Robust Multiarray Analysis
RNA	ribonucleic acid
RNA Pol II	RNA polymerase II
rpm	rounds per minute
RT-PCR	real-time PCR
S	Svedberg
S. cerevisiae	*Saccharomyces cerevisiae*
Sc	synthetic complete
SDS	sodium dodecyl sulfate
sec	second(s)
Ser	serine
SH	thiol group
SIM	SUMO-interaction motif
SRH	second region of homology
STUbL	SUMO-targeted ubiquitin ligase
Sub	substrate
SUMO	small ubiquitin-like modifier
Swi/Snf	switching defective/sucrose non-fermentable
TAP	tandem affinity purification
TBE	tris, boric acid, EDTA
TBS-T	tris-buffered saline with Tween-20
TCA	trichloro acidic acid
TCR	transcription coupled repair
TE	Tris EDTA
TLS	translesion synthesis
Tris	Tris(hydroxymethyl)-aminomethane
Trp	tryptophan
Ub	ubiquitin
UBA	ubiquitin-associated domain
UBD	ubiquitin-binding domain
UBL	ubiquitin-like
UBX	ubiquitin regulatory X
Ufd	ubiquitin-fusion degradation
UIM	ubiquitin-interacting motif
UTR	untranslated region
V	Volt
v/v	volume per volume
VBM	VCP binding motif
VCP	valosine-containing protein
VIM	VCP interaction motif
vs.	versus
WB	western blot
WCE	whole cell extract
WGA	Whole Genome Amplification
WT	wild-type
w/v	weight per volume
Y	tyrosine
YPD	yeast bactopeptone dextrose

Danksagung

Zuerst möchte ich mich sehr herzlich bei meinem Betreuer Stefan Jentsch für seine großartige Unterstützung in allen wissenschaftlichen, sowie persönlichen Belangen bedanken. Die vielen wissenschaftlichen Diskussionen mit Ihm und seine globale biologische Denkweise haben nicht nur zum Erfolg dieser Arbeit, sondern auch maßgeblich zu meiner persönlichen Entwicklung beigetragen. Besonders dankbar bin ich Stefan für sein großes Vertrauen in meine wissenschaftlichen Fähigkeiten und die außergewöhnliche wissenschaftliche Freiheit die ich in seinem Labor hatte. Ferner möchte ich die freundschaftliche Atmosphäre die Stefan im Umgang mit mir und allen anderen Doktoranden pflegt hervorheben. Gerade diese Eigenschaft macht Stefan zu einem besonderen Chef mit dem man jederzeit persönliche Anliegen besprechen kann und auch neben der Arbeit persönlich verbunden ist.

Zudem danke ich den Mitgliedern der Prüfungskommission an der LMU München für Ihre Bereitschaft diese Arbeit zu begutachten.

Mein besonderer Dank gilt Sven Schkölziger, der mich für mehr als 2 Jahre als Technischer Assistent unterstützt hat. Neben seiner hervorragenden Arbeit möchte ich Ihm für die tolle gemeinsame Zeit im Labor danken.

Meinen Dank möchte ich auch Alex Strasser für die Herstellung von Antikörpern, Kerstin Maier für die Unterstützung beim Anfertigen von *Microarrays* und Assa Yeroslaviz, sowie Bianca Habermann für die bioinformatische Analyse von *Microarray* Daten aussprechen.

Des Weiteren möchte ich mich bei allen ehemaligen und derzeitigen Kollegen in der Abteilung Jentsch für das sehr angenehme Arbeitsklima bedanken. Einen besonderen Dank möchte ich meinen langjährigen direkten Labornachbarn Irina, Dirk, Ben und Qin für die hilfsbereite und freundschaftliche Zusammenarbeit aussprechen. Ebenso möchte ich mich bei Kenji, Sven, Claudio, Jörg, Dirk und Sean, den derzeitigen und ehemaligen Mitgliedern des fast verwachsenen Nachbarlabors bedanken. Ihr Alle habt zu einer lustigen und positiven Arbeitsatmosphäre beigetragen und viele von Euch sind nicht nur Kollegen sondern auch Freunde! Claudio, Jörg, Tim, Julian, Flo, Ivan und Steven danke ich für Ihre stetige Bereitschaft und Geduld wissenschaftliche Fragen und Ergebnisse intensiv mit mir zu diskutieren. Jörg, Markus, Ben und Flo danke ich für das kritische Korrekturlesen dieser Arbeit. Ferner möchte ich mich sehr herzlich bei Klara, allen Technischen Assistenten und bei den Mitarbeitern unserer Medienküche für Ihren fortwährenden Einsatz für die Abteilung bedanken.

Ebenfalls möchte ich Jörg, Alex und Klaus für die schöne gemeinsame Zeit am MPI mit vielen Kaffeepausen und tiefgründigen Diskussionen, sowie für Ihre langjährige Freundschaft danken.

Ein besonderes Dankeschön gebührt auch dem Boehringer Ingelheim Fond für die finanzielle, aber auch persönliche Förderung. Vielen Dank an das BIF Team um Claudia, Anja, Kerstin und Sandra für die Unterstützung und die tolle gemeinsame Zeit in Hirschegg und Lautrach!

Mein größter Dank gilt meiner Familie, die mich fortwährend unterstützt hat und alle meine Entscheidungen mitgetragen hat. Insbesondere möchte ich meinen Eltern danken, die jederzeit für mich da waren und ohne die mein Lebensweg so nicht möglich gewesen wäre. Daher möchte ich Ihnen Beiden, aber insbesondere meinem leider viel zu früh verstorbenen Vater diese Arbeit widmen.

Zuletzt möchte ich mich von ganzem Herzen bei meiner Freundin Stefanie für Ihre Liebe, Unterstützung und ihr Verständnis bedanken. Ohne Sie wäre mein Leben nicht komplett!